Coordination Chemistry Reviews, 100 (1990) 453–539
Elsevier Science Publishers B.V., Amsterdam – Printed in The Netherlands

MECHANISTIC ASPECTS OF THE METAL ION PROMOTED HYDROLYSIS OF NUCLEOSIDE 5′-TRIPHOSPHATES (NTPs)

HELMUT SIGEL

Institute of Inorganic Chemistry, University of Basle, Spitalstrasse 51, CH-4056 Basle (Switzerland)

(Received 13 March 1989)

CONTENTS

0010-8545/90/$30.45

ABBREVIATIONS

Ado	adenosine
ADP^{3-}	adenosine 5′-diphosphate
AMP^{2-}	adenosine 5′-monophosphate
ε-AMP^{2-}	$1,N^6$-ethenoadenosine 5′-monophosphate
$AMP \cdot NO^{2-}$	adenosine 5′-monophosphate $N(1)$-oxide
ATP^{4-}	adenosine 5′-triphosphate
ε-ATP^{4-}	$1,N^6$-ethenoadenosine 5′-triphosphate
Bpy	2,2′-bipyridyl
CDP^{3-}	cytidine 5′-diphosphate
CTP^{4-}	cytidine 5′-triphosphate
Dien	diethylenetriamine = bis(2-aminoethyl)amine = 1,4,7-triazaheptane
Dpa	di(2-picolyl)amine
GDP^{3-}	guanosine 5′-diphosphate

GMP^{2-}	guanosine 5′-monophosphate
GTP^{4-}	guanosine 5′-triphosphate
I	ionic strength
IDP^{3-}	inosine 5′-diphosphate
IMP^{2-}	inosine 5′-monophosphate
ITP^{4-}	inosine 5′-triphosphate
M^{n+}	metal ion
M(γ)	this means that the metal ion is coordinated to the terminal γ-phosphate group of a triphosphate chain (Fig. 1); correspondingly, M(β, γ) is the abbreviation for a metal ion bound to the β and γ phosphate groups; etc.
MTP^{4-}	methyltriphosphate
NDP^{3-}	nucleoside 5′-diphosphate
NMP^{2-}	nucleoside 5′-monophosphate
NTP^{4-}	nucleoside 5′-triphosphate
PO_4	if nothing else is specified, the formula PO_4 represents all related species which might be present in solution, i.e. H_3PO_4, $H_2PO_4^-$, HPO_4^{2-} and PO_4^{3-}
$RiMP^{2-}$	D-ribose 5′-monophosphate
R–TP	triphosphate with one terminal non-coordinating organic residue, e.g. MTP^{4-}
tn	trimethylenediamine = 1,3-diaminopropane
Tris	2-amino-2(hydroxymethyl)-1,3-propanediol = tris(hydroxymethyl)amino-methane
Trp	tryptophan
TTP^{4-}	thymidine 5′-triphosphate
$TuMP^{2-}$	tubercidin 5′-monophosphate = 7-deaza-AMP^{2-}
UTP^{4-}	uridine 5′-triphosphate

A. INTRODUCTION

(i) Emphasis and scope of the review, together with some definitions

From known metabolic pathways and the extent of the world's biomass, Boyer [1] has recently estimated that ATP, and ADP and inorganic phosphate from which it is formed, participate in more chemical reactions than any other compound on the Earth's surface except water. A human being for instance uses and resynthesizes about his own body weight of ATP daily [2]. Considering this and the fact that the enzyme-catalyzed hydrolysis of ATP to ADP and inorganic phosphate is the main source of energy for most biological processes [3] it is not surprising that the biochemical significance of an understanding of the thermodynamics of the hydrolysis of ATP [4] was recognized already more than 50 years ago by Meyerhof and Lohmann [5].

As enzymic reactions involving ATP and other nucleoside 5′-triphosphates (NTPs) are metal ion dependent [6–12], the metal–NTP complexes being usually the substrates [3,12], the formation [13,14], stability [15–17], structure [17–20] and reactivity [21–23] of NTP–metal ion complexes and of related species [24–30] are receiving much attention. Among the transfers of phosphoryl and nucleotidyl groups [12] in nature, the transfer of a phosphoryl group to water is the simplest of these processes; it appears likely to provide some insight into transphosphorylations, and it is relatively easy to study in vitro:

$$NTP + H_2O \text{ —\$ } NDP + PO_4 \qquad (1)$$

In fact, the metal ion promoted dephosphorylation of NTPs in aqueous solution to the corresponding diphosphates and orthophosphate [31,32] has long been recognized [31,33,34]. It is of interest to note in this connection that strong evidence exists [35] for a single-step direct phosphoryl transfer from ATP to water in the yeast inorganic pyrophosphatase catalysis of this reaction, i.e. the phosphoryl transfer does not involve formation of a phosphorylated enzyme intermediate.

In connection with eqn. (1) it may be pointed out that here and in the remainder of this review, if nothing else is specified, the formula PO_4 represents all related species which may be present in solution, i.e. H_3PO_4, $H_2PO_4^-$, HPO_4^{2-} and PO_4^{3-}. The term "dephosphorylation" will from now on refer to the transfer of a phosphoryl group to a water molecule (eqn. (1)). The term "hydrolysis" may also refer to this or a closely related process, but for the most part the expression "hydrolysis" will be used in connection with the formation of hydroxo complexes of metal ions. In addition, the terms monomeric or dimeric complexes mean that one or two NTP^{4-} species are in the complex together with at least the corresponding number of M^{n+}; for example, $M_2(NTP)$ is a monomeric (but binuclear) nucleotide complex whereas $[M(NTP)]_2^{4-}$ is a dimeric complex.

To gain some insight into transphosphorylation mechanisms the metal ion promoted dephosphorylations of the nucleoside 5′-triphosphates shown in Fig. 1 are compared. This approach is chosen because differences in reactivity must originate from the structural differences of the nucleic base moieties. In this review the emphasis will be on studies from my own group, which involve substitution-labile divalent metal ions such as Mg^{2+}, Mn^{2+}, Ni^{2+}, Cu^{2+}, Zn^{2+} or Cd^{2+}. However, metal centers of other oxidation states have also been examined previously by various groups. Thus early studies demonstrated that lanthanide ions and/or lanthanide hydroxide gels can be good promoters for the dephosphorylation of ATP [36–38] as well as for the hydrolysis of phosphate esters [39]; corresponding observations have recently been made with Y^{3+} and La^{3+} in systems with ATP and UTP [40].

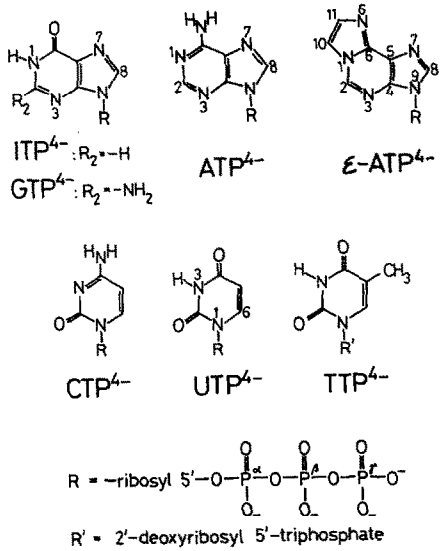

Fig. 1. Structures of several nucleoside 5′-triphosphates (NTP^{4-}), together with the labeling system for the triphosphate chain. It should be noted that the phosphate groups in the NTPs are labeled α, β, and γ, where γ refers to the terminal phosphate group. To facilitate comparisons (see Section H) between the ϵ-adenine and the adenine residues in ϵ-ATP^{4-} (equal to $1,N^6$-etheno-ATP^{4-}) and ATP^{4-} respectively, the conventional atom numbering for adenines is adapted [28]. Obviously, the analogous nucleoside 5′-monophosphates (NMP^{2-}) have the corresponding structures with only a single phosphate group.

More recent work has also shown that certain cobalt(III) complexes can be very effective in promoting ATP dephosphorylation [32,40–44], in addition to the hydrolysis of ADP [45,46], triphosphate [23,47,48], pyrophosphate [23,49,50] and orthophosphate esters [46,51]. Large enhancements in ATP dephosphorylation rates have also been reported for VO_2^+ and VO^{2+} in the presence of oxidants [23,52]. Finally, it may be added that recently much attention has been given to the facilitated hydrolysis of all kinds of orthophosphate esters by divalent metal ions [53].

(ii) Some remarks on the historical development of the subject

Owing to its biological importance, ATP was at the focus of most of the early studies. However, the results presented up to the mid-seventies on the composition and structure of the reactive complexes in the M^{2+}-promoted dephosphorylation of ATP were contradictory and equivocal. For example, some authors concluded that in the reactive complex the metal ion should be coordinated to the β- or to the α- and β-phosphate groups [31,34,54] and that an interaction between the purine moiety [31], i.e. N-7 (see Fig. 1)

[34,55], and the metal ion is required. Others deduced that hydroxo-bridged dimeric species of the kind $[M(ATP)(OH)]_2^{6-}$, with $M^{2+} = Cu^{2+}$ or Zn^{2+}, are reactive [56,57] and that the metal ion is not bound to the adenine group in the reactive ATP complex, the function of the adenine moiety being ring stacking in the dimer to facilitate the formation of the transition state [57,58]. It has also been suggested that a complex containing two metal ions per triphosphate chain may be the reactive species, thus resembling a tetrasubstituted pyrophosphate [59].

Most of these contradictions were due to incomplete knowledge on the stability and structure of ATP and other NTP complexes in solution; however, recent studies have improved the situation in this respect [17–20,60,61]. For example, the evaluations which led to the proposal that $[Cu(ATP)(OH)]_2^{6-}$ is the reactive complex in the Cu^{2+}/ATP system [56] were based on early (incorrect) equilibrium constants for Cu^{2+}–ATP–hydroxo complexes [62] (see also refs. 55 and 63) which had obviously been determined without knowing that Cu^{2+} is an excellent promoter of ATP dephosphorylation [55]. Today, one realizes that the liberation of phosphate according to eqn. (1), as well as an initial contamination of ATP with phosphate, can simulate hydroxo complex formation due to the appearance of "additional" protons in a potentiometric pH tritration [55]; the circulus viciosus inherent in this situation is evident.

However, all these contradictions are now resolved [64,65] and it is amazing to see that several of the features asked for earlier, and mentioned above, appear also in the structure given now (see Fig. 20 in Section E(v)) for the reactive complex in the M^{2+}-promoted ATP dephosphorylation. Considering only the still valid conclusions and suggestions one may note the following: (i) Tetas and Lowenstein [31] concluded in 1962–1963 "that the ions which are particularly active in catalyzing the hydrolysis of ATP interact with the adenine ring system". This was reinforced by Schneider and Brintzinger [34] in 1964 and ten years later by Buisson and Sigel [55], when they concluded that the M^{2+}–N-7 interaction is essential, and also by Miller and Westheimer [59] in 1965–1966 from a comparison of the rate of dephosphorylation in the M^{2+}/methyl and M^{2+}/γ-phenylpropyl triphosphate systems with that in M^{2+}/ATP systems (see Section C(ii)). (ii) Schneider and Brintzinger [34] also concluded that in the active species the metal ion should be coordinated to the β-phosphate group. Tetas and Lowenstein [31] asked for α,β coordination, which was also deduced by Cooperman [6,54] in 1969 from a study of the hydrolysis of asymmetrical diesters of pyrophosphate (see Section E(v)). (iii) Miller and Westheimer [59] have suggested that "a complex containing two metal ions per triphosphate may be the reactive species", a suggestion which is indeed correct (Section E(ii)). (iv) In 1967–1968, Spiro et al. [56] concluded that the reactive species

is a dimer. This was taken up by Feldman [57,58] in 1972 who suggested further that in the dimer "the two adenine rings are stacked", (though there is no hydroxo bridge; see Section E(ii)).

B. MEASUREMENTS OF NTP DEPHOSPHORYLATION AND EVALUATION PROCEDURES

To give the interested reader an idea about the experimental procedures, the most pertinent features of these are summarized below. In fact, for any judgement on the validity of the conclusions, familiarity with the experiments and their evaluation is a precondition.

(i) Determination of dephosphorylation rates

All dephosphorylation experiments described in the following sections were carried out at $I = 0.1$ M ($NaClO_4$) and also mostly at 50 °C (water bath). As buffers inhibit the metal ion accelerated dephosphorylation of NTPs [66] (see below), the pH of the solutions was adjusted with NaOH or $HClO_4$ [40,55,64–66]. As the pH changes somewhat in such unbuffered solutions, it was measured each time a sample for the phosphate determination was taken. The concentration of liberated phosphate from the conversion of NTP to NDP and PO_4 [31,32] was determined after careful standardizations with molybdate reagent in samples taken at suitable intervals, using an adaptation [34] of the method developed by Hirata and Appleman [67]. After mixing the sample with the molybdate–$HClO_4$ reagent and volume adjustment, the probe was kept for 2 min in a bath at 25 °C prior to spectrophotometric measurements. The method using molybdate reagent has been criticized with undue arguments [68]. In fact, results obtained with molybdate reagent are in good agreement [40] with measurements using ^{31}P NMR or an enzymic method [32]. The following definitions hold: [NTP] at time t is given by $[NTP]_t = [NTP]_0 - [PO_4]_t$, where $[NTP]_0$ is the initial concentration of NTP, and $[NTP]_t$ and $[PO_4]_t$ are concentrations at time t.

The (pseudo) first-order rate constant k (s^{-1}), which is generally used for comparisons [34], was determined from the slope of the straight-line portion of a log $[NTP]_t$/time plot. The corresponding pH_{av} was obtained by averaging the pH values measured for those samples that gave points on the straight-line portion. In Fig. 2, three representative examples are shown [55]; others are given in the figures in refs. 66 and 69. With this procedure, the results of Schneider and Brintzinger (Fig. 1 in ref. 34) were exactly reproducible. The dephosphorylation of the NTPs was in most cases followed for

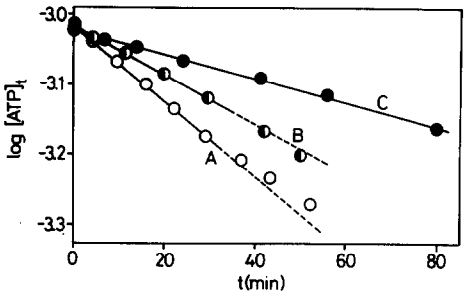

Fig. 2. Determination of the first-order rate constant k (s^{-1}) from plots of log $[ATP]_t$ vs. time t for the Cu^{2+}-promoted dephosphorylation of ATP in aqueous reaction solutions of various pH: $[ATP]_{tot(t=0)} = [Cu^{2+}]_{tot} = 10^{-3}$ M; $I = 0.1$ M, $NaClO_4$; 50 °C. For the evaluation, only this part of a kinetic run was used where the points did fit a straight line portion (solid parts of lines A, B and C): line A, $m = -0.220/39.0 = -5.65 \times 10^{-3}$, $k = (5.65 \times 10^{-3} \times 2.303)/60 = 2.17 \times 10^{-4}$ s^{-1}; line B, $m = -0.106/32.8 = -3.24 \times 10^{-3}$, $k = (3.24 \times 10^{-3} \times 2.303)/60 = 1.24 \times 10^{-4}$ s^{-1}; line C, $m = -0.110/60.0 = -1.833 \times 10^{-3}$, $k = (1.833 \times 10^{-3} \times 2.303)/60 = 7.04 \times 10^{-5}$ s^{-1}. The corresponding pH values, i.e. pH_{av} were determined from the same part of an experiment: line A, 6.70, 6.54, 6.38, 6.25, 6.17, 6.10, $pH_{av} = 6.36$; line B, 6.52, 6.38, 6.28, 6.18, 6.09, $pH_{av} = 6.29$; line C, 7.82, 7.75, 7.68, 7.59, 7.46, 7.37, 7.24, $pH_{av} = 7.56$. The values for k at pH_{av} 6.36, 6.29 and 7.56 are part of the pH–rate profile for the Cu^{2+}/ATP system shown in Fig. 5 (vide infra). (Redrawn from Fig. 1 of ref. 55 (Biochim. Biophys. Acta, 1974) with permission of Elsevier.)

about 20–30% reaction, the data covering the first 5–10% reaction being generally the most useful for the evaluation, especially for the calculation of v_0 (see next paragraph).

For mechanistic considerations, where an exact relationship between rate and pH is essential [64], the initial rate of NTP dephosphorylation, $v_0 = d[PO_4]/dt$ ($M\ s^{-1}$), was determined from the slope of the tangent of the $[PO_4]_t$/time curve at time $t = 0$. The corresponding initial pH of the reaction solution, i.e. pH_0, was determined analogously. To obtain v_0 for a given system at a particular pH_0, at least two experiments were carried out in this range of pH (one slightly above and the other below the desired value) and these results were then interpolated to the desired pH_0. An example of this procedure is shown in Fig. 3 [64]; further examples are given in the figures in refs. 55 and 69. Usually v_0 is reproducible to $\pm 10\%$, but for a very rapid reaction and/or an unstable pH, the error limit may increase to about $\pm 25\%$.

The two quantification methods for the dephosphorylation rates may be transformed into each other by the relation $v_0 = d[PO_4]/dt = k[NTP]$, and by also taking into account that pH_0 is usually larger than pH_{av} by about 0.2 log units.

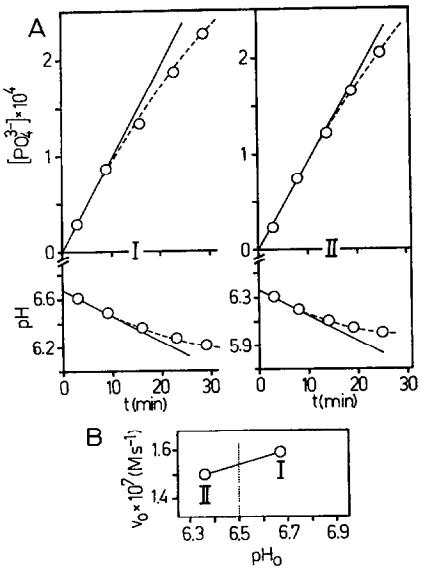

Fig. 3. Determination of the initial rate v_0 (M s^{-1}) and the corresponding initial pH, pH_0 (A), and the interpolation (B) for v_0 at pH_0 6.50. A, Cu^{2+}-promoted dephosphorylation of ATP in aqueous solution; $[ATP]_{tot(t=0)} = 0.9\times10^{-3}$ M, $[Cu^{2+}]_{tot} = 1.1\times10^{-3}$ M (there is a printing error in the concentrations given in ref. 64); $I = 0.1$ M, $NaClO_4$; 50 °C. Initial rate for case I and extrapolation to $t = 0$: $v_0 = d[PO_4^{3-}]/dt = 1.91\times10^{-4}/(20\times60) = 1.59\times10^{-7}$ M s^{-1} (pH_0 6.67). For case II: $v_0 = 1.80\times10^{-4}/(20\times60) = 1.50\times10^{-7}$ M s^{-1} (pH_0 6.36). B, interpolation from the above results at pH_0 6.50 gives $v_0 = 1.54\times10^{-7}$ M s^{-1}; this value corresponds to the top point of the experimental series at pH_0 6.50 shown in Fig. 15B (vide infra in Section E(ii)). (Partial reproduction from Fig. 1 in ref. 64 (J. Am. Chem. Soc., 1976) with permission of the American Chemical Society.)

(ii) Inhibition of the metal ion promoted NTP dephosphorylation by buffers

Buffers such as 2-amino-2-(hydroxymethyl)-1,3-propanediol (Tris), 2-[bis(2-hydroxyethyl)amino]-2-(hydroxymethyl)-1,3-propanediol (Bistris) and triethanolamine (Tea) are well known to form complexes with metal ions, including mixed-ligand complexes involving ATP [70]. Considering that all buffers that are proton acceptors are also potential ligands for metal ions, one expects that the presence of a buffer will affect the reactivity of an M^{n+}/NTP system.

Indeed, the examples in Fig. 4 show the effect of acetate, Tris and borate buffers on the Zn^{2+}-promoted dephosphorylation of ATP in a Zn^{2+}/ATP 1 : 1 system ($[ATP] = 10^{-3}$ M) at 80 °C [66]. Already low buffer concentrations of 5×10^{-3} M have a significant effect on the dephosphorylation rate; the larger concentrations of 0.1 M lead to strong inhibition, with a reactivity nearly as low as that of free ATP. In addition, the maximum of the pH–rate

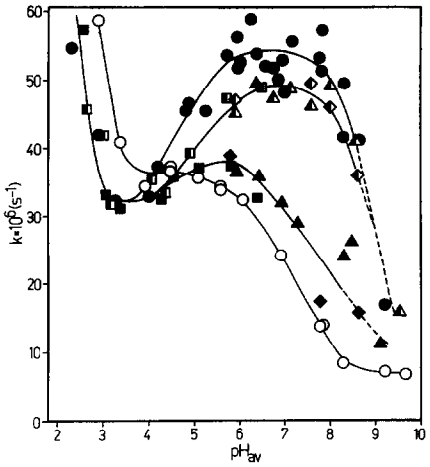

Fig. 4. Influence of buffers at 80 °C ($I = 0.1$ M, $NaClO_4$) on the dephosphorylation of Zn^{2+}/ATP as a function of pH characterized as the first-order rate constants, k (s^{-1}): ATP (○, 10^{-3} M) and Zn^{2+}/ATP (●, $[ATP] = [Zn^{2+}] = 10^{-3}$ M). Zn^{2+}/ATP (also each 10^{-3} M) in the presence of 5×10^{-3} M acetate (◧), Tris (◆) or borate (▲), and in the presence of 0.1 M acetate (■), Tris (◆) or borate (▲). The broken line portions indicate uncertainty due to precipitation. (Reproduced from Fig. 4 of ref. 66 (Eur. J. Biochem., 1976) with permission.)

profile of the dephosphorylation is shifted to lower pH values [66]. Other buffers composed of imidazole [55] or phosphate [64,65] also inhibit the reactivity of M^{2+}/ATP systems.

These observations explain why different pH–rate profiles are found by different groups, for example, for the Zn^{2+}/ATP system [31,66]. It is evident that any study aiming to reveal the effect of metal ions on NTP dephosphorylations must be carried out in buffer-free solutions; otherwise no reliable conclusions can be drawn.

(iii) Influence of temperature on the NTP dephosphorylation

The slope of the pH–rate profile for free ATP in Fig. 4 at 80 °C corresponds approximately to that observed at 50 °C [66], although the rate is significantly higher at 80 °C. The pH–rate profile of the Zn^{2+}/ATP 1 : 1 system shows not only an increased rate at 80 °C but also a rather broad maximum in the pH range 5.8–7.8 (Fig. 4) which contrasts with the sharp maximum at pH 8 at 50 °C [66] (vide infra, Fig. 13). However, it is still evident that an increase in temperature shifts the maximum of the pH–rate profile to lower pH. This corresponds to observations with the Cu^{2+}/ATP 1 : 1 system [55], where the maximum of the pH–rate profile is for 25 °C at pH 7.3 and for 50 °C at pH 6.5.

From experiments of the kind indicated (with [NTP] = 10^{-3} M) one may also estimate the activation energy E_A for the NTP dephosphorylation in the different systems. For the species $H(ATP)^{3-}$ (or $H(NTP)^{3-}$) which dominates at pH 5, one obtains $E_A \approx 109$ kJ mol^{-1}, and for ATP^{4-} (or NTP^{4-}) at pH 9.5, $E_A \approx 134$ kJ mol^{-1} [66]. The activation energies in the presence of metal ions are lower than for ATP^{4-} alone: $E_A \approx 88$ kJ mol^{-1} for the Zn^{2+}/ATP 1:1 system at pH 8 [66], and about 100 kJ mol^{-1} for the Cu^{2+}/ATP 1:1 system in the pH range 6.0–6.6 [55].

These results indicate that great care should be exercised if conclusions are drawn from experiments with different systems carried out at different temperatures. All experiments considered in the following sections were done at 50 °C.

C. DEPHOSPHORYLATION OF FREE NTPs AND INFLUENCE OF Cu^{2+} OR Cu(2,2′-BIPYRIDYL)$^{2+}$

A summary of the dephosphorylating properties of the six natural nucleoside 5′-triphosphates shown in Fig. 1 is provided in Fig. 5, where the first-order rate constants k for the several systems are plotted as a function of pH [65]. Some of the main conclusions follow.

(i) The dephosphorylation process in uncomplexed triphosphates with one terminal organic residue (R–TP)

The results in Fig. 5 show that all common NTPs (Fig. 1) including ATP and also methyltriphosphate [34] (see also Fig. 3 in ref. 71) display virtually identical dephosphorylation rates in the absence of metal ions [65]. In other words, protonations (e.g. at N-1 in ATP [72]) or deprotonations (e.g. from N-1 in ITP [73]) at the nucleic base portion do not alter the hydrolysis rate, i.e. only protonations of the triphosphate chain have to be considered and therefore the reasoning below holds for any triphosphate with one terminal organic residue (R–TP).

The entire pH–rate profile for free NTPs in Fig. 5 from pH 2–10 may be fitted by only two equilibrium and three rate constants [65]. For free R–TPs the observed first-order rate constant k_{obsd} for hydrolysis according to eqn. (1) is given by eqn. (2), where the subscripts 2, 4 and 9 for the rate constants k refer to the corresponding pH ranges in the pH–rate profile of free NTPs in Fig. 5:

$$k_{obsd}[\text{R–TP}]_{tot} = k_2[\text{H}_2(\text{R–TP})^{2-}] + k_4[\text{H(R–TP)}^{3-}] + k_9[\text{R–TP}^{4-}] \quad (2)$$

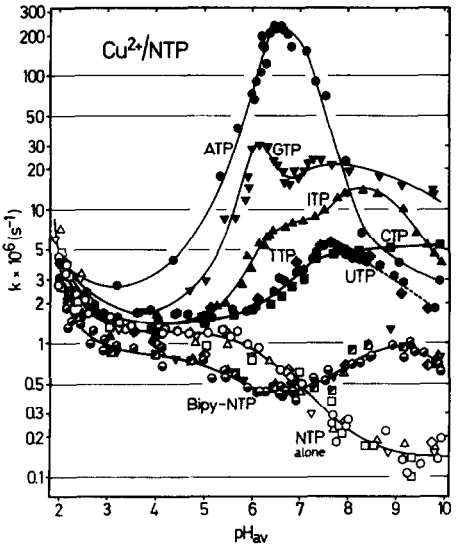

Fig. 5. Comparison of the Cu^{2+}-promoted dephosphorylation of ATP (●), ITP (▲), GTP (▼), CTP (■), UTP (●) and TTP (◆) (always in the ratio 1 : 1) in aqueous solution as a function of pH, characterized as the first-order rate constants k (s^{-1}). In addition, ATP (○), ITP (△), GTP (▽), CTP (□), UTP (○), and TTP (◇) are given alone; and ATP (◒), ITP (◭), GTP (◬), CTP (◩), UTP (◍) and TTP (◈) are given also in the presence of Cu^{2+} and 2,2′-bipyridyl (1 : 1 : 1). The concentration of each reagent was always 10^{-3} M, when present; $I = 0.1$ M, $NaClO_4$; 50 °C. The broken line portion indicates uncertainty due to precipitation. (Reproduced from Fig. 1 in ref. 65 (J. Am. Chem. Soc., 1984) with permission of the American Chemical Society.)

The acidity constants of $H_2(R\text{–}TP)^{2-}$ are defined by eqns. (3) and (4):

$$K^{H}_{H_2(R\text{–}TP)} = [H^+][H(R\text{–}TP)^{3-}]/[H_2(R\text{–}TP)^{2-}] \quad (3)$$

$$K^{H}_{H(R\text{–}TP)} = [H^+][R\text{–}TP^{4-}]/[H(R\text{–}TP)^{3-}] \quad (4)$$

The corresponding values are $pK^{H}_{H_2(R\text{–}TP)} \approx 2.0$ [15,74] and $pK^{H}_{H(R\text{–}TP)} = 6.5$ [61], in agreement with the two inflection points observed in the pH–rate profile for free NTP in Fig. 5.

Evaluation of the data for the three rate constants in eqn. (2) gives $k_9 = 0.14 \times 10^{-6}$ s^{-1}, $k_4 = 1.2 \times 10^{-6}$ s^{-1} and $k_2 \approx 9 \times 10^{-6}$ s^{-1} [65]; hence the dephosphorylation tendency increases in the series $R\text{–}TP^{4-} < H(R\text{–}TP)^{3-} < H_2(R\text{–}TP)^{2-}$. This result agrees with an earlier conclusion [75] reached from studies of the hydrolysis of a variety of phosphate esters: rates are enhanced by protonation of the anionic forms.

Each of the three rate constants in eqn. (2) may characterize either of two kinetic pathways or a combination of both [65]; i.e. an addition–elimination

pathway (by attack of water) via a pentacoordinate oxyphosphorane intermediate, or an elimination–addition pathway via elimination of a monomeric metaphosphate anion, PO_3^- (which then adds water). The metaphosphate pathway with a tricoordinate phosphorus becomes more favored the more anionic the reacting species is. The contribution of the two pathways to hydrolysis of the several ATP species has not definitively been resolved [76]. Assuming that the pentacoordinate addition–elimination pathway predominates, it is concluded [65] that throughout the entire NTP pH–rate profile in Fig. 5, free R–TP dephosphorylation proceeds by nucleophilic water attack and nowhere does hydroxide significantly contribute as a nucleophile.

It may be added that during hydrolysis of ATP in 3 M $HClO_4$ the direct production of orthophosphoric acid is about 20 times faster than the production of pyrophosphoric acid [77]. This is different in the alkaline pH range; at pH > 8.5, depyrophosphorylation of ATP^{4-} becomes significant [78].

(ii) Promotion of NTP dephosphorylation by Cu^{2+}

The remarkable point in the preceding section was the observation that the nucleic base moieties have no influence on the dephosphorylation of uncomplexed NTPs. This situation changes drastically in the presence of metal ions such as Cu^{2+} (Fig. 5) or Zn^{2+} [64,66,71]. Clearly, only the base moieties can be responsible for the differences observed between the individual Cu^{2+}/NTP 1 : 1 systems in Fig. 5. In addition, the acceleration of the reaction can be large, e.g. at pH 6.5, Cu^{2+} facilitates in a 1 : 1 ratio the dephosphorylation of ATP by a factor of about 300 (see also Section J).

A more careful comparison of the results summarized in Fig. 5 reveals that in the presence of Cu^{2+} only the purine-NTPs differ markedly, while the pyrimidine-NTP/Cu^{2+} systems have the same properties up to pH 8. This latter result is understandable as there is no metal ion–nucleic base interaction in M(pyrimidine-NTP)$^{2-}$ complexes [60,61] with the exception of $Cu(CTP)^{2-}$, in which a weak base-backbinding of the phosphate-coordinated Cu^{2+} occurs, i.e. about one-third of $Cu(CTP)^{2-}$ exists as a weak macrochelate [61], but this backbinding is evidently not strong enough to affect the dephosphorylation process (see also Section H(iv)). Consequently, all three pyrimidine-NTP/Cu^{2+} systems [71] have essentially the same dephosphorylating properties as the methyltriphosphate/Cu^{2+} system [34] (see also Fig. 6, vide infra); the corresponding mechanistic aspects will be discussed together in Section D. The differences at pH > 8 between the Cu^{2+}/CTP system on the one hand and the Cu^{2+}/UTP and Cu^{2+}/TTP systems on the other (Fig. 5) are due to the deprotonation at N-3 [60,73]

which can occur only in $M(UTP)^{2-}$ and $M(TTP)^{2-}$ but not in $M(CTP)^{2-}$ (see Fig. 1).

For $M(purine\text{-}NTP)^{2-}$ complexes the metal ion–nucleic base interaction is important [60], as has been worked out especially carefully for the $M(ATP)^{2-}$ species [17,61]. In fact, the metal ion–N-7 interaction significantly influences the dephosphorylation process of the Cu^{2+}/purine-NTP systems shown in Fig. 5, though it should be mentioned already here that the differences in reactivity between the Cu^{2+} 1:1 systems in the pH range 2–7.5 are more a reflection of the decreasing stacking tendency, ATP > GTP > ITP [65] (Section E(vi)). The main emphasis in the discussion of mechanistic aspects will be on M^{2+}/ATP systems (Section E), but ITP and GTP will also be considered shortly (Section F).

(iii) Protection of NTPs towards dephosphorylation by mixed-ligand complex formation

The properties of the 2,2′-bipyridyl/Cu^{2+}/NTP systems (Fig. 5) [64,66,71] in the pH range 2–10 are in accord with the points mentioned: the formation of ternary $M(Bpy)(NTP)^{2-}$ complexes leads to intramolecular stacks between the base residues and the pyridyl rings [15,20,28,79–81]. Consequently the metal ion–nucleic base interaction is prevented and indeed all Bpy/Cu^{2+}/NTP systems have the same dephosphorylating properties (Fig. 5). However, there is one further important point: in the pH range up to 7 the $Cu(Bpy)(NTP)^{2-}$ complexes, which have a very high degree of formation, are even more stable towards dephosphorylation than free ATP (Fig. 5). This observation [64,82] has allowed the growth of crystals of mixed-ligand $M(Bpy)(ATP)^{2-}$ complexes and has thus led to the first X-ray studies of ATP complexes with substitution-labile metal ions [83,84].

The protecting effect on NTPs is not unique to Cu^{2+} systems, nor to the presence of 2,2′-bipyridyl. It occurs, for example, also in the Zn^{2+}/Bpy/ATP system [66,85] as well as in mixed-ligand NTP complexes with imidazole [55], tryptophanate, phosphate etc. [65,86]. Evidently, coordination of any ligand (including the unidentate OH^-, NH_3 and imidazole) to $M(ATP)^{2-}$ releases N-7 from the coordination sphere of the metal ion [87,88] (see also Sections D(ii) and E(iii)). These results may be meaningful for biological systems, e.g. regarding the transport of hydrolysis-sensitive phosphates (Section L).

D. THE METAL ION PROMOTED DEPHOSPHORYLATION PROCESS OF SIMPLE TRIPHOSPHATES (R–TPs)

The discussion in Section C(ii) of the results given in Fig. 5 emphasized that the Cu^{2+}/UTP and Cu^{2+}/TTP 1:1 systems show identical properties

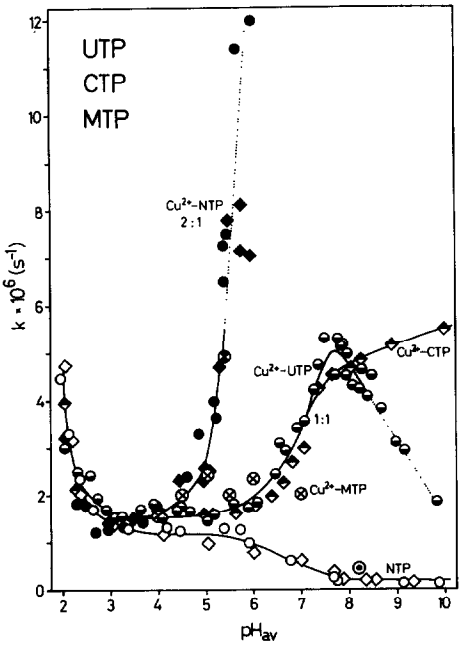

Fig. 6. First-order rate constants, k (s^{-1}), for the dephosphorylation of UTP (○, ⊖, ●) and CTP (◇, ◈, ◆) in aqueous solution as a function of pH: NTP alone (○, ◇), Cu^{2+}/NTP (1:1) (⊖, ◈), and Cu^{2+}/NTP (2:1) (●, ◆); $[NTP]_{tot} = 10^{-3}$ M; $I = 0.1$ M, $NaClO_4$; 50 °C. The dotted line portions indicate uncertainty due to precipitation. For further comparison the corresponding data for methyltriphosphate [34] are also shown: MTP (⊙), Cu^{2+}/MTP (1.1:1) (⊗), and Cu^{2+}/MTP (2:1) (⊛); $[MTP]_{tot} = 10^{-3}$ M; 50 °C. (Reproduced from Fig. 3 in ref. 71 (Eur. J. Biochem., 1983) with permission.)

in the pH range 2–10. Furthermore, in the pH range 2–8 all three Cu^{2+}/pyrimidine-NTP systems, i.e. including CTP (see Fig. 1), behave in the same way, as the pyrimidine base residue is not influencing the dephosphorylation reaction (at pH > 8, UTP and TTP lose the proton at N-3 [73,89]). This conclusion is confirmed by the results in Fig. 6 where the first-order rate constants, k (s^{-1}), for the dephosphorylation of several CTP, UTP and methyltriphosphate (MTP) systems are plotted as a function of pH [71]; the data for the MTP systems are taken from the work of Schneider and Brintzinger [34]. It is evident that the available MTP data fit well, within the limits of experimental error, to the corresponding three pH–rate profiles defined by the CTP and UTP data. Hence we are considering here the simplest case, i.e. the results discussed in this section are representative of the properties of a triphosphate with one terminal non-coordinating organic residue (R–TP).

(i) Comparison between the rate of dephosphorylation and the distribution of complex species in M^{2+}/R–TP systems

In the upper parts of Figs. 7 and 8, again the first-order rate constants, k (s^{-1}), for the dephosphorylation reaction of several M^{2+}/CTP 1 : 1 systems

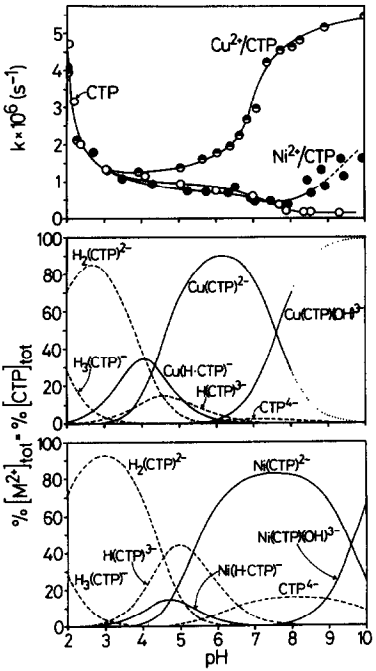

Fig. 7. Comparison of the variation (upper part) of the Cu^{2+}-promoted (⊖) [69] and Ni^{2+}-promoted (●) [66] dephosphorylation of CTP (alone, ○) [69] in aqueous solution at 50 °C, characterized by first-order rate constants k (s^{-1}), as a function of pH (each reactant when present was 10^{-3} M; $I = 0.1$ M, $NaClO_4$; the broken line portion indicates uncertainty due to precipitation) with the effect (lower parts) of pH at 25 °C ($I = 0.1$ M, $Na^+ ClO_4^-$/NO_3^-) on the concentration of the species present in an aqueous solution of CTP and Cu^{2+} or Ni^{2+} (each 10^{-3} M); these results are given as the percentage of the total M^{2+} present (equal to total CTP); the broken lines refer to the free CTP species and the solid lines to the CTP complexes. The results of the middle and lower parts were computed with the following equilibrium constants: $pK^{H}_{H_3(CTP)} \approx 1.6$ ($\approx pK^{H}_{H_3(ATP)}$ [72]), $pK^{H}_{H_2(CTP)} = 4.55 \pm 0.03$, $pK^{H}_{H(CTP)} = 6.55 \pm 0.02$, $\log K^{Cu}_{Cu(H\cdot CTP)} = 3.80 \pm 0.06$, $\log K^{Ni}_{Ni(H\cdot CTP)} = 2.70 \pm 0.25$, $\log K^{Cu}_{Cu(CTP)} = 6.03 \pm 0.03$, $\log K^{Ni}_{Ni(CTP)} = 4.52 \pm 0.02$ (all values from ref. 61), $pK^{H}_{Cu(CTP)(H_2O)} = 7.6$ [73,89] (this value describes the situation well in the pH range up to 8, possibly even 9, then matters may become more complicated and therefore at pH > 8 the lines are dotted; this conclusion is made in analogy to the Cu^{2+}/ATP system, cf. refs. 55 and 63), $pK^{H}_{Ni(CTP)(H_2O)} = 9.58 \pm 0.15$ [73]. The diprotonated $M(H_2 \cdot CTP)$ complexes were ignored in the calculations as the appropriate constants are unknown; however, such species would probably exist only below pH 3.

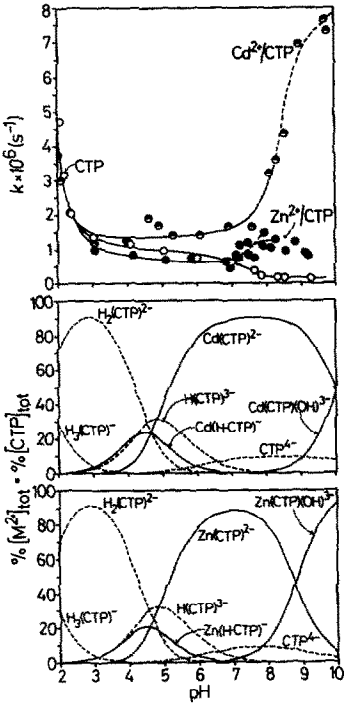

Fig. 8. Comparison of the variation (upper part) of the Cd^{2+}-promoted (⊖) [65] and Zn^{2+}-promoted (●) [66] dephosphorylation of CTP (alone: ○) [69] in aqueous solution at 50 °C, characterized by first-order rate constants k (s^{-1}), as a function of pH (each reactant, when present, was 10^{-3} M; $I = 0.1$ M, $NaClO_4$; the broken line portions indicate uncertainty due to precipitation) with the effect (lower parts) of pH at 25 °C ($I = 0.1$ M, $Na^+ ClO_4^-$/NO_3^-) on the concentration of the species present in an aqueous solution of CTP and Cd^{2+} or Zn^{2+} (each 10^{-3} M); these results are given as the percentage of the total M^{2+} present (equal to total CTP); the broken lines refer to the free CTP species and the solid lines to the CTP complexes. The results of the middle and lower parts were computed with the following equilibrium constants: $pK^H_{H_3(CTP)} \approx 1.6$ ($\approx pK^H_{H_3(ATP)}$ [72]), $pK^H_{H_2(CTP)} = 4.55 \pm 0.03$, $pK^H_{H(CTP)} = 6.55 \pm 0.02$, $\log K^{Cd}_{Cd(H\cdot CTP)} = 3.15 \pm 0.06$, $\log K^{Zn}_{Zn(H\cdot CTP)} = 3.05 \pm 0.07$, $\log K^{Cd}_{Cd(CTP)} = 5.05 \pm 0.04$, $\log K^{Zn}_{Zn(CTP)} = 5.03 \pm 0.05$ (all values from ref. 61), $pK^H_{Cd(CTP)(H_2O)} = 10.0$ [88], $pK^H_{Zn(CTP)(H_2O)} = 8.79 \pm 0.05$ [73]. The diprotonated $M(H_2 \cdot CTP)$ complexes were ignored in the calculations as the appropriate constants are unknown; however, such species would probably exist only below pH 3.

are plotted as a function of pH. Although these rates were measured at 50 °C [65,66,69] and the distribution of the complex species in the middle and lower parts of Figs. 7 and 8 refer to 25 °C [61], the dephosphorylation rates of CTP parallel the formation of the $M(CTP)(OH)^{3-}$ species. Considering that an increase in temperature from 25 to 50 °C considerably favors the formation of hydroxo complexes in triphosphate systems [55] it is especially evident for the Cu^{2+} and Cd^{2+} systems that the rate increases

with increasing concentration of $Cu(CTP)(OH)^{3-}$ and $Cd(CTP)(OH)^{3-}$. The dephosphorylation experiments with Ni^{2+} and Zn^{2+} are somewhat hampered by precipitation but the results still confirm the conclusion given and show that
the reactivity parallels the formation of $Ni(CTP)(OH)^{3-}$ and $Zn(CTP)(OH)^{3-}$.

One may add that the degrees of formation of $M(UTP)^{2-}$ complexes are similar to those of the corresponding $M(CTP)^{2-}$ species seen in Figs. 7 and 8. Differences in the distribution curves occur at higher pH values with the release of the proton from N-3 and the formation of deprotonated $M(UTP-H)^{3-}$ and $M(UTP-H)(OH)^{4-}$ complexes [71]; this holds also for M^{2+}/TTP systems. The formation of these N-3 ionized species is responsible for the decreasing dephosphorylation rate at pH > 8, observed for the Cu^{2+}/UTP or Cu^{2+}/TTP systems (Figs. 5 and 6).

The reactivity in Ni^{2+}/UTP, Cu^{2+}/UTP and Zn^{2+}/UTP systems is also connected with the formation of $M(UTP)(OH)^{3-}$ species [71]; comparisons with Fig. 5 indicate further that the same may be surmised at least for $Cu(TTP)(OH)^{3-}$. Hence overall one may conclude that the most reactive species in M^{2+}/R–TP dephosphorylations is connected with the formation of the $M(R-TP)(OH)^{3-}$ complex.

(ii) Evidence for an intramolecular attack by coordinated OH^- in M^{2+}/R–TP systems

That in the most reactive species of the metal ion promoted R–TP dephosphorylation the metal ion is not simply needed for the neutralization of the negatively charged triphosphate chain is evident from a comparison of the middle and lower parts in Figs. 7 and 8 with the corresponding upper parts. The reactivity of the $M(R-TP)^{2-}$ complex is in all systems evidently very low. This together with the observations summarized in Section D(i) indicate that the formation of $M(R-TP)(OH)^{3-}$ leads to intramolecular attack by OH^- in the reactive complex.

This suggestion agrees with the observation that all Cu^{2+}/Bpy/NTP systems are very unreactive (Section C(iii); Fig. 5): $Cu(Bpy)(NTP)^{2-}$ complexes [90], as well as the $Cu(Bpy)(NTP-H)^{3-}$ species formed with those NTPs having an ionizable base residue [73,89] are very stable and their degree of formation in 1 : 1 : 1 systems is therefore very high [55,69,71,73]. Clearly, in these complexes the equatorial positions of the Jahn–Teller distorted coordination sphere of Cu^{2+} are occupied by the two nitrogen atoms of 2,2′-bipyridyl and two oxygen atoms of the triphosphate chain; there is no strong binding site left for the coordination of OH^- and hence these complexes are not dephosphorylation sensitive as they are not suited to

to intramolecular nucleophilic attack by OH^-. This is why $Cu(Bpy)(R\text{–}TP)^{2-}$ is unreactive even at pH 10 (Fig. 5).

Similarly, the ternary Ni^{2+} and Zn^{2+} systems with UTP or CTP and 2,2′-bipyridyl are also more stable toward dephosphorylation than the corresponding binary systems [71]. In fact, it is evident that any kind of mixed-ligand complex formation will be in competition with the formation of $M(R\text{–}TP)(OH)^{3-}$, which is also a mixed-ligand complex. This competition, and as a consequence, the inhibition of the dephosphorylation reaction is nicely seen in Fig. 9, where the initial rate v_0 of the reaction (eqn. (1)) is plotted as a function of increasing amounts of a ligand L added to the Cu^{2+}/UTP 1:1 system at pH_0 7.80. Obviously the amino-acid anion, L-tryptophanate (Trp^-), suppresses the formation of $Cu(UTP)(OH)^{3-}$ by formation of $Cu(UTP)(Trp)^{3-}$; the stability of this ternary complex [71] is of the same order as that of the more thoroughly studied $Cu(ATP)(Trp)^{3-}$ analog [91,92]. Correspondingly, the addition of hydrogen phosphate to Cu^{2+}/UTP inhibits the reaction by formation of $Cu(UTP)(PO_4)^{5-}$ [71]; that not mainly $Cu(UTP)(HPO_4)^{4-}$ is formed is evident from the smaller influence of AMP^{2-} (Fig. 9) which leads to the formation of $Cu(UTP)(AMP)^{4-}$

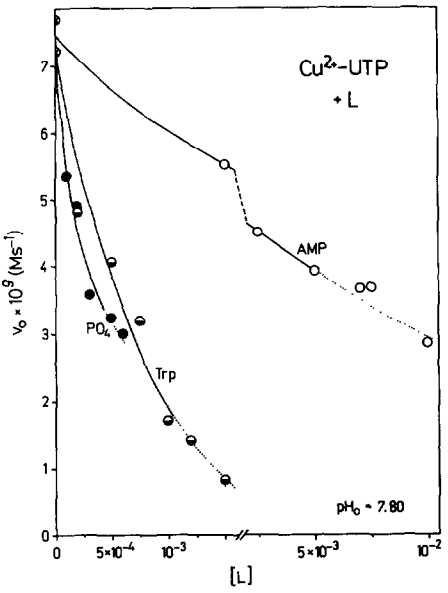

Fig. 9. Inhibition of the Cu^{2+}-promoted dephosphorylation of UTP in aqueous solution (characterized as the initial rate v_0 (M s^{-1})) by the addition of further ligands (L), i.e. phosphate (●), L-Trp (◒) or AMP (○), at pH_0 7.80. $[Cu^{2+}]_{tot} = [UTP]_{tot} = 10^{-3}$ M; $I = 0.1$ M, $NaClO_4$; 50 °C. The dotted line portions indicate uncertainty due to precipitation. (Reproduced from Fig. S4 of ref. 71 (Eur. J. Biochem., 1983) with permission.)

[71]. This conclusion is justified as it is well known [93] that the coordinating properties of HPO_4^{2-} and AMP^{2-} are to a first approximation rather similar.

To conclude, inhibition of the formation of $M(R-TP)(OH)^{3-}$ inhibits also the dephosphorylation reaction; this together with the other arguments given above and a further one described in the next section suggest that in the most reactive species in an $M^{2+}/R-TP$ system the reaction proceeds by intramolecular nucleophilic attack, i.e. via an $M(OH)^+$ unit. Indeed, that a correctly positioned OH^- in an M(OH) unit can be a potent nucleophile [94–96] despite its reduced basicity [94,95] is well known and has been implied for OH^- bound to, for example, Zn^{2+} [97,98], Co^{3+} [32,45,95,99] and Cu^{2+} [100,101].

(iii) Dephosphorylation rate in $M^{2+}/R-TP$ 2 : 1 systems, and relation between the rate and the concentration of $M^{2+}/R-TP$

There are many indications that the coordination of more than one metal ion to an oligophosphate promotes the hydrolysis of a P–O–P bond particularly well (see for example refs. 21, 22, 32, 49 and 59). Indeed, in Fig. 6 it is seen from the first-order rate constants, k (s^{-1}), plotted as a function of pH, that CTP, UTP and methyltriphosphate in the presence of two equivalents of Cu^{2+} are considerably more reactive than the corresponding 1 : 1 systems [71]. The promoting effect of an excess of metal ions is confirmed by the results shown in the upper part of Fig. 10 where the initial rate of the UTP dephosphorylation, $v_0 = d[PO_4]/dt$ (M s^{-1}), is plotted as a function of increasing Cu^{2+} concentration at a constant pH (pH_0 5.00); these observations correspond to those made with Cu^{2+} and CTP [64] and are certainly a general feature of such systems.

To obtain a clear picture of the composition of a reactive complex, Job's method of continuous variation [102] is advantageously employed. The measured initial rates, v_0, are plotted vs. the ratios $[M^{2+}]/([M^{2+}] + [R-TP])$, keeping $[M^{2+}] + [R-TP]$ constant. Hence a maximal rate at values of 0.33, 0.5 or 0.67 indicates a composition for the reactive species of M^{2+}: R–TP = 1 : 2, 1 : 1, or 2 : 1 respectively. Such experiments have been carried out for Cu^{2+}/CTP [64] and Cu^{2+}/UTP [71]; two examples are shown in the middle and lower parts of Fig. 10. These results prove that the most reactive species contains two metal ions and one $R-TP^{4-}$. As unbound Cu^{2+} in about 2×10^{-3} M solutions begins to hydrolyze at a pH of approximately 5, i.e. it forms hydroxo complexes, it is to be expected that a $Cu_2(R-TP)$ species, in which the coordination spheres of the two Cu^{2+} ions are certainly not saturated, is also partly hydrolyzed at a pH of about 5.

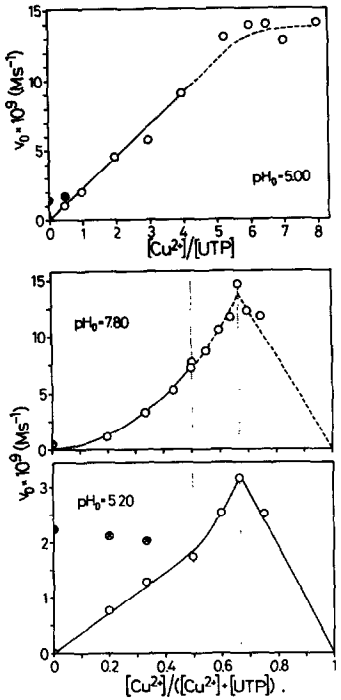

Fig. 10. Upper part: Dependence of the initial rate v_0 (M s^{-1}) for the Cu^{2+}-promoted dephosphorylation of UTP in water on the ratio $[Cu^{2+}]/[UTP]$ with $[UTP]_{tot} = 10^{-3}$ M at pH_0 5.00. Lower parts: Job's series for the aqueous Cu^{2+}/UTP system at pH_0 7.80 and 5.20 at $[Cu^{2+}]_{tot} + [UTP]_{tot}$ = constant = 2×10^{-3} M. The vertical dotted lines give the positions of the ratios Cu^{2+} : UTP = 1 : 1 or 2 : 1 (see text). For all three parts, $I = 0.1$ M, $NaClO_4$; 50 °C. The measured points (⊗) were corrected for the dephosphorylation rate of uncomplexed UTP by assuming that the 1 : 1 complex, $Cu(UTP)^{2-}$, is completely formed. The broken line portions indicate uncertainty due to precipitation. This figure is a combination of the data given in Figs. S5 and S6 in ref. 71.

Indeed, this view is supported by an evaluation of the slope of the pH–rate profile for the 2 : 1 systems in Fig. 6. A plot of log k vs. log $[H^+]$ for these 2 : 1 systems gives a straight line in the pH range 5–6 with a slope of -1, indicating that the reaction rate is proportional to $1/[H^+]$, i.e. proportional to $[OH^-]$ [71]. As this proportionality is connected with the presence of Cu^{2+}, this means, in agreement with Section D(ii), that the nucleophile is intramolecularly provided by a $Cu(OH)^+$ unit. Hence, on the basis of the arguments presented so far the most reactive species is best formulated as a monomeric but binuclear $M_2(R\text{–}TP)(OH)^-$ species.

This conclusion is confirmed by the following reasoning (see for example ref. 103), which in fact was already used for the deduction of $v_0 \propto 1/[H^+]$

given above. For any reaction

$$aA + bB + cC + \ldots \longrightarrow \text{products} \tag{5}$$

the reaction rate v is given by

$$v = k[A]^a[B]^b[C]^c \ldots \tag{6}$$

Transformed into a logarithmic form, one obtains eqn. (7):

$$\log v = \log k + a \log [A] + b \log [B] + c \log [C] + \ldots \tag{7}$$

If in an experiment the concentrations of all reactants, except A, are kept constant, all corresponding terms also become constant and eqn. (7) simplifies to the straight-line equation (eqn. 8):

$$\log v = \log k' + a \log [A] \tag{8}$$

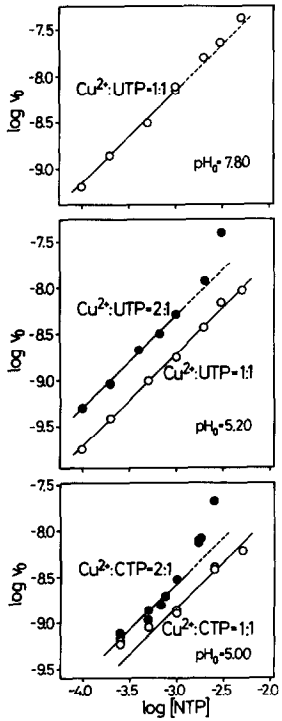

Fig. 11. Relationship between the initial dephosphorylation rates v_0 (M s^{-1}) of UTP (upper and middle parts) or CTP (lower part) and the total concentrations of Cu^{2+} and NTP in aqueous solution at different values of pH_0. Dependence of log v_0 on log $[NTP]_{tot}$ = log $[Cu^{2+}]_{tot}$ (○) or log $[NTP]_{tot}$ = log $(1/2[Cu^{2+}]_{tot})$ (●); I = 0.1 M, $NaClO_4$; 50 °C. The solid lines are drawn with the slope $m = 1$ (see text); the broken line portions indicate the regions of uncertainty due to precipitation. This figure is a combination of the data given in Figs. 4 and 11 in refs. 71 and 64 respectively.

Hence the relation between the initial rate v_0 and the concentration of M^{2+}/R–TP may be determined from a series of experiments in which the concentration of M^{2+}/R–TP is varied, but all the other conditions are kept constant. This means, if according to eqn. (9)

$$\log v_0 = \log k' + a \log [M^{2+}/R\text{–}TP] \tag{9}$$

$\log v_0$ is plotted vs. log [R–TP] for experiments with $[M^{2+}]:[R\text{–}TP] = 1:1$ or 2:1, the slope $m = a$ of the straight lines gives the order of the corresponding reaction. From the results of experiments summarized in Fig. 11 it is seen that in all cases the data [64,71] fit straight lines with a slope of unity, i.e. the dephosphorylation reaction proceeds in the 1:1 and 2:1 systems via monomeric complexes. The corresponding result has been obtained [40] for the Ni^{2+}/UTP and Zn^{2+}/UTP systems.

(iv) The dephosphorylation process and structure of the most reactive species in M^{2+}/R–TP systems

From pH 2 to 8 all Cu^{2+}/R–TP 1:1 systems display virtually identical pH–rate profiles (Figs. 5–7); the same is true for the corresponding Zn^{2+} and Ni^{2+} systems in the pH ranges 2–9 and 2–10 respectively [71]. Comparison of these results with the species distributions as a function of pH given in Figs. 7 and 8 shows that above pH 5, 6 and 6.5 the degrees of formation of $Cu(R\text{–}TP)^{2-}$, $Zn(R\text{–}TP)^{2-}$ and $Ni(R\text{–}TP)^{2-}$ are high, and that therefore the dephosphorylation in the 1:1 solutions with Cu^{2+}, Zn^{2+} and Ni^{2+} may be assigned to nucleophilic water attack on the $M(R\text{–}TP)^{2-}$ complexes in the pH ranges 5–6, 6–7 and 6.5–8 respectively.

The specific rate constant for water attack on $Cu(R\text{–}TP)^{2-}$ was estimated as $k_6 \approx 1.5 \times 10^{-6}$ s^{-1} [65]; the rate constants' subscripts define again the pH (see Section C(i)). Estimation of the corresponding specific rate constants, based on Figs. S1 and S2 in ref. 71 and on Figs. 7 and 8 in Section D(i) by including also the Cd^{2+}/CTP 1:1 system, gives $k_6 \approx 1.3 \times 10^{-6}$ s^{-1} for $Cd(R\text{–}TP)^{2-}$, $k_6 \approx 0.7 \times 10^{-6}$ s^{-1} for $Zn(R\text{–}TP)^{2-}$, and $k_7 \approx 0.5 \times 10^{-6}$ s^{-1} for $Ni(R\text{–}TP)^{2-}$. All these rate constants are rather similar; they differ only within a factor of three. The values decrease in the order $Cu^{2+} > Cd^{2+} > Zn^{2+} > Ni^{2+}$, which is also the order of the metal ion substitution rates [13,104]. Hence this might indicate that part of the reaction proceeds by intramolecular water attack, as has been suggested for other systems [99–101,105] (however, see Section E(iv)), but the given order could also be connected with rearrangement equilibria (see for example eqns. (10) and (11)) leading to $M_2(R\text{–}TP)$ species (see also the related discussion in Section G). In any case, all these values are close to that given in Section C(i) for water attack on the free $H(R\text{–}TP)^{3-}$ species ($k_4 = 1.2 \times 10^{-6}$ s^{-1}), which

confirms that $M(R-TP)^{2-}$ complexes are not very reactive with regard to R–TP dephosphorylation.

A significant metal ion promotion of the R–TP dephosphorylation is observed in the pH range where hydroxo complexes form (Section D(ii); Figs. 7 and 8). The most pertinent points from the preceding sections in this respect are the following: Job's series show that the most reactive species has a Cu^{2+} : R–TP composition of 2 : 1 (Fig. 10); this together with the result in Fig. 11 that this species is of a monomeric nature and that evaluation of the pH–rate profile for the 2 : 1 systems in the pH range 5–6 of Fig. 6 provides evidence for $v_0 \propto [OH^-]$ gives for the most reactive species the composition $M_2(R-TP)(OH)^-$.

The reaction scheme with the probable structure of the reactive complex and its reaction mode is depicted in Fig. 12 [71]. The coordination of one metal ion to a triphosphate leads commonly to $(\alpha),\beta,\gamma$ coordination [11,17,18,106–109]. In Fig. 12 it is proposed that the coordination of a second metal ion forces one metal ion to the γ-phosphate group (which is the most basic site) and the other into the α,β position, thus causing a labilization of the γ group (see also Section I). In addition, it should be emphasized that evidence has already been given in Sections D(ii) and D(iii) for an intramolecular nucleophilic attack by coordinated OH^- at the terminal phosphate group in the most reactive species in M^{2+}/R–TP systems, and this conclusion is confirmed by arguments based on specific rate constants as outlined in ref. 65.

For the reactivity observed in M^{2+}/R–TP 1 : 1 systems in the alkaline pH range (Figs. 6–8), the situation as given in Fig. 12 offers two explanations.

(a) The $(\alpha),\beta,\gamma$-chelated metal ion of $M(R-TP)^{2-}$ releases partly in an intramolecular equilibrium the $(\alpha),\beta$ group(s) with formation of the $M(R-TP)(OH)^{3-}$ hydroxo complex; the same release could partially also occur in

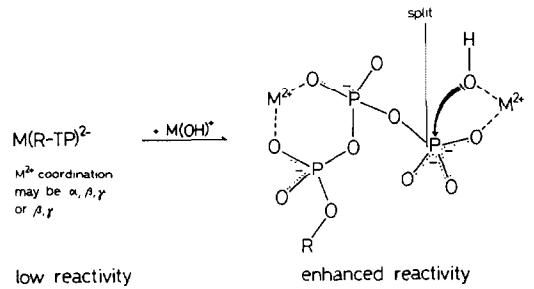

Fig. 12. Probable structure of the reactive complex formed during the metal ion promoted dephosphorylation of organic triphosphates (R–TP) undergoing only a metal ion–phosphate coordination like methyltriphosphate or (most) pyrimidine-nucleoside 5′-triphosphates. (Reproduced from Fig. 5 in ref. 71 (Eur. J. Biochem., 1983) with permission.)

already formed $M(R\text{–}TP)(OH)^{3-}$ complexes. Such a species with an $M(OH)^{+}$ unit coordinated to the γ group, the α,β groups being free, should also show some reactivity.

(b) The positions of the equilibria

$$2M(R\text{–}TP)(OH)^{3-} \rightleftharpoons M_2(R\text{–}TP)(OH)^{-} + R\text{–}TP^{4-} + OH^{-} \quad (10)$$

$$M(R\text{–}TP)(OH)^{3-} + M(R\text{–}TP)^{2-} \rightleftharpoons M_2(R\text{–}TP)(OH)^{-} + R\text{–}TP^{4-} \quad (11)$$

may be such that a small percentage of $M_2(R\text{–}TP)(OH)^{3-}$ is formed. As the reactivity of the 2 : 1 complexes is larger than that of the 1 : 1 species (see for example, Fig. 10), the formation of relatively small amounts of $M_2(R\text{–}TP)(OH)^{3-}$ would be enough to explain the observed reactivity.

It is evident that either explanation (a) or (b), or a combination of both could actually be responsible for the observed reactivity.

Possible reasons for the efficiency differences observed between the metal ions employed in the M^{2+}/R–TP systems regarding the dephosphorylation reaction will be discussed in Section G.

E. THE METAL ION FACILITATED DEPHOSPHORYLATION OF ADENOSINE 5′-TRIPHOSPHATE (ATP)

In discussing the results in Fig. 5 it was pointed out in Section C(ii) that the promotion of the dephosphorylation reaction by Cu^{2+} is most effective in the case of ATP; the reactivity of the Cu^{2+}/NTP 1 : 1 systems decreases in the order ATP > GTP > ITP > pyrimidine-NTPs. The properties of the pyrimidine-NTP systems correspond to those of simple triphosphate monoesters with a non-coordinating terminal organic residue (R–TP), which in the simplest case is a methyl group. Therefore the R–TP systems were considered first (Section D); next, the properties of the most reactive nucleotide, ATP, will be discussed. It is evident from the structures in Fig. 1 and the kinetic results in Fig. 5 that the dephosphorylation reaction of ATP in the presence of metal ions must be influenced by the adenine residue.

(i) Comparison of the effect of different metal ions on the dephosphorylation of ATP

Considering the remarkable properties of the Cu^{2+}/ATP 1 : 1 system in Fig. 5, it is appropriate to compare first these properties with those of other M^{2+}/ATP systems. In Fig. 13 examples of first-order rate constants, k (s^{-1}), for the dephosphorylation of ATP in the presence of Ni^{2+}, Cu^{2+}, Zn^{2+} or Cd^{2+} are plotted as a function of pH [64,65]. The corresponding results are given for the Mn^{2+}/ATP 1 : 1 system in the upper part of Fig. 14

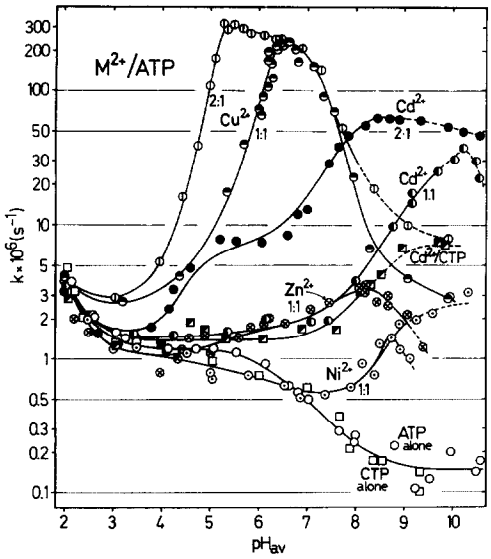

Fig. 13. First-order rate constants k (s^{-1}) for the dephosphorylation of ATP in aqueous solution as a function of pH: ATP alone (○), Ni^{2+} : ATP = 1 : 1 (⊙, regarding the extension of the two broken line portions see text in Section E(i)), Cu^{2+} : ATP = 1 : 1 (◓), Zn^{2+} : ATP = 1 : 1 (⊗), Cd^{2+} : ATP = 1 : 1 (◐), and Cu^{2+} : ATP = 2 : 1 (⊕) or Cd^{2+} : ATP = 2 : 1 (●). For comparison the corresponding data are also given for CTP alone (□) and Cd^{2+} : CTP = 1 : 1 (◩). $[NTP]_{tot} = 10^{-3}$ M; $I = 0.1$ M, $NaClO_4$; 50 °C. The broken line portions indicate uncertainty due to precipitation. This figure combines part of the results of Figs. 2 and 3 in refs. 64 and 65 respectively.

[66]; the lower part of this figure shows the influence of pH on the concentration of the species present in a 10^{-3} M aqueous solution of Mn^{2+} and ATP. These distribution curves for the Mn^{2+}/ATP 1 : 1 system in the lower part of Fig. 14 are to a large extent also representative of the situation in the corresponding systems with Ni^{2+}, Zn^{2+} or Cd^{2+}; at least as far as the degree of formation of $M(ATP)^{2-}$ is concerned (see also Fig. 18C; vide infra), as the stabilities of $Ni(ATP)^{2-}$, $Zn(ATP)^{2-}$ and $Cd(ATP)^{2-}$ are quite alike [17,61]. The stability of $Cu(ATP)^{2-}$ is somewhat higher and that of $Mg(ATP)^{2-}$ somewhat lower [17,61], but still the maximal degree of formation of $M(ATP)^{2-}$ differs only little in 10^{-3} M solutions of M^{2+} and ATP: it reaches about 80%, 90% and 95% for $Mg(ATP)^{2-}$, $Zn(ATP)^{2-}$ and $Cu(ATP)^{2-}$ respectively. It is evident that the different promotional effects of the metal ions on ATP dephosphorylation in the pH range of about 5–8 cannot be explained by different degrees of formation of the $M(ATP)^{2-}$ species.

From the initial rates of ATP dephosphorylation, v_0 (M s^{-1}), collected in Table 1, it follows that Mg^{2+} is the poorest promoter and that Mn^{2+} is not

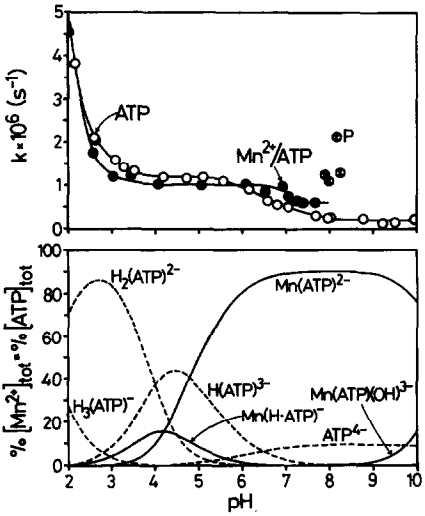

Fig. 14. Upper part: First-order rate constants, k (s^{-1}), for the dephosphorylation of ATP (○) and ATP in the presence of one equivalent Mn^{2+} (●) in aqueous solution as a function of pH [66]; $[ATP]_{tot} = 10^{-3}$ M; $I = 0.1$ M, $NaClO_4$; 25 °C. Results from solutions in which Mn^{2+} was partially oxidized to Mn^{3+} (see text in Section E(i)) are also shown (⊛); P indicates precipitation. Lower part: Effect of pH at 25 °C ($I = 0.1$ M, $Na^+ ClO_4^-/NO_3^-$) on the concentration of the species present in an aqueous solution of Mn^{2+} and ATP (each 10^{-3} M); the results are given as the percentage of the total Mn^{2+} present (equal to total ATP); the broken lines refer to the free ATP species and the solid lines to the ATP complexes. The results were computed with the following equilibrium constants: $pK^{H}_{H_3(ATP)} \approx 1.6$ [72], $pK^{H}_{H_2(ATP)} = 4.00 \pm 0.01$, $pK^{H}_{H(ATP)} = 6.47 \pm 0.01$, $\log K^{Mn}_{Mn(H \cdot ATP)} = 2.74 \pm 0.06$, $\log K^{Mn}_{Mn(ATP)} = 5.01 \pm 0.05$ (all values from ref. 61), $pK^{H}_{Mn(ATP)(H_2O)} = 10.7$ [73]. The diprotonated $Mn(H_2 \cdot ATP)$ complex was ignored in the calculations as the corresponding constant is unknown; however, such species would probably exist only below pH 3.

significantly better. With regard to biological systems this observation is important, as there are also conditions which allow Mg^{2+} to participate effectively in the reaction (see Section E(iv); Fig. 19). At pH below 6, Ni^{2+}, Zn^{2+} and Cd^{2+} show no significant promotion of the reaction, although Cd^{2+} especially becomes a good promoter in the alkaline pH region. By far the most effective is Cu^{2+}: at pH 6.5 it promotes the dephosphorylation of ATP in the 1 : 1 system by a factor of about 300 (see also Section J).

The mentioned low reactivity of the Mg^{2+} and Mn^{2+} systems is in agreement with the earlier conclusion [34,64] about the importance of the M^{2+}–N-7 interaction; the direct form of this interaction is very low in $Mg(ATP)^{2-}$ and reaches only about 10% in $Mn(ATP)^{2-}$ [17,61]. In the other $M(ATP)^{2-}$ complexes mentioned, macrochelate formation is more pronounced [17,61]; hence the M^{2+}–N-7 interaction is certainly an important aspect but it cannot be the only one as this interaction does not differ

TABLE 1

Comparison of the initial rate of dephosphorylation, v_0 (M s^{-1}), of ATP in 10^{-3} M solutions in the presence of equivalent amounts of several metal ions ($I = 0.1$, $NaClO_4$; 50 °C). All initial rates are given as $v_0 \times 10^8$. (This table is reprinted from the "Supplementary Material" (Table S1) of ref. 65 (J. Am. Chem. Soc., 1984) by permission of the American Chemical Society.)

M^{2+}	$v_0 \times 10^8$ for $[M^{2+}]:[ATP] = 1:1$		
	pH_0 5.5	pH_0 7.5	pH_0 9.5
None	0.11	0.032	0.015
Mg^{2+}	0.096	0.045	0.039
Mn^{2+}	0.10	0.060	– [a]
Ni^{2+}	0.075	0.05	0.2 [b]
Cu^{2+}	2.5	7.5	0.34
$Cu(Bpy)^{2+}$	0.060	0.052	0.1
Zn^{2+}	0.15	0.25	0.1 [b]
Cd^{2+}	0.15	0.25	2.4

[a] Precipitation occurs and the rate increases drastically due to partial oxidation of Mn^{2+} to Mn^{3+} (see ref. 66 and Fig. 14). [b] This value is an estimation due to trace amounts of precipitation.

enough for these metal ions to explain the results in Figs. 13 and 14 and in Table 1. However, the promoting role of the adenine residue is confirmed by a comparison of the reaction rates in the alkaline pH range of the Cd^{2+}/ATP and Cd^{2+}/CTP 1:1 systems in Fig. 13.

A further important difference between the metal ions considered is their tendency to form hydroxo complexes [65]:

$$M(ATP)^{2-}_{(aq)} \rightleftharpoons M(ATP)(OH)^{3-} + H^+ \qquad (12)$$

Indeed, the values of $pK^{H}_{M(ATP)(H_2O)}$ follow the order Cu^{2+} (8.2) < Zn^{2+} (8.9) < Ni^{2+} (9.4) < Cd^{2+} (10.1) < Mn^{2+} (10.7) < Mg^{2+} (> 11) [55,73,88]. This order parallels exactly the order of the pH values at which the maximum rates of dephosphorylation are observed at the M^{2+}/ATP 1:1 ratio, despite the fact that the maximum in the Ni^{2+}/ATP system is obscured due to precipitation (Fig. 13). These results indicate that in the reactive complex an $M(OH)^+$ unit is involved, just as has been concluded for the M^{2+}/R–TP systems in Section D. However, it is also evident, by comparing the given values of $pK^{H}_{M(ATP)(H_2O)}$ with the peaks in Fig. 13, that too much hydroxo complex formation inhibits the reaction, a problem to be addressed further in Section E(iii).

In connection with the preceding paragraph the dephosphorylation of ATP in the presence of Mn^{2+} warrants some further comments (Fig. 14). Reliable measurements could in this case only be carried out in the pH

range below 8 [66]. At higher pH, Mn^{2+} is oxidized to Mn^{3+}, a reaction which is favored by the presence of phosphates [92,110,111] and which could not be completely prevented by flushing N_2 through the solutions [66]; they still turned slightly yellowish. However, this change in the oxidation state of manganese from II to III does not only enhance its affinity for phosphate groups but also its tendency to form hydroxo complexes, and this is presumably the reason for the steep increase in the dephosphorylation rate (see also Section L).

(ii) Metal ion composition of the reactive species, and relation between the rate of dephosphorylation and the concentration of M^{2+}/ATP

Figure 13 contains, besides the pH–rate profiles of 1:1 systems, two examples of pH–rate profiles for 2:1 systems, i.e. with Cu^{2+} and Cd^{2+}. In

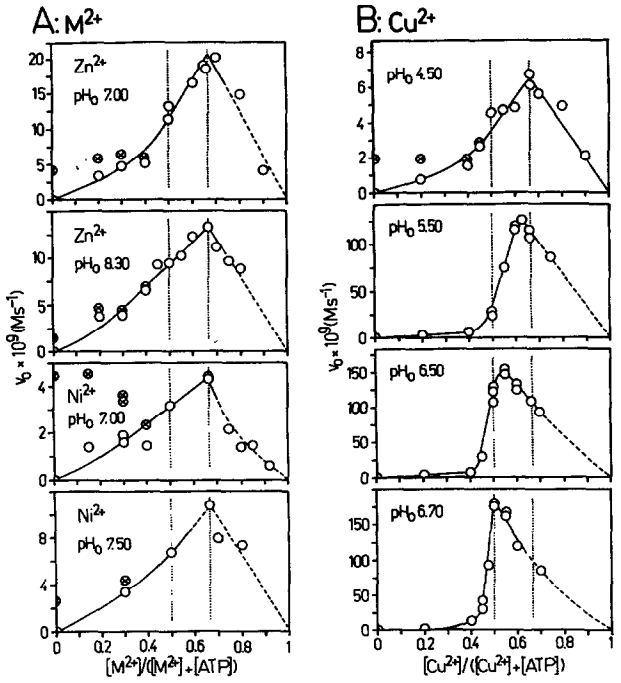

Fig. 15. Job's series for aqueous M^{2+}/ATP systems at different values of pH_0 ($I = 0.1$ M, $NaClO_4$; 50 °C). The vertical dotted lines give the positions of the ratios M^{2+} : ATP = 1:1 or 2:1 (see text). The broken line portions indicate uncertainty due to precipitation. The measured points (⊗) were corrected for the dephosphorylation rate of uncomplexed ATP by assuming that the corresponding 1:1 complex, $M(ATP)^{2-}$, is completely formed. A, for the Zn^{2+} or Ni^{2+}/ATP systems: $[M^{2+}]_{tot} + [ATP]_{tot}$ = constant = 5×10^{-3} M. B, $[Cu^{2+}]_{tot} + [ATP]_{tot}$ = constant = 2×10^{-3} M. This figure is a combination of the results given in Figs. 6 and 7 in ref. 64.

both cases the 2 : 1 systems are mostly more reactive and the onset of the promotion occurs always at a lower pH compared with that in the 1 : 1 systems [65]. The corresponding observation has also been made with the Ni^{2+}/ATP and Zn^{2+}/ATP 2 : 1 systems [64], as well as with the M^{2+}/R–TP systems (Section D).

Experiments carried out according to Job's method of continuous variation (see Section D(iii)) help to clarify the situation; some examples of such plots are shown in Fig. 15. The experiments with the Ni^{2+} and Zn^{2+} systems [64] prove that the most reactive species has two metal ions bound to ATP. The corresponding experiments with Cd^{2+}/ATP at pH_0 7.20, 8.20 and 9.00 confirm this result (supplementary material from ref. 65). In fact the formation of M_2(NTP) species is well known [13,64,112–115] and also in accord with the results in Section D.

Close examination of the pH–rate profiles in Fig. 13 for the Cu^{2+}/ATP 2 : 1 and 1 : 1 systems indicates that the situation with this metal ion might be more complicated because in the pH range from about 6.3 to 8 both systems show the same dephosphorylation rate, indicating that the second equivalent of Cu^{2+} might not participate in the reaction in this pH region. Indeed, the experimental data in Fig. 16 support the view that the Cu^{2+} : ATP ratio in the active species depends on the pH. The final proof that this assumption is correct is seen from the Job's series in Fig. 15B. It is clear that

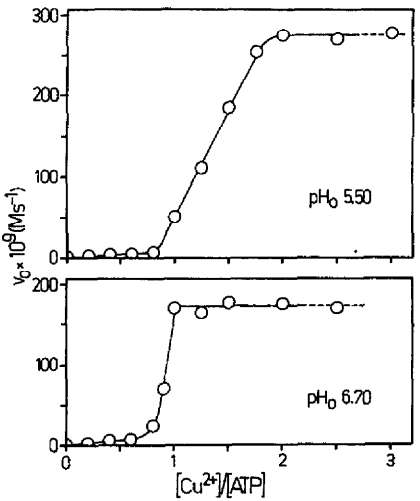

Fig. 16. Dependence of the initial rate v_0 (M s^{-1}) for the Cu^{2+}-promoted dephosphorylation of ATP in water on the ratio $[Cu^{2+}]/[ATP]$ with $[ATP]_{tot} = 10^{-3}$ M ($I = 0.1$ M, $NaClO_4$; 50 °C). The broken line portions indicate uncertainty due to precipitation. (Reproduced from Fig. 4 in ref. 64 (J. Am. Chem. Soc., 1976) with permission of the American Chemical Society.)

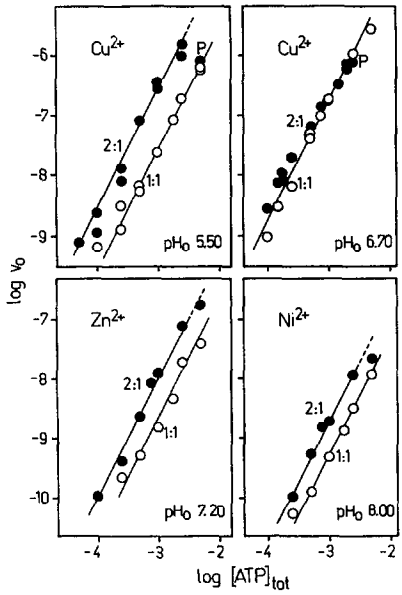

Fig. 17. Relationship between the initial dephosphorylation rates v_0 (M s^{-1}) of ATP and the total concentrations of M^{2+} and ATP in aqueous solution for different metal ions at various values of pH_0. Dependence of log v_0 on log $[ATP]_{tot}$ = log $[M^{2+}]_{tot}$ (○) or log $[ATP]_{tot}$ = log $(1/2[M^{2+}]_{tot})$ (●); $I = 0.1$ M, $NaClO_4$; 50 °C. The solid lines are drawn with the slope $m = 2$ (see text); the broken line portions indicate uncertainty due to precipitation. In the experiments labeled P, precipitation was also observed. (Reproduced from Fig. 9 in ref. 64 (J. Am. Chem. Soc., 1976) with permission of the American Chemical Society.)

the most reactive species at pH 4.5 contains Cu^{2+}/ATP in the ratio 2:1, and at pH 6.7 in the ratio 1:1. This observation is unique for Cu^{2+}/ATP among the systems studied and will be discussed further in Section E(v). It may be added that a Job's series at pH 8.5 gave no clear results owing to precipitation [64].

Experiments based on the reasoning indicated in Section D(iii) in connection with eqns. (5)–(9) showed that the rate of dephosphorylation depends on the square of the reactant concentration in the M^{2+}/ATP 1:1 as well as in the 2:1 systems [64,65]. Some examples of the corresponding plots with log v_0 vs. log $[ATP]_{tot}$ are shown in Fig. 17; analogous results were obtained for Cd^{2+}/ATP at pH_0 7.20, 8.20 and 9.20 (supplementary material from ref. 65).

There is one further point. Since the most reactive species contain M^{2+} and ATP in the ratio 2:1, one may expect that under the conditions with M^{2+}/ATP in the ratio 0.5:1 the reactivity will be considerably reduced. With Cu^{2+} being the most effective promoter (Fig. 13), this expectation was checked [65] and confirmed in 10^{-3} M ATP solutions (see also Fig. 22; vide

infra). However, plots of log v_0 vs. log $[ATP]_{tot}$ at pH_0 6.70 and 7.60 showed that even under an unfavorable Cu^{2+}/ATP 0.5 : 1 condition, all experimental data still fit on straight lines with a slope of two (supplementary material from ref. 65).

Hence under all conditions and for all M^{2+}/ATP systems studied [64,65] the dephosphorylation rate depends on the square of the reactant concentration, which may be rationalized with the monomer–dimer equilibria given in eqns. (13) and (14):

$$2M(ATP)^{2-} \rightleftharpoons [M(ATP)]_2^{4-} \tag{13}$$

$$2M_2(ATP) \rightleftharpoons [M_2(ATP)]_2 \tag{14}$$

Assuming both equilibria are far to the left, then the dimer concentration will be proportional to the square of the total concentration because $K_D = [\text{dimer}]/[\text{monomer}]^2$. Consequently, if the dimers are the reactive complexes, the slopes of the plots log v_0 vs. log $[\text{reactant}]_{tot}$ will be two while for the monomer as the reactive species it would be unity. Indeed, self-association via aromatic ring stacking of ATP and other nucleotides is well known [28,60,72,116,117], and it is evident that the dimer in this process is on the way from the monomer to an oligomer. Calculations based on known equilibrium constants indicate [65] that under the conditions of the experiments (for example Fig. 17) about 85% or more of the total ATP is present as the monomer, i.e. the dimer is indeed always a minority species as required by the above considerations.

The result that the most efficient promotion of the dephosphorylation reaction of ATP by M^{2+} proceeds via dimeric complexes is important, and it contrasts with the metal ion facilitated dephosphorylation of R–TPs, including the pyrimidine-NTPs, in which the rate-determining step always occurs in a monomeric intermediate (Section D and Fig. 12). It is therefore appropriate to summarize in this connection also some ^1H NMR shift experiments which prove self-association via nucleic base stacking of ATP and of some of its complexes [60,117]. The variation of the upfield shifts for H-2 and H-8 of the adenine residue and H-1′ of the ribose ring as a function of the concentration can be well described for ATP^{4-} [60,72] and $Mg(ATP)^{2-}$ [28,60] by the isodesmic model of indefinite non-cooperative self-association. This model is based on the assumption that, for example, for $Mg(ATP)^{2-}$, the equilibria (15) are all characterized by the same equilibrium constant (eqn. (16)):

$$[Mg(ATP)]_n^{2n-} + Mg(ATP)^{2-} \rightleftharpoons [Mg(ATP)]_{n+1}^{(2n+2)-} \tag{15}$$

$$K = [(Mg(ATP))_{n+1}]/[(Mg(ATP))_n][Mg(ATP)] \tag{16}$$

As expected, owing to the difference in charge (see ref. 28), self-association

is more pronounced for $Mg(ATP)^{2-}$ than for ATP^{4-}, but there is, also as expected, no indication of a direct M^{2+}–N-7 interaction in the $Mg(ATP)^{2-}$ system [17,28,60]. Its properties of self-stacking are therefore representative for those systems in which also no M^{2+}–N-7 interaction occurs, as in $Ca(ATP)^{2-}$.

By ^1H NMR shift measurements the self-association of $Zn(ATP)^{2-}$ or $Cd(ATP)^{2-}$ is also easily demonstrated, but the calculations [60] show that the self-association is considerably more pronounced and also that the above-mentioned simple isodesmic model is inadequate to explain the experimental data. However, a model which, owing to an intermolecular bridge by a metal ion coordinated to the phosphate residue of one ATP and to the base moiety of the neighbor, especially favors the formation of dimers

$$2M(ATP)^{2-} \rightleftharpoons [M(ATP)]_2^{4-} \tag{17}$$

and which also allows that these metal-ion-bridged dimers stack with each other as well as with monomeric $M(ATP)^{2-}$

$$[M(ATP)]_2^{4-} + [M(ATP)]_n^{2n-} \rightleftharpoons [M(ATP)]_{2+n}^{(4+2n)-} \tag{18}$$

is able to explain the experimental observations. The downfield shifts observed for H-8 of self-associated $[Zn(ATP)^{2-}]_\infty$ and $[Cd(ATP)^{2-}]_\infty$ in comparison with $[Mg(ATP)^{2-}]_\infty$ (see Table 2) prove bridge formation under participation of N-7. Indeed, these results confirm the previous deduction [64], based on several indirect hints and observations, that in the dimer the

TABLE 2

Evidence from ^1H NMR shift experiments [a] for an M^{2+}–N-7 interaction in monomeric $M(ATP)^{2-}$ and in self-stacked $[M(ATP)]_n^{2n-}$ complexes, from a comparison of the chemical shifts (ppm) of H-8 between monomeric (δ_0 at $I = 0.1$, $NaNO_3$) and between completely stacked, i.e. polymeric, (δ_∞ at $I \approx 2$) species in D_2O at 27 °C

System	Monomers		Polymers	
	δ_0 of H-8	Downfield shift [b] $\Delta\delta_0$	δ_∞ of H-8	Downfield shift [b] $\Delta\delta_\infty$
ATP^{4-}	8.563 ± 0.004		7.92 ± 0.06	
$Mg(ATP)^{2-}$	8.527 ± 0.009		8.02 ± 0.04	
$Zn(ATP)^{2-}$	8.61 ± 0.01 [c]	0.08 ± 0.02	8.36 ± 0.06	0.34 ± 0.10
$Cd(ATP)^{2-}$	8.74 ± 0.01 [c]	0.21 ± 0.02	8.49 ± 0.08	0.47 ± 0.12

[a] The data are abstracted from Tables III, IV and V of ref. 60. The errors given with the chemical shifts, δ, are twice the standard deviation. [b] Shift difference $\Delta\delta$ for H-8 between the data for $Zn(ATP)^{2-}$ or $Cd(ATP)^{2-}$ and those for $Mg(ATP)^{2-}$. The errors given are the sum of the errors of the values used for the calculation of $\Delta\delta$. [c] Graphically extrapolated values; the error is estimated.

two adenine bases are stacked and that metal ions bridge the two ATPs by coordinating to the phosphate chain of one ATP and to the N-7 of the other. It may be added that in monomeric $Zn(ATP)^{2-}$ and $Cd(ATP)^{2-}$, N-7 also participates in complex formation as is evident from the data in Table 2, i.e. macrochelates are formed by coordination of a metal ion to the phosphate chain and to N-7 of the same ATP^{4-}. These macrochelates are well quantified today [17,61] and it is certainly fair to assume that all those metal ions which form such monomeric macrochelates, like Co^{2+}, Ni^{2+} or Cu^{2+}, are also able to promote under higher reactant concentrations the formation of $[M(ATP)]_2^{4-}$ dimers by an intermolecular bridge of the kind described.

In summary, the adenine residue itself is responsible for self-stacking and this property distinguishes ATP a priori from the R–TP systems (Section D). Furthermore, certain metal ions with a relatively pronounced affinity for N sites, such as Zn^{2+} or Cd^{2+}, are able to favor especially the formation of dimeric stacks. This together with the results of Job's series leads so far to the conclusion that the most reactive species which occurs in low concentration in the dephosphorylation process has the composition $[M_2(ATP)]_2$, except in the case of Cu^{2+} where in a limited pH range also a species of the composition $[Cu(ATP)]_2^{4-}$ is quite reactive. Finally, from the discussion in Section E(i) it became apparent that an $M(OH)^+$ unit also plays a role in the reaction; this last problem is addressed in the following section.

(iii) Interplay between hydroxo complex formation and the reaction rate in M^{2+}/ATP systems

In the metal ion promoted dephosphorylation of those triphosphate systems in which no M^{2+}–N-7 interaction occurs, the most reactive species has the composition $M_2(R–TP)(OH)^-$ (Fig. 12), and consequently the reaction rate levels off at about that pH at which the hydroxo complex $M(R–TP)(OH)^{3-}$ is fully developed, as is well seen for Cu^{2+}/CTP in Figs. 5–7 and for Cd^{2+}/CTP in Figs. 8 and 13. An alteration occurs only in those M^{2+}/R–TP systems which undergo a side-reaction, such as the ionization at N-3 in UTP or TTP, with increasing pH. This means that the pH–rate profiles of the M^{2+}/ATP as well as of the other purine-NTP systems differ in an important aspect: in all cases the dephosphorylation rate reaches a *maximum* at a certain pH (see for example Figs. 5 and 13). Hence the implications from the ascending as well as from the descending sides of the peaks in the pH–rate profiles now need to be discussed [65].

For example, unbound Cd^{2+} in a 2 mM solution begins to hydrolyze, i.e. forms hydroxo species, at pH about 7–7.5; therefore a partial hydrolyzation is also expected in a Cd^{2+}/ATP 2 : 1 system (Fig. 13), because ATP^{4-} is not able to saturate the coordination spheres of both Cd^{2+} ions. Indeed,

evaluation of the ascending side of the 2 : 1 pH–rate profile by a plot of log k vs. log $[H^+]$ (see reasoning in Section D(iii) in connection with eqns. (5)–(9)) gives a straight line in the pH range 7–8 with a slope close to -1, indicating that a $Cd(OH)^+$ unit is involved. Similar properties are expected for other metal ion systems, and in fact plots of log k (or log v_0) vs. pH give for a certain pH range on the ascending side of the peak (Figs. 5 and 13) the following results. A slope of unity is observed for the Cu^{2+}/ATP 1 : 1 system [55]; for the corresponding systems with Zn^{2+}, Ni^{2+} or Cd^{2+} the slopes are somewhat below unity, while for the 2 : 1 systems the slope in the case of Cu^{2+} is slightly larger than unity; it is about unity for Cd^{2+}, as mentioned above, and for Zn^{2+} and Ni^{2+} it is somewhat less than unity. A slope of unity means that the reaction rate is proportional to $1/[H^+]$, i.e. to $[OH^-]$, while a slope below unity indicates that also H_2O acts as a nucleophile [66]; a slope larger than unity is only observed in the Cu^{2+} 2 : 1 system, indicating that two reactive sites are present in the reactive dimeric intermediate (see Fig. 20 in Section E(v)).

That the ascending sides of the peaks are observed in different pH ranges in the individual systems, despite the fact that above pH 5.5 the degree of formation of $M(ATP)^{2-}$ has always reached 80% or more (see the various figures with distribution curves), suggests that the metal ion is not simply needed for the neutralization of the negatively charged phosphate groups. This suggests in addition that the nucleophilic attack of OH^- is not intermolecular but intramolecular. This is further confirmed by the parellelism between reactive pH range and hydroxo complex formation as discussed in Section E(i), i.e. an $M(OH)^+$ unit is part of the reactive intermediate.

It is further evident that the peaks of the rates in the M^{2+}/ATP 2 : 1 systems (see for example Fig. 13) [64,65] occur always well before the pH equals the values of $pK^{H}_{M(ATP)(H_2O)}$ (eqn. (12)) for the corresponding $M(ATP)^{2-}$ complexes, i.e. well before $M(ATP)(OH)^{3-}$ reaches its maximum concentration. However, the descending sides of all peaks in the pH–rate profiles, be it a 2 : 1 or 1 : 1 system, correlate closely with the $pK^{H}_{M(ATP)(H_2O)}$ values (Section E(i)), indicating that the formation of $M(ATP)(OH)^{3-}$ is connected with a structural rearrangement which inhibits the reactivity. As the formation of mixed-ligand complexes with $M(ATP)^{2-}$ leads to a release of N-7 from the coordination sphere of the metal ion [87], the same could be surmised for $M(ATP)(OH)^{3-}$, which is indeed the case [88]. From the ^1H NMR shift experiments shown in Fig. 18B it is seen that with increasing concentration of $Cd(ATP)(OH)^{3-}$ (Fig. 18C) the shifts of H-2 and H-8 move back to the position in free ATP, showing a release of N-7 from the coordination sphere of Cd^{2+}, which is paralleled by a decreasing rate of dephosphorylation (Fig. 18A). This demonstrates well the interrelations

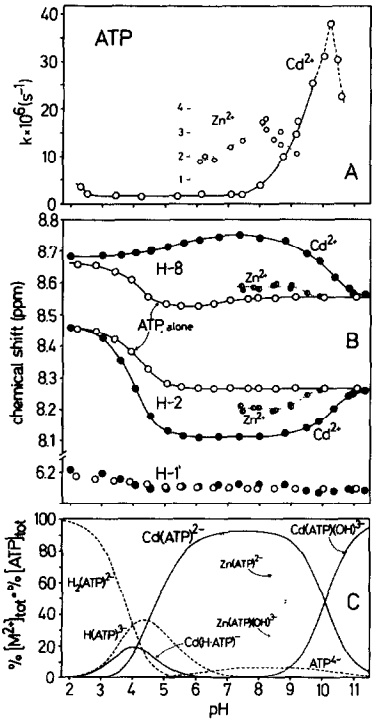

Fig. 18. Comparison of the variation of (A) the Cd^{2+}-promoted dephosphorylation of ATP (each 10^{-3} M) in aqueous solution at 50 °C as a function of pH ($I = 0.1$, $NaClO_4$; cf. Fig. 13), with (B) the chemical shift of H-2, H-8 and H-1′ in the ^1H NMR spectra of ATP (○; 5×10^{-3} M) and of ATP in the presence of Cd^{2+} (●; 1:1 ratio, 5×10^{-3} M) in D_2O at 27 °C ($I = 0.1$, $NaNO_3$) as a function of "pH" (i.e. no correction according to pD = pH meter reading +0.40 was applied, allowing direct comparisons of experiments carried out in H_2O and D_2O; cf. footnote 66 in ref. 65), and with (C) the effect of pH at 25 °C ($I = 0.1$ M, $NaNO_3$) on the concentration of the species present in an aqueous solution of Cd^{2+} and ATP (each 10^{-3} M); the results are given as the percentage of the total Cd^{2+} present (equal to total ATP). The broken lines indicate the free ATP species and the solid lines the ATP complexes. Further comparisons are shown with dotted lines inserted: (A) the Zn^{2+}-promoted dephosphorylation of ATP (note the fivefold expanded scale; cf. Fig. 13); (B) the chemical shift of H-2 and H-8 for Zn^{2+}/ATP (◐); and (C) the formation of $Zn(ATP)^{2-}$ and $Zn(ATP)(OH)^{3-}$. The experimental conditions for the measurements with Zn^{2+} correspond to those given for Cd^{2+}. Use of the recently revised set of equilibrium constants given in refs. 17 and 61 would not significantly alter the species distributions shown in part C. The threefold protonated $H_3(ATP)^-$ species (cf. Fig. 14, lower part) and the diprotonated $M(H_2 \cdot ATP)$ complexes were ignored in the calculations for part C; however, such species exist only below pH 3.5. (Reproduced from Fig. 4 in ref. 65 (J. Am. Chem. Soc., 1984) with permission of the American Chemical Society.)

between Cd^{2+}/N-7 release, $Cd(ATP)(OH)^{3-}$ formation and decreasing dephosphorylation rate (for further details, see ref. 65).

Changes in the chemical shifts by the coordination of Zn^{2+} to ATP^{4-} are less pronounced, but nevertheless it is evident from the dotted lines in Fig. 18 that all the conclusions outlined for Cd^{2+}/ATP are also valid for Zn^{2+}/ATP. Interestingly, substitution of Cd^{2+} for the native Zn^{2+} in human carbonic anhydrase B shifts the apparent pK_A for esterase activity from 7.0 in the native enzyme to 9.1 in the Cd^{2+}-substituted enzyme [118–120]. This shift corresponds exactly to the 2.1 pH units between the two peaks in Fig. 18A.

A comparison similar to that made for Cd^{2+} and Zn^{2+}/ATP in Fig. 18 is possible for Cu^{2+}/ATP by employing selective line-broadening ^1H NMR experiments (see Fig. 5 in ref. 65). These experiments confirm that N-7 becomes increasingly inaccessible for Cu^{2+} in the pH range from about 7.5 to 9, which agrees with the formation of $Cu(ATP)(OH)^{3-}$ ($pK^{H}_{Cu(ATP)(H_2O)}$ = 8.2 in 10^{-3} M solution [55]) and the descending side of the pH–rate profile (Figs. 5 and 13) of the dephosphorylation reaction.

To conclude, the results of this section confirm that the M^{2+}–N-7 interaction plays a crucial role in the formation of the reactive species of the M^{2+}-promoted ATP dephosphorylation and that an $M(OH)^+$ unit is involved. The results demonstrate further that an excess of OH^- destroys the reactive complex.

(iv) On the role of the second metal ion: effect of the addition of further M^{2+} on the reactivity of the Cu^{2+}/ATP 1 : 1 system

The Job's series described in Section E(ii) showed that in the Cu^{2+}/ATP system in the lower pH range a 2 : 1 complex is the most reactive species (Fig. 15B). This is also evident from the upper parts of Figs. 16 and 19, where it is seen that addition of 1 equivalent of Cu^{2+} to a Cu^{2+}/ATP 1 : 1 system at pH_0 5.50 promotes the reaction already to its maximum rate, indicating that this 2 : 1 complex is relatively stable but also very reactive. In order to learn more about the role of the second metal ion, the experiments shown in Fig. 19 were carried out [65]. To the Cu^{2+}/ATP 1 : 1 system, increasing amounts of Mg^{2+}, Ni^{2+}, Zn^{2+} or Cd^{2+} were added, as well as increasing amounts of the 1 : 1 complexes of Cu^{2+} and diethylenetriamine (Dien) or di(2-picolyl)amine (Dpa); $Cu(Dien)^{2+}$ and $Cu(Dpa)^{2+}$ are nearly 100% formed under the conditions used.

From the experiments at pH_0 5.50, shown in the upper part of Fig. 19, it follows that the addition of metal ions other than Cu^{2+} is less effective, although Zn^{2+} still promotes the activity of the Cu^{2+}/ATP 1 : 1 system considerably. As the second Cu^{2+} acts in the reactive complex in the form of

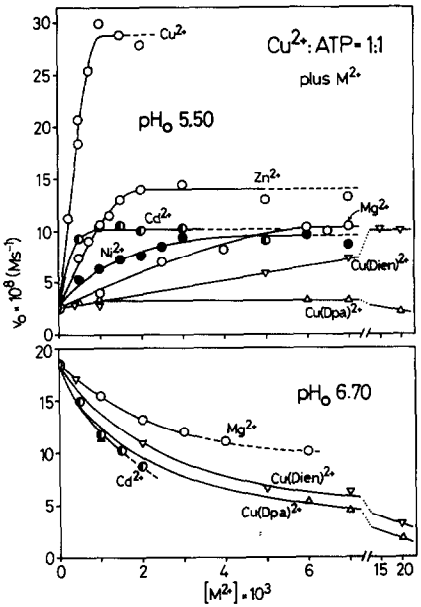

Fig. 19. Dependence of the initial rate, v_0 (M s^{-1}), of the Cu^{2+}-promoted dephosphorylation of ATP ($[Cu^{2+}]_{tot} = [ATP]_{tot} = 10^{-3}$ M) in aqueous solution on the addition of divalent metal ions (○, ◐, ●) or the Cu^{2+} 1:1 complexes with diethylenetriamine (Dien, ▽) and di(2-picolyl)amine (Dpa, △) at pH_0 5.50 (upper part) and 6.70 (lower part); $I = 0.1$, $NaClO_4$; 50 °C. The broken line portions indicate uncertainty due to precipitation. (Reproduced from Fig. 6 in ref. 65 (J. Am. Chem. Soc., 1984) with permission of the American Chemical Society.)

$Cu(OH)^+$ (see the discussion of slopes in Section E(iii)), it seems reasonable to assume that Zn^{2+} analogously acts in part as $Zn(OH)^+$ but that some reactivity in this system must also be attributed to a nucleophilic water attack. This latter assumption agrees with the properties of the systems containing Cd^{2+}, Ni^{2+} or Mg^{2+}; these ions also promote the reactivity but they do not form hydroxo complexes at pH 5.5; therefore they could only carry water as a nucleophile.

In agreement with the reasoning given in Section C(i) [65] regarding dephosphorylation of the free R–TP species it is also proposed here that water attack does not occur in an intramolecular fashion (as suggested for other systems [99–101,105]). This conclusion is based on the following arguments. (a) It is difficult to see why Cd^{2+}, Ni^{2+} and Mg^{2+} should "activate" or "position" the bonded attacking water molecule in exactly the same manner. It is easier to understand that they reach the same limiting value (see Fig. 19, upper part) by assuming the same structure of the reactive species and an intermolecular water attack. Different concentrations are

needed to reach the limiting rate value because these metal ions have somewhat different coordination tendencies toward phosphate groups (Cd^{2+} > Ni^{2+} > Mg^{2+} [17,61]). (b) $Cu(Dien)^{2+}$ also reaches the same limiting rate value even though there is no water molecule left in the equatorial coordination sphere of Cu^{2+}, which could be used for the attack, after coordination of $Cu(Dien)^{2+}$ to $Cu(ATP)^{2-}$. Clearly, for the apical water molecules in $Cu(Dien)^{2+}$, again the arguments of point (a) would hold. It may further be added that $Cu(Dien)(OH)^{+}$ is formed only at high pH, i.e. with $pK^{H}_{Cu(Dien)(H_2O)} = 9.5$ [121]. Hence it is concluded that $[Cu(ATP)M]_2$ is the most reactive species under these conditions (Fig. 19, upper part) and that it undergoes intermolecular H_2O attack when $M^{2+} = Mg^{2+}$, Ni^{2+}, Cd^{2+} or $Cu(Dien)^{2+}$.

The addition of 1 equivalent of Dien or Dpa alone at pH_0 5.50 to the Cu^{2+}/ATP 1 : 1 system reduces the rate dramatically to about 1/20 [65]; this result is expected for these Cu^{2+} sequestering ligands. With $Cu(Dpa)^{2+}$ it appears that the promoting and inhibiting effects offset each other (Fig. 19; upper part). This means the promotion occurs as with $Cu(Dien)^{2+}$, while the inhibition is probably due to stacking between the pyridyl rings of Dpa and the purine system of the adenine residue. Such stacking interactions are well known [15,28,79–81,83,84,91,117] and they are expected to influence the structure of the dimeric intermediate. That both $Cu(Dien)^{2+}$ and $Cu(Dpa)^{2+}$ are able to coordinate to $Cu(ATP)^{2-}$ is evident from the results at pH_0 6.70 (Fig. 19, lower part), which will be discussed below.

From the above-mentioned results regarding the upper part of Fig. 19, two further important conclusions follow: (a) In $Cu(Dien)^{2+}$ and $Cu(Dpa)^{2+}$, only a single equatorial binding site is left for coordination to $Cu(ATP)^{2-}$. As the coordination tendency of the apical Cu^{2+} positions is very weak, this suggests that the second metal ion (or complex) coordinates to $Cu(ATP)^{2-}$ (or its dimeric derivative) only in a monodentate fashion and that no four-membered chelate is formed in the reactive species. (b) From the properties of the Cu^{2+}/ATP system in the presence of Mg^{2+} or $Cu(Dien)^{2+}$ it is clear that the second metal ion does not interact with N-7, because such a role could not be taken over by either of these two ions. Both these points are important for the formulation of the reactive intermediates (Figs. 20 and 21; vide infra). In addition, it is revealing to see, regarding biological systems, that Mg^{2+} promotes the dephosphorylation, provided it is correctly positioned by "outside" forces (see also Section L).

The Cu^{2+}/ATP ratio is 1 : 1 in the reactive dimer at pH 6.7 (Figs. 13, 15 and 16), and the results summarized in the lower part of Fig. 19 are in accord with this view: the addition of Mg^{2+} or Cd^{2+} and $Cu(Dpa)^{2+}$ or $Cu(Dien)^{2+}$ inhibits the reactivity at pH_0 6.70 in the Cu^{2+}/ATP 1 : 1 system. The explanation is evident; any additional metal ion coordination to

the triphosphate impairs the coordinated Cu^{2+} so that it becomes in part released. As the added metal ions or metal ion complexes promote the reaction less effectively than Cu^{2+}, the dephosphorylation rate in the system is therefore decreased.

(v) Composition and structure of the reactive species in the M^{2+}-promoted dephosphorylation of ATP

From the preceding sections it is evident that (i) the reactive intermediate contains an M^{2+} : ATP ratio of 2 : 1 for all metal ions studied (with the single exception of Cu^{2+} at higher pH; see Figs. 16 and 17, and below), (ii) the intermediate is of a dimeric nature, and (iii) the attack occurs preferably via OH^- in an *intra*molecular fashion through an $M(OH)^+$ unit, in which OH^- can still be a potent nucleophile as already discussed in Section D(ii). Consequently the most reactive intermediate has the composition $[M_2(ATP)]_2(OH)^-$, although *inter*molecular attack of water on $[M_2(ATP)]_2$ may also occur to some extent as we have seen in Section E(iv) in connection with Fig. 19.

Considering the results mentioned and also the crucial metal ion–N-7 interaction (Section E(iii)), as well as the ^1H NMR shift evidence [60] (Section E(ii)) that ions such as Zn^{2+} or Cd^{2+} promote the formation of dimers during the self-association process of ATP by bridging neighboring ATP species, the structure shown in Fig. 20 is proposed for the reactive intermediate [65]. In agreement with the conclusions for Fig. 12 (Section D(iv)), coordination of two metal ions to a triphosphate forces one metal ion

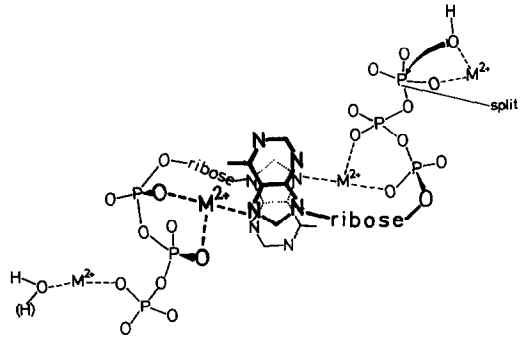

Fig. 20. Proposed structure of the reactive $[M_2(ATP)]_2(OH)^-$ dimer, which occurs in low concentrations during the metal ion promoted dephosphorylation of ATP. The intramolecular attack of OH^- is indicated on the right-hand side, while the left-hand side is ready to transfer also into the reactive state by deprotonation of the coordinated water molecule or to undergo an intermolecular water attack (corresponding to the dimeric $[M_2(ATP)]_2$ species). (Reproduced from Fig. 7 in ref. 65 (J. Am. Chem. Soc., 1984) with permission of the American Chemical Society.)

to the γ-phosphate group (which is the most basic site) and the other into the α,β position, in this way causing labilization of the γ group. It is the shift of the one metal ion into the α,β position which is facilitated by its simultaneous binding to N-7 of the neighboring ATP, and owing to this additional N-7 interaction, purine-NTPs are dephosphorylated much faster than pyrimidine-NTPs (Fig. 5); the latter do not have this additional support in achieving the reactive species (see Figs. 12 and 20 and also Section I).

With the already mentioned single exception of Cu^{2+}, over the whole range from pH 2 to 10 the 2 : 1 mixture is always more reactive than the 1 : 1 mixture for all M^{2+}/ATP systems studied and indeed, Job's series showed throughout a 2 : 1 composition for the reactive dimeric species. The reactivity in M^{2+}/ATP 1 : 1 systems (see for example Fig. 13) may therefore be explained analogously to the situation further outlined below for the Cu^{2+}/ATP 1 : 1 system at pH > 6.5 (Fig. 21), but for the 1 : 1 systems with Ni^{2+}, Zn^{2+} or Cd^{2+} and for the Cu^{2+}/ATP 1 : 1 system at pH < 6.5 it may also be explained on the basis of Fig. 20 by assuming that the position of equilibria (19)–(21)

$$2M(ATP)(OH)^{3-} \rightleftharpoons M_2(ATP)(OH)^{-} + ATP^{4-} + OH^{-} \quad (19)$$

$$M(ATP)(OH)^{3-} + M(ATP)^{2-} \rightleftharpoons M_2(ATP)(OH)^{-} + ATP^{4-} \quad (20)$$

$$M_2(ATP)(OH)^{-} + M(ATP)^{2-} \rightleftharpoons M_3(ATP)_2(OH)^{3-} \quad (21)$$

or of any related equilibria is such that few percent of $M_3(ATP)_2(OH)^{3-}$ are formed. In this species, two metal ions stabilize the dimer via bridging and the third coordinates to one of the two γ-phosphate groups to facilitate nucleophilic attack.

However, this explanation (eqns. (19)–(21)) does not satisfy the observations for the Cu^{2+}/ATP 1 : 1 system at pH ≥ 6.5, because Job's series showed (Fig. 15B) that from pH > 6.7 the Cu^{2+}/ATP ratio is 1 : 1 in the reactive dimer. Indeed, at pH > 6.5 the 2 : 1 and 1 : 1 systems share the same reactivity (Fig. 13 and lower part of Fig. 16). This indicates that the second Cu^{2+} simply hydrolyzes away in this pH range and is no longer available for promotion of the dephosphorylation; hence the reactive species has the composition $[Cu(ATP)]_2(OH)^{5-}$. It is also assumed for this complex that both Cu^{2+} bridge an ATP dimer. The reaction is then initiated by a partial release of the (α),β group from the coordination sphere of Cu^{2+} upon deprotonation of a coordinated water molecule. This latter Cu^{2+} would then be coordinated in the reactive intermediate to N-7 of one ATP and the γ-phosphate group of the other ATP, allowing intramolecular attack of a coordinated OH^{-} as shown in Fig. 21. It is evident that with progressing

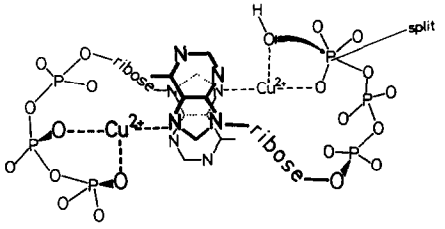

Fig. 21. Tentative structure of the reactive $[Cu(ATP)]_2(OH)^{5-}$ dimer, which occurs in low concentrations during the Cu^{2+}-promoted dephosphorylation of ATP at pH ≥ 6.5 (see text). The intramolecular attack of OH^- is indicated on the right-hand side, while the left-hand side shows a Cu^{2+} ion stabilizing the dimer by coordination to the γ,β-phosphate groups of one ATP and to N-7 of the other. (Reproduced from Fig. 8 in ref. 65 (J. Am. Chem. Soc., 1984) with permission of the American Chemical Society.)

hydroxo complex formation the bridging to N-7 and the stability of the dimer will be affected [65], leading to $Cu(ATP)(OH)^{3-}$ (or derivatives thereof [63]) and a decreasing reactivity.

As already indicated above, for metal ions other than Cu^{2+} the reactivity of M^{2+}/ATP 1 : 1 systems may also be explained by a reactive intermediate corresponding to that in Fig. 21, provided it is also postulated for these cases that the reactivity of this intermediate is lower than that of the intermediate shown in Fig. 20. With this assumption the results of Job's series (for Zn^{2+}, Ni^{2+} and Cd^{2+}) [64,65] would also be satisfied. Finally, it may be emphasized that detailed mechanistic considerations evaluating specific rate constants and using Cu^{2+} as an example [65] suggest for the ATP systems special structural features not present in the R–TP systems (Section D). This agrees with the conclusions presented, and the "special structural features" are borne out by a comparison of Figs. 20 and 21 with Fig. 12.

In the present context, two recent studies of the Cu^{2+}/ATP [122] and Zn^{2+}/ATP [68] 1 : 1 systems in aqueous solution at 50 °C should also be mentioned; both studies confirm the dimeric nature of the reactive complex. However, the importance of the M^{2+}–N-7 interaction for the reaction process is challenged and instead two roles are attributed to N-1. It is concluded that (i) "when a reactive dimer form is produced... the Cu^{2+} ion binds the N-1 position of the ring of one ATP molecule and O^- of the γ-phosporyl group of the other" [122], and (ii) in connection with $[Zn(ATP)]_2^{4-}$,... "the N-1 atom of the adenine ring fulfills the function of a general basic catalyst which cleaves a proton from the H_2O molecule coordinated at the γ-phosphate group" [68]. These suggestions are *not* in agreement with the experimental facts; the following, to name just two, are to be outlined further also in other sections: (i) AMP^{2-} is able to take over the role of the structuring ATP^{4-} in the dimer (Figs. 20 and 21) while

$TuMP^{2-}$ (7-deaza-AMP^{2-}) is not [65], despite the increased basicity of N-1 in $TuMP^{2-}$ compared with AMP^{2-} [29]; the crucial point here is that $TuMP^{2-}$ lacks the N-7 site (see also Section E(vi)). (ii) The mechanistic properties of the Cu^{2+}/ITP or GTP systems in the lower pH range correspond to those of Cu^{2+}/ATP (see Section F), despite the fact that N-1 of ITP and GTP carries a proton (see Fig. 1) and has therefore no basic properties; the corresponding mechanistic properties are in agreement with the presence of an N-7 site in all three NTPs.

(vi) Further details on the structures of the reactive ATP species: promotion of the reactivity in M^{2+}/ATP systems by AMP and related purine-NMPs, and inhibition by other ligands, including 7-deaza-AMP (TuMP)

Considering the delicacy of the structures in Figs. 20 and 21 it is evident that the addition of any ligand with a greater coordination tendency toward the metal ion than that of N-7 will inhibit the reactivity. Consequently, ligands such as 2,2′-bipyridyl (Section C(iii); Fig. 5) or tryptophan (Fig. 22) inhibit the dephosphorylation reaction by forming ternary complexes of the $M(Bpy)(ATP)^{2-}$ [15,20,28,79–81] and $M(ATP)(Trp)^{3-}$ type [28,81,91,123]. Dien and Dpa also drastically inhibit the reaction in the Cu^{2+}/ATP 1:1

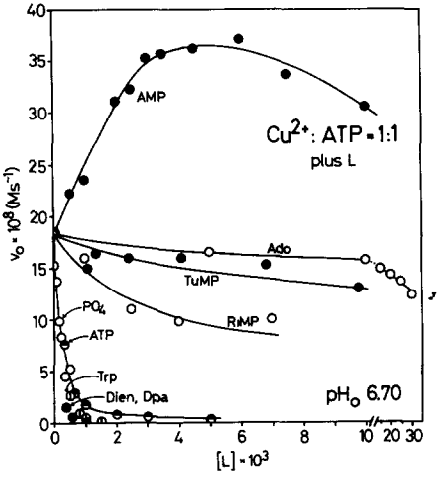

Fig. 22. Dependence of the initial rate v_0 (M s^{-1}) of the Cu^{2+}-promoted dephosphorylation of ATP ($[Cu^{2+}]_{tot} = [ATP]_{tot} = 10^{-3}$ M; $I = 0.1$ M, $NaClO_4$; 50 °C) in aqueous solution at pH_0 6.70 on the addition of further ligands (L), i.e. AMP (●), adenosine (○), TuMP (●), RiMP (○), ATP (◒), PO_4 (○), L-Trp (◑), Dien (●) or Dpa (●). (Reproduced from Fig. 9 in ref. 65 (J. Am. Chem. Soc., 1984) with permission of the American Chemical Society.)

system, as does an excess of ATP (Fig. 22) [65]. This latter result implies that $Cu(ATP)_2^{6-}$, the species most probably formed, which would be a stacked complex, shows no reactivity.

One could view the reactive species shown in Figs. 20 and 21 also by saying that one ATP is needed to bring the other into the reactive state; i.e. one could say that ATP may act as its own enzyme. Indeed, addition of AMP^{2-} to the Cu^{2+}/ATP 1:1 system further promotes the reaction as is seen in Fig. 22. It may be recalled that this contrasts with the observation in the Cu^{2+}/UTP 1:1 system (Fig. 9) where the addition of AMP leads to inhibition of the reaction (as does the addition of phosphate or tryptophan). On the basis of Fig. 21 the promotion mentioned can only mean that in the $[Cu(ATP)]_2^{4-}$ dimers, part of ATP^{4-} is replaced by AMP^{2-} to give a $Cu_2(ATP)(AMP)^{2-}$ complex and that this species has a higher stability, thus leading to a larger concentration of a reactive species. This assumption is quite feasible because charge repulsion in the stack will be less. In addition, bridging of the two ligands by Cu^{2+} will probably be easier on one side of the "dimer" as the phosphate chain is shorter, and in this way the Cu^{2+} on the other side of the stack can possibly reach its reactive state more readily. Clearly, AMP^{2-} with the N-7 and its phosphate group is able to take over the role of the "structuring" ATP^{4-}, thus creating mixed AMP/ATP stacks and forcing more ATP into the reactive form. The addition of too much AMP will of course lead to unreactive AMP stacks, which will also bind Cu^{2+} and in this way inhibit the reaction, i.e. a maximum in the [AMP]–rate profile is expected and actually observed (Fig. 22).

The corresponding experiments at pH_0 7.20 in the Zn^{2+}/ATP 1:1 system were strongly hampered by precipitates, but the observations summarized in Fig. 23 still allow the conclusion to be drawn that the overall properties are a reflection of those described in the preceding paragraph for the Cu^{2+} system. That the effects seen in Fig. 23 seem to be real, despite the precipitate, is also confirmed by a more detailed evaluation. Addition of tryptophan strongly inhibits the reaction, while AMP apparently has only a "slight" influence. It should be emphasized that formation of a simple Zn(AMP) precipitate (see also ref. 29) is expected to inhibit the reaction owing to removal of Zn^{2+} from the reactive ATP complex. Furthermore, by calculating apparent stability constants (see eqn. (1) in ref. 124), valid at pH 7.2, for the two corresponding binary complexes (with the equilibrium constants given in refs. 29 and 92 respectively) it becomes evident that the affinities of AMP^{2-} and Trp^- for Zn^{2+} at pH 7.2 are very similar: $\log K^{Zn}_{Zn(AMP)/app} = 2.34$ and $\log K^{Zn}_{Zn(Trp)/app} = 2.48$. Hence this suggests that the affinities of AMP^{2-} and Trp^- towards $Zn(ATP)^{2-}$ are also similar. The observed differences are therefore most probably not due to different

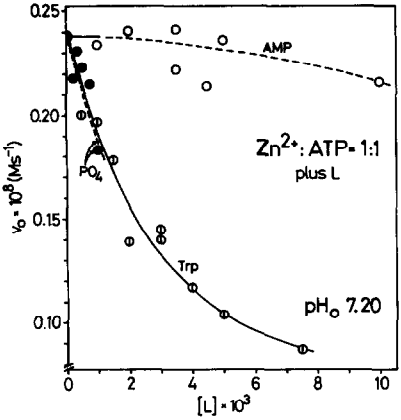

Fig. 23. Dependence of the initial rate v_0 (M s^{-1}) of the Zn^{2+}-promoted dephosphorylation of ATP ($[Zn^{2+}]_{tot} = [ATP]_{tot} = 10^{-3}$ M; $I = 0.1$ M, $NaClO_4$; 50 °C) in aqueous solution at pH_0 7.20 on the addition of ligands (L), i.e. AMP (○), PO_4 (●) or L-Trp (Φ). The broken line portions indicate uncertainty due to precipitation. (Reproduced from the "Supplementary Material" (Fig. S5) in ref. 65 (*J. Am. Chem. Soc.*, 1984) with permission of the American Chemical Society.)

degrees of formation of the corresponding mixed-ligand complexes but rather are due to different structures, i.e. AMP^{2-} is able to replace one of the two ATP^{4-} ions in the reactive species (Fig. 20).

The importance of bridging on both sides of the reactive species in the Cu^{2+}/ATP system (Fig. 21) is confirmed by the inhibitory effect of adenosine (see Fig. 22); adenosine can only stack and/or undergo a weak M^{2+}–N-7 interaction, but it cannot lead to a double bridge. Correspondingly, ribose 5′-monophosphate ($RiMP^{2-}$) and phosphate also inhibit the reaction; that $RiMP^{2-}$ inhibits less indicates that phosphate coordinates as PO_4^{3-}. However, most important in this respect is the result that tubercidin 5′-monophosphate ($TuMP^{2-}$ = 7-deaza-AMP^{2-}, i.e. N-7 in AMP is replaced by a CH unit; see Fig. 24) also *inhibits* the dephosphorylation reaction as

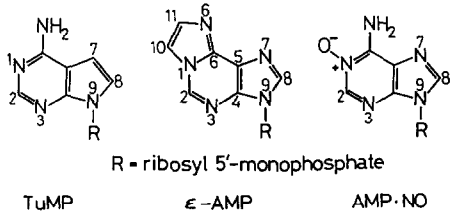

Fig. 24. Structures of AMP derivatives: $TuMP^{2-}$, tubercidin 5′-monophosphate (= 7-deaza-AMP^{2-}); ε-AMP^{2-}, 1,N^6-ethenoadenosine 5′-monophosphate; $AMP \cdot NO^{2-}$, adenosine 5′-monophosphate $N(1)$-oxide.

seen in Fig. 22. This observation definitely proves that simultaneous stacking and phosphate coordination is *not* enough for promotion, and that N-7 is a crucial part of the base moiety. Only metal ion bridging of the dimeric adenine-stack via N-7 leads to the reactive intermediate!

On the basis of the results summarized in Fig. 22 it is expected that the promoting effect of AMP on the dephosphorylation of a Cu^{2+}/ATP 2:1 system should even be more dramatic than that of a 1:1 system. Indeed, the addition of a fivefold excess of AMP^{2-} leads to a threefold increase in the rate in the 2:1 system at pH_0 6.70, as seen in Fig. 25. Moreover, it was now interesting to see [65] if IMP^{2-} and GMP^{2-} could take over the role of AMP^{2-}, as both these nucleotides have a purine residue with an N-7 site. In fact, the observations in Fig. 25 show that IMP and GMP can take over the role of AMP, though only in a less efficient way. This result cannot be due to a smaller coordination tendency of N-7 in IMP and GMP because the corresponding nucleoside complexes are somewhat more stable than those with adenosine [20,30,60]. The lower efficiency must be due to the stacking properties. The self-association tendency of the nucleosides (and nucleo-

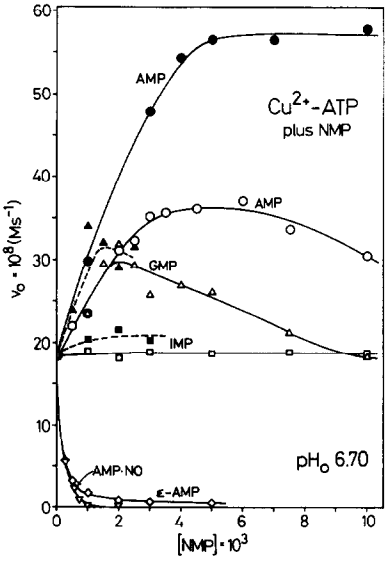

Fig. 25. Influence of purine-nucleoside 5′-monophosphates and derivatives (NMP) on the initial rate v_0 (M s^{-1}) of dephosphorylation of the 1:1 (open symbols ○, △, □, ◇, ▽; $[Cu^{2+}]_{tot} = [ATP]_{tot} = 10^{-3}$ M) and 2:1 (solid symbols ●, ▲, ■; $[Cu^{2+}]_{tot} = 2 \times 10^{-3}$ M and $[ATP]_{tot} = 10^{-3}$ M) Cu^{2+}/ATP systems in aqueous solution at pH_0 6.70: AMP (○, ●), GMP (△, ▲), IMP (□, ■), ε-AMP (◇) and AMP·NO (▽). The broken lines indicate uncertainty due to precipitation. $I = 0.1$ M, $NaClO_4$; 50 °C. (Reproduced from Fig. 10 in ref. 65 (J. Am. Chem. Soc., 1984) with permission of the American Chemical Society.)

tides) decreases in the series adenosine > guanosine > inosine [60,116,117], and this reflects exactly the order of decreasing efficiency, AMP^{2-} > GMP^{2-} > IMP^{2-}, in promoting the dephosphorylation reaction (Fig. 25). In addition, these results again confirm that N-7 is involved in the bridging process by the metal ion (Figs. 20 and 21), because N-1 of IMP and GMP is not available for coordination in this pH range.

How sensitive the structure of the reactive intermediate is, also becomes clear from the addition experiments (Fig. 25) with $1,N^6$-ethenoadenosine 5′-monophosphate (ϵ-AMP^{2-}) and adenosine 5′-monophosphate *N*(1)-oxide ($AMP \cdot NO^{2-}$) (see Fig. 24). The stacking properties of ϵ-AMP^{2-} [28,125] are very similar to those of AMP^{2-} and the same may be surmised for $AMP \cdot NO^{2-}$. However, both AMP derivatives form rather stable chelates with Cu^{2+} at pH 6.7. In Cu(ϵ-AMP) the metal ion is bound to the phosphate group and the N-6,N-7 site [28,125,126] and in $Cu(AMP \cdot NO{-}H)^{-}$ to the ionized *o*-amino *N*-oxide group [127]. This leads to different orientations of the metal ion in space, and consequently both AMP derivatives are strong inhibitors of the dephosphorylation in the Cu^{2+}/ATP system (Fig. 25).

F. M^{2+}-FACILITATED DEPHOSPHORYLATIONS OF THE 5′-TRIPHOSPHATES OF INOSINE (ITP) AND GUANOSINE (GTP)

The properties of the purine moiety are crucial for the Cu^{2+}-promoted dephosphorylation process of purine-nucleoside 5′-triphosphates as was indicated already in Section C(ii) in connection with the results shown in Fig. 5. The reaction in the pH range up to 7.5 is more accelerated by Cu^{2+} with ITP and GTP than with the pyrimidine-NTPs, but less so than with ATP. The reactivity decreases in the Cu^{2+}/NTP systems in the pH range 2–7.5 in the order ATP > GTP > ITP > pyrimidine-NTP (= R–TP). Regarding the order within the purine-NTPs, one must conclude that different stacking properties are most probably the reason for the different reactivities. This agrees with the results in Fig. 25 (Section E(vi)) where the promoting effect of NMPs on the Cu^{2+}/ATP systems decreases in the order AMP > GMP > IMP. Indeed, there is no M^{2+} or H^{+} binding property that could account for the observed order of the dephosphorylation rates. All H^{+} and M^{2+} binding to the base moieties follow the order adenosine < inosine < guanosine [27,30], whereas the tendency of the bases to stack follows the order adenosine > guanosine > inosine [60,116,117]. Hence this comparison supports the conclusion already outlined (Section E) that stacking interactions are important in forming the kinetically active dimers (Figs. 20 and 21).

The kinetic properties of the M^{2+}/ITP and GTP systems have not yet been studied in detail. However, similarly to the situation described in

Section E(iii), the pH–rate profiles for the Cu^{2+} 1 : 1 systems with ITP and GTP show a (first) maximum or shoulder at a pH close to the maximum in the pH–rate profile of Cu^{2+}/ATP (Fig. 5). Indeed, the initial rate v_0 from the ascending side of the peaks is also proportional to $1/[H^+]$, i.e. to $[OH^-]$ (footnote 65 in ref. 65). In addition, at pH_0 5.70, plots of log v_0 vs. log $[Cu^{2+}/NTP]$ yield straight lines with a slope of two for both ITP and GTP, showing that the reactive species is a dimer, and Job's series, also at pH_0 5.70, gives a Cu^{2+}/NTP ratio of 2 : 1 for this species [128]. Hence these results suggest the composition $[Cu_2(NTP)]_2(OH)^-$ for the reactive intermediate and this composition agrees with the proposed structure for the reactive dimer given in Fig. 20 where ATP^{4-} simply has to be replaced by ITP^{4-} or GTP^{4-}, as well as with the conclusions outlined in the preceding paragraph. Moreover, the reactivity of the Cu^{2+}/ITP 1 : 1 system at pH_0 5.70 can also be further promoted by the addition of IMP; this result corresponds to that shown in Fig. 22 for the Cu^{2+}/ATP/AMP system and therefore the corresponding discussion in Section E(vi) is also valid here.

However, from the pH–rate profiles given in Fig. 5 it is already evident that the kinetic properties of the Cu^{2+}/ITP and GTP systems are more complicated than those of the Cu^{2+}/ATP system. The pH–rate profiles of the former have two maxima (or at least shoulders) indicating that in different pH regions different reactive species are operating. Indeed, plots of log v_0 vs. log $[Cu^{2+}/NTP]$ give slopes for ITP and GTP at pH > 6 which are smaller than two, e.g. at pH_0 8.40, slopes of 1.4 are obtained [128] for both NTPs, indicating that in this upper pH range now in addition a monomeric reactive complex gains influence. Job's series ($pH_0 \geq 7.5$) still show a Cu^{2+}/NTP ratio of 2 : 1 for the most reactive species [128]. As in this pH range the proton from N-1 is liberated in $Cu(ITP)^{2-}$ and $Cu(GTP)^{2-}$ [66,69,73], one may presume that $Cu_2(NTP–H)(OH)^{2-}$ is the reactive monomeric intermediate and that the higher reactivity compared with that of $Cu_2(R–TP)(OH)^-$ (see Section D; Fig. 5) is due to purine-ring backbinding of one of the two Cu^{2+} ions. This would then be a new reactive species not discussed so far, but analogous to that described for the Cu^{2+}/ε-ATP system in Section H(iv). The importance of species derived from $M(NTP–H)^{3-}$ to the reactivity in the upper pH range is also evident from the pH–rate profile obtained for the Zn^{2+}/ITP and GTP systems [66]. However, before a final decision on the detailed structure of these reactive intermediates in the upper pH range can be made more experimental work is needed.

G. POSSIBLE REASONS FOR THE EFFICIENCY DIFFERENCES AMONG METAL IONS IN THE PROMOTION OF DEPHOSPHORYLATION REACTIONS

In M^{2+}/ATP 1 : 1 systems, the pH at which the *maximum* promotion occurs increases, beginning with Cu^{2+} at pH 6.5, within the series Cu^{2+} <

$Zn^{2+} < Ni^{2+} \lesssim Cd^{2+}[< Mn^{2+} < Mg^{2+}]$ (see Fig. 13); the position of Ni^{2+} in this order is somewhat uncertain due to precipitation (Fig. 13), and Mn^{2+} and Mg^{2+} are tentatively added (Table 1). For M^{2+}/ITP and GTP 1:1 systems, only studies with Cu^{2+} [69], Zn^{2+} and Ni^{2+} [66] have been made, and for these three metal ions the same order as given above is observed. For triphosphates with a non-coordinating organic residue (R–TP; Section D) the M^{2+}/CTP 1:1 systems are taken as representative examples. In these cases the pH is taken at which the *onset* of increased reactivity occurs to establish the following order, beginning with Cu^{2+} at pH 6, $Cu^{2+} < Zn^{2+} < Cd^{2+} \lesssim Ni^{2+}$, in which again the position of Ni^{2+} is somewhat uncertain due to precipitation (Figs. 7 and 8).

The differences among the metal ions regarding the "active" pH range certainly do not originate in different degrees of formation of the $M(NTP)^{2-}$ species; their degree of formation is large for all systems already from a pH of about 5.5 on (see for example Figs. 7, 8, 14 and 18). The important point is clearly hydroxo complex formation (Sections D(i) and E(i)). Estimations of the negative logarithms of the acidity constants, $pK^{H}_{M(NTP)(H_2O)}$ (eqn. (12)), are for the metal ions mentioned (pK_a values in parentheses) and for $NTP^{4-} = ATP^{4-}$: Cu^{2+} (8.2) < Zn^{2+} (8.9) < Ni^{2+} (9.4) < Cd^{2+}(10.1) < Mn^{2+} (10.7) < Mg^{2+} (> 11); for $NTP^{4-} = CTP^{4-}$: Cu^{2+} (ca. 7.6) < Zn^{2+} (8.8) < Ni^{2+} (9.6) < Cd^{2+} (10.0) < Mn^{2+} (10.9) < Mg^{2+} (> 11) [55,73,88] (see also legend to Fig. 7). It is evident that the tendency of these metal ions to form hydroxo complexes follows the reverse order compared with the orders given for the "active" pH ranges, i.e. the lower the pH at which a metal ion forms hydroxo complexes, the lower the pH at which this metal ion is promoting the dephosphorylation reaction. There may be some uncertainty with Ni^{2+}, but in principle this view is certainly correct and in agreement with the reaction mechanisms described (Sections D and E). In addition, it is also confirmed by observations at trivalent metal ions: $(tn)_2Co^{3+}$ forms hydroxo species at a lower pH than Y^{3+} or La^{3+} and in M^{3+}/ATP or UTP 2:1 systems at pH 5.5, $(tn)_2Co^{3+}$ is a more effective promoter of the dephosphorylation [40] (vide infra Section J(ii); Table 5). Hence one of the reasons why different metal ions accelerate the dephosphorylation of NTPs differently relates to their different abilities to form hydroxo complexes.

The fact that the above orders for M^{2+}/ATP and M^{2+}/CTP systems regarding the "active" pH range of the metal ions correspond to each other should not obscure the other fact that the reactivity of a given metal ion with different NTPs can differ significantly. On the basis of the available information the following four series can be established.

(a) Cu^{2+}: ATP > GTP > ITP > CTP = R–TP (Fig. 5).

(b) Cd^{2+}: ATP > CTP = R–TP (Fig. 13).

(c) Zn^{2+}: ITP > GTP > ATP > CTP = R–TP [66].

The order for the Cu^{2+}/purine-NTPs follows the self-association tendency of the nucleic base moieties as discussed in Section F. That CTP is always at the lowest end of the reactivity order for Cu^{2+}, Cd^{2+} and Zn^{2+} is in accord with the observation that the organic residues in the R–TP systems are not participating in the reaction and therefore not facilitating it. Consequently, this leads to different reactive complexes for R–TPs and purine-NTPs as discussed in connection with Fig. 12 (Section D(iv)) and Figs. 20 and 21 (Section E(v)). The above order for the purine-NTPs in the presence of Zn^{2+} may at first sight appear surprising. However, this order refers to the pH range around 8–9 and here N-1 of ITP and GTP (Fig. 1) may be deprotonated, leading to complexes of the $Zn(ITP–H)^{3-}$ and $Zn(GTP–H)^{3-}$ type [60,66] for which a different reaction path is expected, as indicated in Section F. Indeed, that the kind of reaction path may dictate the reactivity of a system will become further obvious in Section H.

Before the situation in the Ni^{2+}/NTP systems (the above series (d)) is discussed, it seems helpful to establish the order for the dephosphorylation of a given NTP by various metal ions, i.e. the maximum of the dephosphorylation rate achieved by metal ions for a given NTP, independent of the pH range, is used to establish the following orders.

(a) ATP: $Cu^{2+} > Cd^{2+} > Zn^{2+} > Ni^{2+}$ (Fig. 13).
(b) GTP: $Cu^{2+} > Zn^{2+} > Ni^{2+}$ [66,69].
(c) ITP: $Cu^{2+} > Zn^{2+} > Ni^{2+}$ [66,69].
(d) CTP (= R–TP): $Cu^{2+} \approx Cd^{2+} > Zn^{2+} \approx Ni^{2+}$ (Figs. 7 and 8).

It must be emphasized that the order for the CTP system is very tentative as the peaks or plateaus in the pH–rate profiles are strongly obscured due to precipitation. However, on the basis of the results obtained for water attack on $M(R–TP)^{2-}$ species (see Section D(iv)) and on the purine-NTPs it is clear that the effectiveness in promoting the dephosphorylation decreases in the order $Cu^{2+} > Cd^{2+} > Zn^{2+} > Ni^{2+}$. This order cannot be due, as outlined before, to different degrees of formation of the complexes, as these are much more similar (e.g. Figs. 7, 8, 14 and 18) than the large differences in the promotional tendencies (Fig. 13). The order for the purine-NTPs also cannot be due to differences in the metal ion affinity of N-7, as this affinity [17,28–30] is relatively similar for the metal ions mentioned and it would certainly not place Ni^{2+} to the end of the series.

Clearly, one is tempted to explain the reactivity order $Cu^{2+} > Cd^{2+} > Zn^{2+} > Ni^{2+}$ of the preceding paragraph with substitution rate effects in the coordination spheres of these metal ions, as the water substitution rates for the divalent aqua metal ions differ considerably and follow exactly the given order [13,104]. Indeed, for M^{2+}/NTP 1 : 1 systems this effect could play a role as rearrangement equilibria (see for example eqns. (10), (11) and (19)–(21)) are probably necessary to achieve formation of a reactive species

in these systems, and observations with M^{3+}/NTP 1 : 1 systems [40] are in accord herewith. Substitution rates for lanthanides are high [13,104] while those for $(tn)_2Co^{3+}$ are certainly more sluggish; correspondingly at pH 7.5, Y^{3+} and La^{3+} facilitate the dephosphorylation of ATP or UTP in 1 : 1 systems (10^{-3} M; 50 °C) [40] by factors of about 700, while with $(tn)_2Co^{3+}$ the factor is only five.

However, this explanation based on the substitution rates cannot generally be valid due to observations made with systems containing excess of metal ions. For example, addition of Mg^{2+}, Ni^{2+}, Cd^{2+} or $Cu(Dien)^{2+}$ to the Cu^{2+}/ATP 1 : 1 system at pH_0 5.50 leads to the same limiting rate of the dephosphorylation process (Section E(iv); Fig. 19). Similarly, $(tn)_2Co^{3+}$, if present in excess, is an excellent promoter of the dephosphorylation of ATP or UTP, e.g. at pH 5.5 in 2 : 1 systems (10^{-3} M; 50 °C) its promotional factor is above 1000, whereas that for Y^{3+} or La^{3+} is only about 70, and under the same conditions at pH 7.5 it is evident, despite some precipitation [40], that $(tn)_2Co^{3+}$ is still as effective as Y^{3+} or La^{3+} (see also Section J(ii)). (Maybe it should also be mentioned in this connection that, compared with many related Co(III) complexes, $(tn)_2Co^{3+}$ rapidly undergoes water substitution, *trans–cis* isomerization and complexation [129], especially in the vicinity of pH 6.5 where $(tn)_2Co(OH)(OH_2)^{2+}$ is maximized, e.g. *trans* → *cis* isomerization proceeds for the hydroxoaqua complex with a half-life of about 1 s at 25 °C.)

Overall, it is evident that aside from kinetic aspects a further feature is needed to explain the low reactivity of the Ni^{2+} systems as well as the near identity of the dephosphorylation rate in all Ni^{2+}/NTP 1 : 1 systems [66], an identity already indicated above. Indeed, the low reactivity and hence the near rate-identity of Ni^{2+}/NTP systems has been explained [64,66] by an α,β,γ coordination of this hexacoordinate metal ion in $Ni(NTP)^{2-}$. This type of binding would render the formation of an α,β-coordinated Ni^{2+} more difficult compared with that of Cu^{2+}, Zn^{2+} and Cd^{2+}, if these latter ions coordinate initially mainly via the β,γ groups, because then a shift into an α,β position (Figs. 12 and 20) would not alter the denticity in the coordination sphere. Clearly, on this aspect of the metal ion–phosphate coordination, for example, in monomeric $M(NTP)^{2-}$ complexes, more work is needed.

H. M^{2+}-FACILITATED DEPHOSPHORYLATION OF 1,N^6-ETHENOADENOSINE 5′-TRIPHOSPHATE (ϵ-ATP). EVIDENCE FOR A LONG-SOUGHT MONOMERIC BACK-BOUND REACTIVE SPECIES IN THE Cu^{2+}/ϵ-ATP SYSTEM

A reactive triphosphate species that is monomeric and in which the α,β coordination of one metal ion at the phosphate chain is facilitated by the

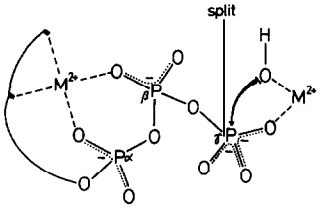

Fig. 26. Simplified structure of a long-sought monomeric reactive complex in which the α,β coordination of one metal ion is facilitated by backbinding to correctly positioned binding sites at the organic residue of the triphosphate to be dephosphorylated. The metal ion–triphosphate coordinations are drawn here in analogy to the structure shown in Fig. 12.

presence of additional binding sites in a sterically favorable position is shown in Fig. 26. A comparison of this structure with that in Fig. 12 makes clear why "backbinding" is an appealing feature. Indeed, the search for such a species was initiated in 1956 by the hypothesis of Szent-Györgyi [130] that macrochelate formation in nucleotide complexes is of importance for biological systems. Consequently, such a reactive complex has long been sought in model studies [6,54] and in NTP dephosphorylations [34,55]. In model studies no significant rate enhancement was observed [6], and for NTP systems other reactive complexes have been identified (Figs. 12, 20 and 21) [65,71]. However, in studies with the ATP derivative $1,N^6$-etheno-ATP (ϵ-ATP; see Fig. 1), it was discovered [86] that its Cu^{2+}-promoted dephosphorylation proceeds via a species like that indicated in Fig. 26, while the Zn^{2+}-facilitated reaction involves a complex analogous to that shown in Fig. 20. It may be mentioned that owing to the scarcity of ϵ-ATP, only a limited number of experiments were carried out [86].

(i) Comparison of the influence of Cu^{2+} and Zn^{2+} on the dephosphorylation rate of ϵ-ATP and some other NTPs

From the pH–rate profile for the dephosphorylation of ϵ-ATP in the absence of metal ions, as shown in Fig. 27, it is evident that ϵ-ATP behaves like any other NTP under these conditions. This result is important because it proves, in accordance with other results (Section C), that alterations at the nucleic base moieties are not reflected in the dephosphorylation rate as long as metal ions are absent. Moreover, this also means that any different properties observed in the presence of metal ions must be a reflection of the nucleic base moiety.

In Fig. 27 the influence of Zn^{2+} on the 1 : 1 systems with ϵ-ATP, ATP and CTP is given. For further comparison the pH–rate profiles for the Cu^{2+} 1 : 1 systems with ϵ-ATP and ATP are also inserted; that for Cu^{2+}/CTP is found in Fig. 5 (for further details see ref. 86). From Fig. 27 it is evident that the

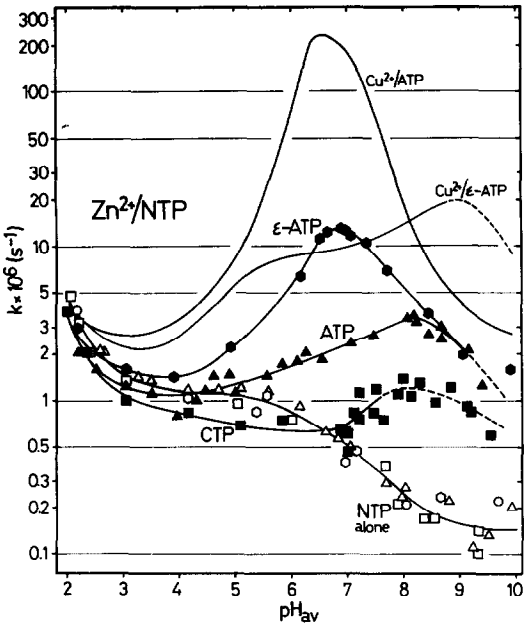

Fig. 27. Comparison of the Zn^{2+}-promoted dephosphorylation of ε-ATP (●), ATP (▲), and CTP (■) (always in the ratio 1:1) in aqueous solution as a function of pH, characterized as the first-order rate constants k (s^{-1}). The corresponding data for ε-ATP (○, ○), ATP (△) and CTP (□) alone are also given. For further comparison the pH rate profiles representing the reactivity of the Cu^{2+}/ε-ATP and Cu^{2+}/ATP 1:1 systems are inserted. The concentration of each reactant (when present) was always 10^{-3} M; $I = 0.1$ M, $NaClO_4$; 50 °C. The broken line portions indicate uncertainty due to precipitation. This figure is a combination of the data given in Figs. 2 and 3 in ref. 86.

dephosphorylation rate in the Cu^{2+}/ATP 1:1 system is more pronounced than in the corresponding system with ε-ATP. However, it is also clear that the Cu^{2+}/ε-ATP 1:1 system is considerably more reactive still than the Cu^{2+}/CTP 1:1 system, the latter being characteristic of a triphosphate with a non-participating organic residue (Section D). This comparison shows that the ε-adenine residue influences the rate and hence participates in the metal ion coordination; this conclusion agrees with spectrophotometric measurements [28,131]. Furthermore, in the Cu^{2+}/ATP system the metal ion is interacting with N-7 (Section E), while in the case of ε-ATP a 1,10-phenanthroline-like coordination to the N-6,N-7 site (see Fig. 1) occurs [28,131]. Hence these different coordinating properties of the two base residues must be responsible for the observed differences in reactivity.

Comparisons in Fig. 27 regarding Zn^{2+} reveal that in the metal-ion-facilitated dephosphorylation of ATP and CTP, Zn^{2+} is considerably less efficient than Cu^{2+}; this agrees with the discussions in Section G. However, in the

in the pH region around 7, Zn^{2+} is clearly a more efficient promoter of the dephosphorylation of ϵ-ATP than Cu^{2+}. This observation is the first hint that different mechanisms might be operating for the dephosphorylation of ϵ-ATP in the presence of these two metal ions. A related aspect in this connection is that for the Zn^{2+}/NTP 1 : 1 systems the reactivity decreases in the pH range 3–10 in the order ϵ-ATP > ATP > CTP, while for the Cu^{2+} 1 : 1 systems the order is ATP > ϵ-ATP > CTP.

(ii) Relations between the reactant compositions of the solutions and the reaction rates

Previous experience is that in general the most reactive NTP species contains more than one metal ion (Figs. 10, 12, 15 and 20) and indeed, the

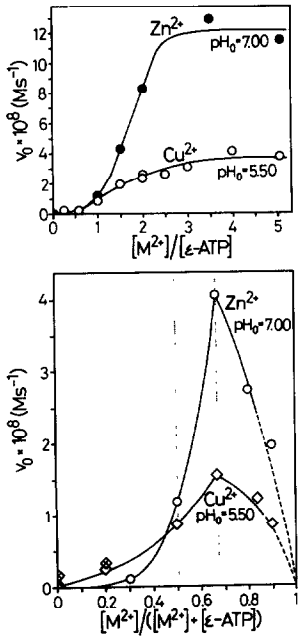

Fig. 28. Upper part. Dependence of the initial rate v_0 (M s^{-1}) for the Cu^{2+}-promoted (○; pH_0 5.50) and Zn^{2+}-promoted (●; pH_0 7.00) dephosphorylation of ϵ-ATP in water on the ratio $[M^{2+}]/[\epsilon\text{-ATP}]$ with $[\epsilon\text{-ATP}]_{tot} = 10^{-3}$ M; $I = 0.1$ M, $NaClO_4$; 50 °C. Lower part. Job's series for the aqueous Cu^{2+}/ϵ-ATP system (◇) at pH_0 5.50 and for the Zn^{2+}/ϵ-ATP system (○) at pH_0 7.00. $[M^{2+}]_{tot} + [\epsilon\text{-ATP}]_{tot}$ = constant = 2×10^{-3} M; $I = 0.1$ M, $NaClO_4$; 50 °C. The measured points (⊗) were corrected for the dephosphorylation rate of uncomplexed ϵ-ATP by assuming complete 1 : 1 complex formation. The broken line portions indicate uncertainty due to precipitation. The vertical dotted lines give the positions of the ratios $[M^{2+}]:[\epsilon\text{-ATP}] = 1:1$ or 2 : 1 (see text in Section D(iii)). This figure is a combination of the data given in Figs. 4 and 5 in ref. 86.

reactivity in 1 : 1 systems of Cu^{2+}/ϵ-ATP and Zn^{2+}/ϵ-ATP may be significantly enhanced by the addition of further metal ions (Fig. 28; upper part); the effect is very pronounced especially in the Zn^{2+} system. Job's method (see Section D(iii)) was used to identify definitely the composition of the reactive complex [86]. From the lower part of Fig. 28 it is evident for both systems that the most reactive species contains two metal ions per ϵ-ATP in accordance with the experience for other triphosphate systems, (see for example Figs. 12 and 15). Therefore it is suggested [86] that the M^{2+}/ϵ-ATP ratio of 2 : 1 is valid over the whole pH range from 4 to 9 and not just at the pH values used in the experiments for Fig. 28.

To learn more about the mechanism of the reaction, i.e. the dependence of the initial rate v_0 ($M\ s^{-1}$) on the total concentration of M^{2+}/ϵ-ATP, the experiments shown in Fig. 29 are reproduced from ref. 86. For both systems at pH_0 7.00 the data fit on straight lines, but for Cu^{2+}/ϵ-ATP a slope of unity is obtained while for Zn^{2+}/ϵ-ATP a slope of two results, indicating (see Section D(iii)) that in the Cu^{2+} system the reaction proceeds via a monomeric complex while in the Zn^{2+} system a dimeric species must be involved.

The results summarized in Fig. 30A show that at pH 7, $Cu(\epsilon\text{-ATP})^{2-}$ is formed to more than 95%. This together with the result in Fig. 29 provide

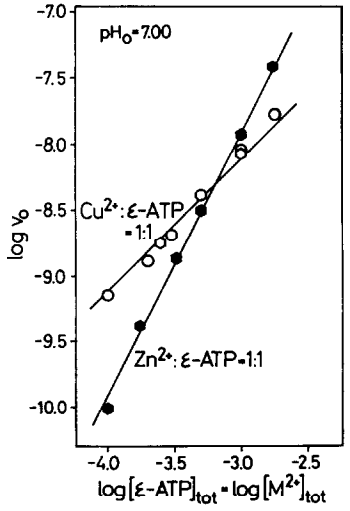

Fig. 29. Relationship between the initial dephosphorylation rate v_0 ($M\ s^{-1}$) of ϵ-ATP and the total concentrations of Cu^{2+} (○, ○) or Zn^{2+} (●) and ϵ-ATP in aqueous solution at pH_0 7.00 showing the dependence of log v_0 on log $[\epsilon\text{-ATP}]_{tot}$ = log $[M^{2+}]_{tot}$; I = 0.1 M, $NaClO_4$; 50 °C. (Reproduced from Fig. 6 in ref. 86 (Inorganic Chemistry, 1986) with permission of the American Chemical Society.)

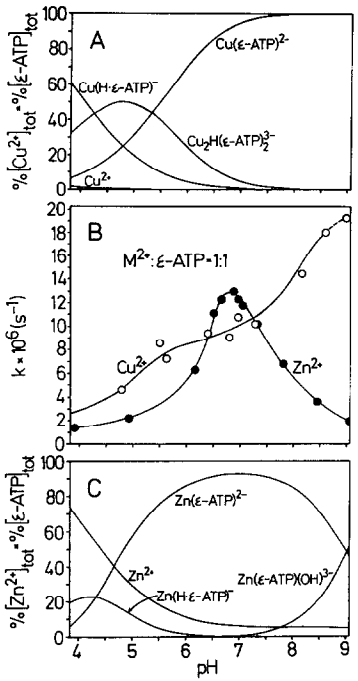

Fig. 30. Comparison of the variation of (B) the Cu^{2+}-promoted (○) and Zn^{2+}-promoted (●) dephosphorylation of ε-ATP (each 10^{-3} M) in aqueous solution at 50 °C as a function of pH ($I = 0.1$ M, $NaClO_4$; cf. Fig. 27), with the effect of pH at 25 °C ($I = 0.1$ M, $NaNO_3$) on the concentration of the species present in an aqueous solution of Cu^{2+} (A) or Zn^{2+} (C) and ε-ATP (each 10^{-3} M). These results were computed with the constants listed in Table I in ref. 86, and they are given as the percentage of the total M^{2+} present (equal to total ε-ATP); for the formation of $Cu(\epsilon\text{-ATP})(OH)^{3-}$ holds probably $pK^{H}_{Cu(\epsilon\text{-ATP})(H_2O)} > 8.5$ [86]. (Reproduced from Fig. 7 in ref. 86 (Inorganic Chemistry, 1986) with permission of the American Chemical Society.)

evidence that the monomeric $Cu(\epsilon\text{-ATP})^{2-}$ complex must be involved in the formation of the most reactive species [86]. The results allow no final conclusion to be drawn about the species responsible for the reactivity at pH < 6.5. Again Cu(ε-ATP) could be involved (at least down to pH 5), but $Cu_2H(\epsilon\text{-ATP})_2^{3-}$ (see Fig. 30A) or a derivative thereof could also have some dephosphorylation reactivity.

Comparisons of Figs. 30B and 30C show that the reactivity decreases with the advent of $Zn(\epsilon\text{-ATP})(OH)^{3-}$. This is especially evident if one remembers that hydroxo complex formation in such systems is favored with increasing temperature [55]. However, at the pH where the dephosphorylation rate reaches its maximum, $Zn(\epsilon\text{-ATP})^{2-}$ is clearly the dominating species. This together with the slope of two shown in Fig. 29 may be rationalized with a

monomer–dimer equilibrium. Hence analogous to the arguments given in Section E(ii) in connection with equilibria (13) and (14), it follows that $[Zn(\epsilon\text{-ATP})]_2^{4-}$ is involved in the formation of the most reactive species in the Zn^{2+}/ϵ-ATP system. Evidence for the formation of such dimers has also been obtained independently from ^1H NMR shift experiments [28,132].

In connection with the results of Fig. 29 it should also be remembered that for all M^{2+}/NTP systems considered so far [64,65,71] the slopes of the straight lines (be it unity or two) obtained by plotting log v_0 vs. log [NTP] were always identical for 1 : 1 and 2 : 1 ratios between M^{2+} and a given NTP (see for example Figs. 11 and 17). The same is now surmised for the two M^{2+}/ϵ-ATP systems.

There is one further aspect to be considered in connection with the lower part of Fig. 28: unbound Cu^{2+} begins to hydrolyze in a 2×10^{-3} M solution at pH ca. 5; hence it is to be expected that, in a species containing two Cu^{2+} and one ϵ-ATP^{4-}, Cu^{2+} will also be partly hydrolyzed in this pH region, because one ϵ-ATP^{4-} is not able to saturate the coordination spheres of two Cu^{2+} ions. The corresponding reasoning holds for Zn^{2+} in the pH region around 7. Hence this indicates that an $M(OH)^+$ unit is involved in the most reactive intermediates [86].

A comparison of Figs. 30B and 30C at pH 5.5 points in the same direction: $Zn(\epsilon\text{-ATP})^{2-}$ is already formed to more than 76%, while the dephosphorylation rate is still far from its maximum. This shows that the pH of a solution is playing an additional role; in other words, this is also an indication of the formation of an $M(OH)^+$ unit within the reactive species, because with increasing pH such a unit will be favored. However, an excess of OH^- destroys the reactive complex as is evident from the formation of $Zn(\epsilon\text{-ATP})(OH)^{3-}$ and in agreement with previous observations (Section E(iii); Fig. 18).

Clearly, the available experiments with the M^{2+}/ϵ-ATP systems give only indirect indications of the intramolecular participation of an $M(OH)^+$ unit in the ϵ-ATP systems, but these are in line with the direct evidence given, for example, in Sections D(ii) and E(iii) for the reactive monomeric and dimeric intermediates in several M^{2+}/NTP systems [65].

However, water attack is also possible: a plot of log k vs. log $[H^+]$ for the 1 : 1 system of Zn^{2+}/ϵ-ATP gives a straight line in the pH range of about 5.9–6.9 with a slope of approximately -0.6. As this is a slope larger than -1 (which would indicate that $v_0 \propto 1/[H^+]$, i.e. $v_0 \propto [OH^-]$), this evaluation provides evidence that not just OH^- attack, via $M(OH)^+$, is occurring. Indeed, for M^{2+}/ATP systems it has already been discussed in Section E(iv) that certain conditions also lead to intermolecular water attack (see also Section D(iv)).

(iii) Composition and structure of the reactive species in the Zn^{2+}-facilitated dephosphorylation of ε-ATP

The facts regarding the composition of the most reactive species in the Zn^{2+}/ε-ATP system may be summarized in the following points: (i) the Zn^{2+} : ε-ATP ratio is 2 : 1 (Fig. 28); (ii) the intermediate is a dimer based on $Zn(\epsilon\text{-ATP})^{2-}$ (Fig. 29); (iii) in accord with previous experience [65], the nucleophilic attack occurs preferably via OH^- in an intramolecular fashion through an $M(OH)^+$ unit (Section H(ii)) [86]. Hence the most reactive intermediate has the composition $[Zn_2(\epsilon\text{-ATP})]_2(OH)^-$, although an intermolecular attack of water on $[Zn_2(\epsilon\text{-ATP})]_2$ may also occur to some extent (Section H(ii)).

Taking into account the crucial metal ion–base interaction (Section H(i)), as well as the evidence from an ^1H NMR shift study [28,132] that Zn^{2+} promotes the self-association of ε-ATP by bridging neighboring ε-ATP species, a structure analogous to that shown in Fig. 20 for ATP systems may be proposed for $[Zn_2(\epsilon\text{-ATP})]_2(OH)^-$. In other words, the adenine moieties in Fig. 20 have to be replaced by the ε-adenine residues with Zn^{2+} coordinated to the N-6,N-7 site [28,133] to describe the situation for the Zn^{2+}/ε-ATP 2 : 1 system. The reactivity in the Zn^{2+}/ε-ATP 1 : 1 system (Fig. 27) is correspondingly explained as in the discussion in Section E(v).

As outlined, the mechanistic properties of the Zn^{2+}/ε-ATP system correspond to those of Zn^{2+}/ATP. However, Fig. 27 shows that the dephosphorylation rate in the 1 : 1 systems is significantly larger for Zn^{2+}/ε-ATP than for Zn^{2+}/ATP, e.g. at pH 7, the ε-ATP system is more reactive by a factor of about five. This experimental fact must be connected with the exchange of the adenine by the ε-adenine moiety (Fig. 1). It appears likely that the larger coordination tendency of the N-6,N-7 site in $\epsilon\text{-ATP}^{4-}$, compared with that of N-7 in ATP^{4-} [28,126], is responsible: this could facilitate bridging of the two NTPs (Fig. 20) and especially promote further the shift of a Zn^{2+} into the reactive α,β-position.

As discussed in Section E(vi), the structure of dimers (Fig. 20) of the $[Zn_2(\epsilon\text{-ATP})]_2(OH)^-$ kind is a delicate matter. Consequently, any ligand with a larger coordination tendency toward Zn^{2+} than that of the N-6,N-7 site of $\epsilon\text{-ATP}^{4-}$ is expected to inhibit the reactivity. Indeed, addition of tryptophan (up to a fivefold excess), leading to the formation of ternary $M(\epsilon\text{-ATP})(Trp)^{3-}$ complexes [28,133], inhibits dephosphorylation in the Zn^{2+}/ε-ATP system (pH_0 7.00; $[\epsilon\text{-ATP}]_{tot} = [Zn^{2+}]_{tot} = 10^{-3}$ M) [86]. Furthermore, from Figs. 30B and 30C it is evident that even the formation of the simple ternary $Zn(\epsilon\text{-ATP})(OH)^{3-}$ complex inhibits the dephosphorylation process. This observation is understandable if one assumes for $Zn(\epsilon\text{-ATP})^{2-}$, as has been proved for several $M(ATP)^{2-}$ systems [65,87,88]

(Section E(iii)), that hydroxo complex formation is connected with a release of the base moiety from the coordination sphere of the metal ion. Indeed, at pH > 8.7 the Zn^{2+} 1 : 1 systems with ϵ-ATP and ATP show the same reactivity, which also at pH > 9.5 approaches that of the Zn^{2+}/CTP 1 : 1 system (see Fig. 27).

(iv) Composition and structure of the reactive species in the Cu^{2+}-facilitated dephosphorylation of ϵ-ATP

The following facts, outlined in Section H(ii), regarding the composition of the most reactive species have to be considered: (i) the Cu^{2+} : ϵ-ATP ratio is 2 : 1 (Fig. 28); (ii) the intermediate is of a monomeric nature (Fig. 29); (iii) there are indications that the nucleophilic attack occurs intramolecularly via a $Cu(OH)^+$ unit [86]. Hence the most reactive intermediate has the composition Cu_2(ϵ-ATP)$(OH)^-$, which corresponds to that deduced for the reactive intermediate in M^{2+}/R–TP systems (Section D; Fig. 12). However, the Cu^{2+}/ϵ-ATP 1 : 1 system at pH 7 is more reactive by a factor of about three than the corresponding CTP system (see Figs. 5 and 27). Hence the increased reactivity of Cu^{2+}/ϵ-ATP has to be attributed to the high affinity of the N-6,N-7 site in the ϵ-adenine residue [28]. Taking this into account [86], the likely structure for the most reactive species formed during the Cu^{2+}-promoted dephosphorylation of ϵ-ATP is given in Fig. 31.

For the observed reactivity shown in Fig. 27 for the Cu^{2+}/ϵ-ATP 1 : 1 system at pH > 5 (see Section H(ii)) several explanations may be offered [86], which are partly related to those given in Section D(iv) for M^{2+}/R–TP 1 : 1 systems.

(i) The position of the equilibrium (22)

$$2Cu(\epsilon\text{-ATP})^{2-} + H_2O \rightleftharpoons Cu_2(\epsilon\text{-ATP})(OH)^- + H^+/\epsilon\text{-ATP}^{4-} \qquad (22)$$

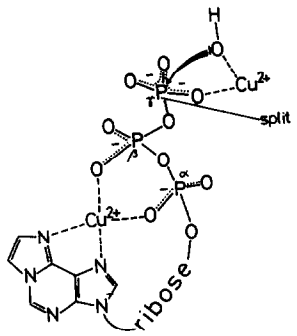

Fig. 31. Probable structure of the reactive Cu_2(ϵ-ATP)$(OH)^-$ complex formed during the Cu^{2+}-promoted dephosphorylation of ϵ-ATP (see text).

may be such that some reactive $Cu_2(\epsilon\text{-ATP})(OH)^-$ species are formed; more of these may be formed according to equilibria (10) and (11) as discussed in Section D(iv).

(ii) $Cu(\epsilon\text{-ATP})^{2-}$ could well be directly suitable for dephosphorylation via water attack. It seems possible that the strong back-binding to the N-6,N-7 site [28] may enforce in an intramolecular equilibrium the formation of some $Cu(\epsilon\text{-ATP})^{2-}$ with only γ-phosphate coordination (instead of the usual β,γ binding) thus favoring an intermolecular water attack at the γ group.

(iii) A further possibility connected with point (ii) is the formation of some $Cu(\epsilon\text{-ATP})(OH)^{3-}$ isomer in which the metal ion is only coordinated to N-6,N-7 and the γ-phosphate group, allowing thus an *intra*molecular attack at the γ phosphorus of an also bound OH^-; clearly, the normally formed $Cu(\epsilon\text{-ATP})(OH)^{3-}$ species is not very reactive as is indicated by the results seen in Fig. 27 at pH > 9.

A reactive species with a structure such as that shown in Fig. 31 is expected to be rather sensitive to the presence of other ligands. Indeed, addition of 2,2′-bipyridyl or tryptophan to the Cu^{2+}/ϵ-ATP 1 : 1 system drastically inhibits the dephosphorylation process (see Fig. 2 and Fig. 8 respectively in ref. 86) owing to the formation of ternary $Cu(Bpy)(\epsilon\text{-ATP})^{2-}$ or $Cu(\epsilon\text{-ATP})(Trp)^{3-}$ complexes [28]. The decrease in reactivity in the Cu^{2+}/ϵ-ATP 1 : 1 system at pH > 9 (Fig. 27) is most probably also due to the formation of a ternary complex, i.e. $Cu(\epsilon\text{-ATP})(OH)^{3-}$ [86]. It is understandable that in this case hydroxo complex formation occurs only at a rather high pH because in $Cu(\epsilon\text{-ATP})^{2-}$ the equatorial part of the Cu^{2+} coordination sphere is saturated and therefore the substitution of N-6 and/or N-7 needs a relatively large OH^- concentration. Indeed, in the pH range of about 10 the reactivities in the Cu^{2+} systems of ATP, ϵ-ATP or CTP become comparable (see Figs. 5 and 27), an observation in accordance with a release of the base moiety in $Cu(\epsilon\text{-ATP})(OH)^{3-}$.

A comparison of the mechanistic details summarized in this and the preceding sections for the Cu^{2+} and Zn^{2+}/ϵ-ATP systems respectively with the results for the corresponding ATP systems (Section E) leads to two obvious questions [86]: (i) Why is the pathway for the dephosphorylation of ATP and ϵ-ATP the same with Zn^{2+} as promoter? (ii) Why does the dephosphorylation reaction in the Cu^{2+}/ATP system proceed via dimers, i.e. via $[Cu_2(ATP)]_2$, $[Cu_2(ATP)]_2(OH)^-$ (Fig. 20) and $[Cu(ATP)]_2(OH)^{5-}$ (Fig. 21), and in the Cu^{2+}/ϵ-ATP system via monomers (Fig. 31)?

This difference in the pathways of the dephosphorylation must be connected with the N-6,N-7 site in ϵ-ATP as this is the only difference from ATP (Fig. 1). Hence the reason could be the increased coordination tendency of the N-6,N-7 site in $\epsilon\text{-ATP}^{4-}$ compared with that of N-7 in ATP^{4-}

[28]; however, this suggestion is not convincing, as a corresponding change in the coordination affinities for Zn^{2+} did not alter the reaction mechanism (Section H(iii)). Therefore it seems more probable that a geometric or steric factor and the degree of saturation of the coordination sphere are responsible for the mechanistic differences. With ATP^{4-} only three equatorial binding sites of the tetragonal Cu^{2+} ion are occupied (β,γ phosphate and N-7), while with ϵ-ATP^{4-} the equatorial positions are saturated (β,γ phosphate, N-6 and N-7), thus probably enforcing the different pathway. Zn^{2+} with the possibility for a hexadentate octahedral coordination sphere is more adaptable with regard to the steric conditions required for dimer formation (Fig. 20).

I. COMMON FEATURES OF THE REACTIVE INTERMEDIATES IN M^{2+}-PROMOTED DEPHOSPHORYLATIONS OF TRIPHOSPHATES

Among the four most reactive intermediates encountered so far in M^{2+}/NTP systems and described in this account three contain an M^{2+}/NTP composition of 2 : 1, as is clearly shown by the results from Job's series; only for the Cu^{2+}/ATP 1 : 1 system the most reactive M^{2+}/ATP ratio is in part 1 : 1. As discussed in Section E(v), this latter system is a special case because at pH $\geq$ 6.5 the second Cu^{2+} simply hydrolyzes away and the 2 : 1 and 1 : 1 systems then display the same reactivity (Fig. 13). It is evident that this observation is closely connected with the large tendency of Cu^{2+} to form hydroxo complexes. The corresponding reactive intermediate is dimeric and has the composition $[Cu(ATP)]_2(OH)^{5-}$, for which the structure given in Fig. 21 was proposed. There is the possibility, as discussed in Section E(v), that an analogous species is also responsible for the reactivity in other M^{2+}/ATP (or purine-NTP) 1 : 1 systems, but this is not certain because for all other metal ions studied the reactivity of the 2 : 1 systems is significantly larger than that of the 1 : 1 systems; hence this question has to remain open. However, the fact that the structures shown in Figs. 20 and 21 are related to each other is obvious and was discussed in Section E(v).

Considering that many of the enzyme–nucleotide systems operating in nature contain two or more metal ions [9,10,134–138], the three reactive intermediates with an M^{2+}/NTP ratio of 2 : 1 appear especially interesting and warrant further discussion. To facilitate comparisons the proposed structures for these three intermediates are collected in Fig. 32.

All three structures in Fig. 32 have in common that one metal ion is coordinated to the terminal γ-phosphate group and the other to the α,β groups. This kind of coordination labilizes the γ-phosphate group and facilitates nucleophilic attack at the γ phosphorus [21,22,65,71]. As coordination of a single metal ion to a triphosphate chain, as in $M(R\text{–}TP)^{2-}$,

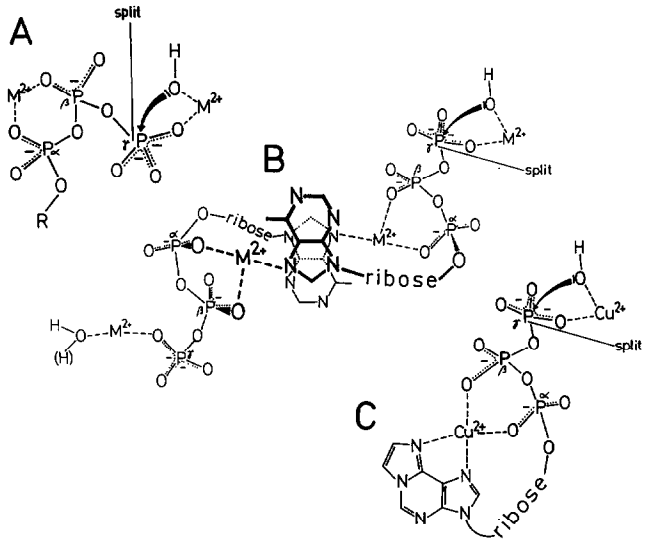

Fig. 32. Comparison of the three types of most reactive species which contain a metal ion-to-nucleotide ratio of 2:1 and which are formed during the metal-ion-promoted dephosphorylations of nucleoside 5′-triphosphates. **A**, Probable structure of the reactive M_2(R–TP)$(OH)^-$ species formed with triphosphates having a non-coordinating organic residue (Section D(iv)). **B**, Proposed structure for the reactive $[M_2(ATP)]_2(OH)^-$ dimer, which occurs in low concentration during the dephosphorylation of ATP and other purine-NTPs (Sections E(v), F and H(iii)). **C**, Example of a monomeric reactive species with metal-ion backbinding to well-positioned sites of the organic residue; the probable structure of the reactive Cu_2(ε-ATP)$(OH)^-$ complex is shown (Section H(iv)).

occurs in an $(\alpha),\beta,\gamma$ fashion, it is understandable why 1 : 1 systems, as long as no mixed-ligand hydroxo complexes are formed, are usually not very reactive. Furthermore, it is evident that the second metal ion has to enforce the reactive M(α,β)–M(γ) structure, and therefore the dephosphorylation process is usually accelerated by an excess of metal ions.

Comparisons between structures **A** and **B** or **C** in Fig. 32 make it quite clear that it is the additional interaction of the metal ion with N-7 in the dimer **B** and with the N-6,N-7 site in the monomer **C** that facilitates the shift of the one metal ion into the α,β position. It is this facilitation that is responsible for the higher reaction rates observed in systems able to form intermediates of the type **B** or **C**.

For triphosphates with a non-coordinating organic residue, such as methyl triphosphate (Section D(iv)), the dephosphorylation proceeds in the presence of excess metal ions by a reactive species as indicated in structure **A**; the reactivity of M_2(R–TP) solely via water attack is low. ATP exhibits a pronounced tendency for self-stacking. This together with the M^{2+}–N-7 interaction leads to the formation of dimeric $[M_2(ATP)]_2$ species (structure **B**) which may be dephosphorylated by an intramolecular attack of coordi-

nated OH^- or (less effectively) under certain conditions via an intermolecular water attack (Sections E(iv)–E(vi) and H(iii)). A reactive species of the kind corresponding to structure **C** in Fig. 32 is so far encountered only in the Cu^{2+}/ε-ATP 2:1 system (Section H(iv)), but there are indications (Section F) that in M^{2+}/ITP and GTP systems in the higher pH range, where $M(NTP-H)^{3-}$ complexes are formed by deprotonation of N-1, an analogous species may become reactive. However, in the lower pH range, dephosphorylation of M^{2+}/ITP and GTP 2:1 systems proceeds via a reaction path involving a species analogous to that given in structure **B** in Fig. 32.

So far not much is known about the metal-ion-promoted dephosphorylation of nucleoside 5′-diphosphates, but Cu^{2+} is able to promote this process in ADP [55] as well as in IDP, GDP and CDP [69]. On the basis of the experience summarized in Fig. 32 one may predict that the most reactive species will contain two metal ions per diphosphate residue leading to an $M(\alpha)$–$M(\beta)$ coordination (similar to structure **A**) thereby labilizing the β group. This type of coordination has again to be enforced by binding of the second metal ion, as in the simple $M(NDP)^-$ 1:1 complex α,β coordination occurs. A facilitated $M(\alpha)$–$M(\beta)$ binding may again be brought about by additional M^{2+} interactions analogous to those shown in structures **B** and **C**.

In connection with the mechanistic aspects it should also be pointed out that the split indicated in the three structures in Fig. 32 is in agreement with studies employing ^{18}O. In the metal-ion-promoted dephosphorylation and also in the enzyme-catalyzed cleavage of the terminal P–O–P bond [139–145], the incorporation of ^{18}O from water occurs into PO_4^{3-}, which is derived from the γ-phosphate group of the NTPs.

Finally, as the nucleophilic attack by a metal ion bound hydroxide occurs in an intramolecular fashion (Fig. 32), the development of a pentacoordinated [146,147] transition state is implied, i.e. a metaphosphate-type [148] intermediate is not expected [65] to develop during a metal-ion-promoted phosphoryl transfer process as considered here.

J. COMPARISON OF THE DEPHOSPHORYLATION RATES IN VARIOUS M^{n+}/NTP SYSTEMS

Considering that experiments with different metal ions have often been carried out under different conditions, and that the reaction path of the dephosphorylation process in different systems may also proceed via different reactive intermediates (see for example Fig. 32), as discussed in Section I, it is not surprising to find conflicting views in the literature regarding the effectiveness of various metal ions in the promotion of NTP dephosphorylations.

Possible reasons for the efficiency differences among metal ions in promoting the dephosphorylation process have already been discussed in Section G. The object of this section is to provide guidance and also some material for comparative analyses of metal ion promoted NTP dephosphorylations. All the experimental data considered refer to identical conditions ($I = 0.1$ M, $NaClO_4$; 50 °C), and the reactivity is (mostly) quantified by the initial rates for phosphate liberation, i.e. $v_0 = d[PO_4]/dt$ ($M\ s^{-1}$). This evaluation method is independent of the order of the reaction, be it first order (structures **A** or **C** in Fig. 32) or second order (Fig. 21 or **B** in Fig. 32), and of the reaction mechanism.

(i) "Pitfalls" in reaction rate comparisons of different systems

In comparing rates of reactions, one should be aware that any comparison is strictly valid only for those conditions under which the data have been obtained. Any extrapolation, for example, to other pH regions or to other concentrations is dangerous.

For example, the effectiveness of Zn^{2+} and Cd^{2+} at the M^{2+}/ATP 1 : 1 ratio in 10^{-3} M aqueous solutions is identical at pH 5.5 and 7.5 (cf. Fig. 13). However, the maximum rates are observed at different pH values: the Zn^{2+} system reaches its peak at pH about 8 and the Cd^{2+} system only at pH 10, i.e. at pH > 8, the reactivity in the Zn^{2+}/ATP 1 : 1 system decreases while it is still increasing in the Cd^{2+} system (Fig. 13). The consequence is a rather similar promotion of the ATP dephosphorylation by Zn^{2+} and Cd^{2+} in the pH range below 8, while at pH 10 the Cd^{2+} system is more reactive by a factor of at least 50.

Similarly, if the Cd^{2+} and Cu^{2+}/ATP 1 : 1 systems are compared (Fig. 13), the promotion by Cd^{2+} at pH 10 is only about 1/6 less pronounced than that by Cu^{2+} at pH 6.5, i.e. the pH where Cu^{2+}/ATP reaches its maximal reactivity, while at pH 7.5, Cd^{2+} is less efficient by a factor of 1/30 than Cu^{2+} at the same pH. Moreover, a comparison of the rates at pH 10 indicates about a tenfold higher reactivity for the Cd^{2+} system.

Another more serious problem in attempting extrapolations relates to the different proportionalities between the initial rates of the dephosphorylation and the concentrations of the reactants. These different proportionalities have often been neglected in the literature, and therefore false comparisons have been made.

To make this important point clearer the initial rates of dephosphorylation for several M^{n+}/NTP 2 : 1 systems at pH_0 5.5 have been collected in Table 3. There are several points to be noted. For example, (i) in 10^{-3} M ATP solutions $(tn)_2Co^{3+}$ is the best promoter of the dephosphorylation reaction with a promotion factor of 1200; Cu^{2+} with a factor of 270 is

TABLE 3

Comparison of the initial rate of dephosphorylation, v_0 (M s^{-1}), for the 2:1 systems of Cu^{2+}/UTP, Cu^{2+}/ATP and $(tn)_2Co^{3+}$/ATP at pH_0 5.5 in 10^{-3} and 10^{-1} M NTP solutions ($I = 0.1$ M, $NaClO_4$; 50 °C). [a] All initial rates are given as $v_0 \times 10^8$

2:1 system	NTP concentration			
	10^{-3} M		0.1 M [b]	
	$v_0 \times 10^8$	PF [c]	$v_0 \times 10^8$	PF [c]
NTP, alone	0.11	*1*	11	*1*
Cu^{2+}/UTP	0.7	*6.4*	70	*6.4*
Cu^{2+}/ATP	30	*270*	300000	*27000*
$(tn)_2Co^{3+}$/ATP[d,e]	130	*1200*	200000	*18000*

[a] The above data are collected from Table I and the text on p. 3320 of ref. 40. [b] These values were calculated from the known proportionalities between the initial rates and the concentrations of the reactants (see ref. 40). [c] The values given in *italics* are the promotion factors (PF) based on the dephosphorylation rate of the corresponding NTP alone. For example, PF = 0.7/0.11 = 6.4. [d] The properties of the $(tn)_2Co^{3+}$/UTP system are hardly different from those of the $(tn)_2Co^{3+}$/ATP system [40]. [e] tn, trimethylenediamine (1,3-diaminopropane).

considerably less effective. (ii) However, in 0.1 M ATP solutions, Cu^{2+} accelerates the ATP dephosphorylation by a factor of 2.7×10^4 and is therefore even more effective than $(tn)_2Co^{3+}$ with a promotion factor of only 1.8×10^4. (iii) For the Cu^{2+}/UTP 2:1 system one arrives at the same low promotion factor of 6.4 for both concentrations, because it is a first-order reaction (i.e. $v_0 \propto [2Cu^{2+}/UTP]$; cf. Section D(iii)), while for the 2:1 systems of Cu^{2+}/ATP and $(tn)_2Co^{3+}$/ATP, quite different promotion factors are obtained because their reaction orders are higher, i.e. $v_0 \propto [2\ Cu/ATP]^2$ (Section E(ii)) and approximately $v_0 \propto [2\ (tn)_2Co^{3+}/ATP]^{1.6}$ (cf. ref. 40) respectively. (It should be noted that here and elsewhere in this section the given proportionalities, i.e. $v_0 \propto [\cdots]$, always refer to the concentration of NTP, while the given equivalents of M^{n+} define the system.)

A further example of rate comparisons at different reactant concentrations is given in Table 4 for some M^{2+}/NTP 1:1 systems at pH_0 7.00. At 10^{-4} M concentrations of ϵ-ATP (Section H), Cu^{2+} promotes the dephosphorylation by a factor of 18, while Zn^{2+} does so only with a promotion factor of 2.4. However, in 10^{-2} M ϵ-ATP solutions, Zn^{2+} with a promotion factor of 240 is, quite unexpectedly, much more effective than Cu^{2+}, which is still promoting the reaction only by the factor of 18. The reason is again the different proportionality between initial rate v_0 and the total reactant concentration. With Cu^{2+} the reaction proceeds via a monomer ($v_0 \propto [Cu^{2+}/\epsilon\text{-ATP}]$; Fig. 31), but with Zn^{2+} via a dimer ($v_0 \propto [Zn^{2+}/\epsilon\text{-ATP}]^2$; Section H(ii); Fig. 20). This example illustrates further the difficulties and

TABLE 4

Comparison of the initial rate of dephosphorylation, v_0 (M s^{-1}), of ε-ATP, ATP and CTP (NTP) in 10^{-4}, 10^{-3} and 10^{-2} M solutions in the presence of equivalent amounts of Cu^{2+} or Zn^{2+} (1:1 ratio) at pH_0 7.00 ($I = 0.1$ M, $NaClO_4$; 50 °C). All initial rates are given as $v_0 \times 10^8$. (This table is reprinted from Table II of ref. 86 (Inorganic Chemistry, 1986) with permission of the American Chemical Society.)

System	Concentration of reactants					
	10^{-4} M		10^{-3} M		10^{-2} M	
	$v_0 \times 10^8$	PF [a]	$v_0 \times 10^8$	PF [a]	$v_0 \times 10^8$	PF [a]
NTP, alone	0.005	*1*	0.05	*1*	0.5	*1*
Cu^{2+}/ε-ATP	0.09	*18*	0.9	*18*	9	*18*
Zn^{2+}/ε-ATP	0.012	*2.4*	1.2	*24*	120	*240*
Cu^{2+}/ATP	0.18	*36*	18	*360*	1800	*3600*
Zn^{2+}/ATP	0.0023	*0.46*	0.23	*4.6*	23	*46*
Cu^{2+}/CTP	0.03	*6*	0.3	*6*	3	*6*
Zn^{2+}/CTP	0.007	*1.4*	0.07	*1.4*	0.7	*1.4*

[a] The values given in italics are the promotion factors (PF) based on the dephosphorylation rate of the corresponding NTP alone. For example, PF = 0.09/0.005 = 18.

"pitfalls" in making general statements about the relative promotional effects of different metal ions in NTP dephosphorylations, because different dependences between rate and concentrations may exist.

In addition, it is obvious from Table 4 that for ATP the Cu^{2+}/Zn^{2+} activity ratio stays constant over the reactant concentration range considered, Cu^{2+} being about 80 times more effective than Zn^{2+} at pH_0 7.00. However, for both ATP 1:1 systems, i.e. with Cu^{2+} or Zn^{2+}, the promotion factors increase with increasing ATP concentration (because $v_0 \propto [M^{2+}/ATP]^2$; Section E(ii)). This is clearly different for the Cu^{2+} or Zn^{2+}/CTP 1:1 systems, for which the promotion factors are low and constant (here $v_0 \propto [M^{2+}/CTP]$; Section D(iii)).

It is evident from the examples given in Tables 3 and 4 that, depending on the reaction conditions employed, one can arrive at different conclusions. Thus at low reactant concentrations, small or moderate accelerations are generally seen, while at high concentrations large rate enhancements may more often be "celebrated". Clearly, the very worst type of comparison is between different systems which have been studied at different concentrations without taking into account the possibly different proportionalities between rate and reactant concentrations.

However, if one wants to "feast" in large promotional factors one may do so by selecting for comparison a system of low reactivity. For example, it may be argued that the rate in Table 3 for the Cu^{2+}/ATP 2:1 system at pH_0 5.5 should *not* be compared with the rate for ATP at the same pH,

because here $H(ATP)^{3-}$ is the species present in solution, while in Cu^{2+}/ATP the promotional effect of Cu^{2+} on ATP^{4-} is measured, because the reactive species is ultimately derived from $Cu(ATP)^{2-}$ (Section E(v)). Hence on the basis of these arguments, the comparison may be made with ATP^{4-} (which exists at pH 9.5), for example, for 0.1 M reactant solutions. Thus $v_0 = 3 \times 10^{-3}$ M s^{-1} for Cu^{2+}/ATP 2:1 at pH_0 5.5 (Table 3) is compared with $v_0 = 1.5 \times 10^{-8}$ M s^{-1} for ATP^{4-} (Tables 1 and 4; pH_0 9.5) and this then gives the impressive promotion factor (PF) of 2×10^5. Certainly such a comparison is also valid, but if applied it must be unequivocally defined.

(ii) Rate comparisons for some M^{n+}/NTP 2:1 systems, and the effect of charge at the metal center on the dephosphorylation rate

In this section the effects of some selected divalent metal ions (Mg, Mn, Ni, Cu, Zn, Cd) and trivalent metal ions (Co, Y, La) on the dephosphorylation process of ATP and UTP in 2:1 systems at pH_0 5.5 and 7.5 will be compared; the corresponding rate data are collected in Table 5. Data for 2:1 systems were selected in accord with the discussed experience available for divalent metal ions (e.g. Fig. 32), and because previous results [40] with $(tn)_2Co^{3+}$, Y^{3+} or La^{3+}/NTP also provide evidence, despite some experimental difficulties experienced with Y^{3+} and La^{3+}, that effective metal ion promotion of NTP dephosphorylation requires the formation of species involving more than one metal ion per NTP. Indeed, for the ATP system there are indications that two complexes which have the compositions $[(tn)_2Co]_2(ATP)^{2+}$ and $[(tn)_2Co]_3(ATP)^{5+}$ are involved in the formation of the most reactive species at pH_0 6.50 [32,40]. Of course, at this pH at least part of the positive charges in these two species or in their derivatives will be compensated by coordinated OH^-.

The data in Table 5 provide evidence that at pH 5.5 and 7.5 some metal ions even inhibit somewhat the dephosphorylation process, most are poor promoters, among them Mg^{2+}, while only a few metal ions are really effective promoters of the dephosphorylation of ATP and UTP in 10^{-3} M NTP solutions. For example, at pH_0 7.5 in a 2:1 ratio Zn^{2+} facilitates the ATP dephosphorylation by a factor of about 40, and Cd^{2+} or Cu^{2+} by promotion factors of 100 and 230 respectively. However, the promotion is really pronounced only with the trivalent ions: for the $(tn)_2Co^{3+}$, Y^{3+} or La^{3+}/ATP systems factors of more than 2000 are obtained. Promotion of the UTP dephosphorylation by the divalent metal ions under the same condition is much poorer, which is expected (see Sections C, D, E, G and I), while with the trivalent ions the promotional effects are comparable with those observed with ATP. This indicates that the nucleic base residues have no influence on the reactivity of the mentioned trivalent metal ions.

TABLE 5

Comparison of the initial rate of dephosphorylation v_0 (M s^{-1}) for M^{n+}/NTP 2:1 systems of 10^{-3} M and 10^{-2} M NTP solutions at pH_0 5.5 and 7.5 (I = 0.1 M, $NaClO_4$; 50 °C). [a] All initial rates are given as $v_0 \times 10^8$

NTP (conc.)	M^{n+}	pH_0 5.5		pH_0 7.5	
		$v_0 \times 10^8$	PF [b]	$v_0 \times 10^8$	PF [b]
ATP	None	0.11	*1*	0.032	*1*
(10^{-3} M)	Mg^{2+}	0.11	*1*	0.050	*1.6*
	Mn^{2+}	0.2	*1.8*	0.15	*4.7*
	Ni^{2+}	0.1	*0.9*	0.14	*4.4*
	Cu^{2+}	30	*270*	7.5	*230*
	Zn^{2+}	0.5	*4.5*	1.2	*38*
	Cd^{2+}	0.7	*6.4*	3.2	*100*
	$(tn)_2Co^{3+}$	130 [c]	*1200*	~ 80 [c]	*~ 2500*
	Y^{3+}	~ 8 [c]	*~ 70*	~ 70 [c]	*~ 2200*
	La^{3+}	~ 7	*~ 65*	70 [c]	*2200*
UTP [d]	None	0.11	*1*	0.032	*1*
(10^{-3} M)	Mg^{2+}	0.062	*0.56*	0.041	*1.3*
	Mn^{2+}	0.1	*0.9*	0.09	*2.8*
	Ni^{2+}	0.064	*0.58*	0.057 [e]	*1.8*
	Cu^{2+}	0.7	*6.4*	—	—
	Zn^{2+}	0.1	*0.9*	~ 0.7 [c]	*~ 22*
	Cd^{2+}	0.13	*1.2*	~ 0.8 [c]	*~ 25*
	$(tn)_2Co^{3+}$	120 [c]	*1100*	65 [c]	*2000*
	Y^{3+}	~ 8 [c]	*~ 70*	~ 70 [c]	*~ 2200*
	La^{3+}	7	*65*	~ 70	*~ 2200*
ATP	None	1.1	*1*	0.32	*1*
(10^{-2} M)	Cu^{2+}	3000	*2700*	750	*2300*
	$(tn)_2Co^{3+}$	~ 5000	*~ 4500*	~ 4000	*~ 12500*
UTP [d]	None	1.1	*1*	0.32 [e]	*1*
(10^{-2} M)	Cu^{2+}	7	*6.4*	—	—
	$(tn)_2Co^{3+}$	~ 5000	*~ 4500*	~ 3000	*~ 9400*

[a] The v_0 values are taken from Tables I and II of ref. 40. [b] The values given in italics are the promotion factors (PF) based on the dephosphorylation rate of the corresponding NTP alone. For example, 0.2/0.11 = 1.8. [c] Measured despite the appearance of a precipitate [40]. [d] The same results have also been obtained with CTP for the following entries: none, Ni^{2+}, Cu^{2+}, Zn^{2+} and Cd^{2+} [40]. [e] Precipitation.

In 10^{-2} M NTP solutions the promotional effects are even more dramatic (see Section J(i)). For example, at a 2:1 ratio and pH_0 5.5, one observes a 2700-fold increase for Cu^{2+}/ATP and about a 4500-fold increase for $(tn)_2Co^{3+}$/ATP or UTP compared with the non-promoted reaction (Table 5). However, it is also evident that the promotion of the dephosphorylation

process in the Cu^{2+}/UTP system is considerably less pronounced: the increase is still only 6.4-fold. Clearly, these reaction patterns, as far as the divalent metal ions are concerned, can now easily be understood: the initial rate for pyrimidine-NTPs is proportional to the concentration of M^{2+}/NTP (i.e. a simple first-order dependency is observed; Section D(iii)), while for ATP it is proportional to the square of the concentration of M^{2+}/ATP (i.e. a second-order dependency is obtained; Section E(ii)).

It is apparent that with $(tn)_2Co^{3+}$, the matter is more complicated (Table 5). Although the ATP and UTP systems behave similarly within experimental error [40], the initial rate increases clearly more than tenfold, but less than 100-fold, in going from NTP concentrations of 10^{-3} to 10^{-2} M. In the 1 : 1 systems, the increase is about 20-fold at pH_0 5.5 and 40-fold at pH_0 7.5 [40], while in the 2 : 1 systems (Table 5) it is about 40- and 50-fold at the respective pH values. This indicates that in the reactive species, complex associations are involved. (As a first approximation one may conclude [40] that for 2 : 1 systems in the NTP concentration range of 10^{-3}–10^{-2} M, the proportionality between initial rate and reactant concentration is represented by $v_0 \propto [2\ (tn)_2Co^{3+}/NTP]^{1.6}$.)

Whatever the factors determining and limiting the reaction rate in the $(tn)_2Co^{3+}$/NTP systems may finally be [40], the 2 : 1 ratio gives systems with a high reactivity toward dephosphorylation (Table 5). Hence the following question arises: what are the reasons for this high reactivity? Is there a charge effect involved?

Before answers are sought, it seems wise to evaluate first the best possible basis to be used in the rate comparisons. In this connection it should be recalled that the promotion of the dephosphorylation of ATP by Cu^{2+} and other divalent metal ions with an M^{2+}–N-7 interaction is much larger than that of pyrimidine-NTPs such as UTP, or of simple triphosphate esters, R–TP (Sections C, G and I). This decreased reactivity of R–TP systems is due to the reduced or even completely missing stacking tendency of these triphosphates and the absence of N-7, or a corresponding binding site, which facilitates the creation of the reactive species in the ATP systems (Fig. 32). It is evident that no explanation based on the nucleic base residue is feasible for an explanation of the reactivity of the $(tn)_2Co^{3+}$/NTP systems because here ATP and UTP behave alike. Hence, as in $(tn)_2Co^{3+}$/NTP systems a metal ion–base interaction plays no role [40], reaction rates of these systems should only be compared with those of M^{2+}/UTP systems if effects other than an M^{n+}–base interaction are to be evaluated. Furthermore, because the tendency to form hydroxo complexes, an important feature in dephosphorylations (Fig. 32), is of a similar order for Cu^{2+} and $(tn)_2Co^{3+}$ [40], an appropriate comparison is between these two metal ions.

The charge in Cu^{2+} and $(tn)_2Co^{3+}$ is obviously different, and the results

of the corresponding M^{n+}/UTP 2:1 systems in Table 5 at pH_0 5.5 and 10^{-3} M UTP solutions indicate that this charge effect is quite significant: $(tn)_2Co^{3+}$ is more effective than Cu^{2+} by a factor of about 170; in 10^{-2} M UTP solutions, but otherwise under the same conditions, this factor is about 700.

That the described difference in reactivity between the Cu^{2+}/UTP and $(tn)_2Co^{3+}$/UTP 2:1 systems is indeed associated with a charge effect is supported by the experiments with Y^{3+} and La^{3+}, despite the fact that they were somewhat hampered by precipitation [40]. In the 2:1 ratio and at pH_0 7.5, all three trivalent metal centers, including $(tn)_2Co^{3+}$, show the same reactivity in 10^{-3} M UTP solutions (Table 5). Under the same conditions but at pH_0 5.5, Y^{3+} and La^{3+} are less effective than $(tn)_2Co^{3+}$ by a factor of about 15 owing to their lower tendency to form hydroxo complexes. The species $(tn)_2Co(OH)(OH_2)^{2+}$ reaches its maximum degree of formation at pH 6.5 [129], while with lanthanide ions hydroxo complex formation only begins at pH > 6.5 [149].

(iii) Dephosphorylation rates in ATP systems containing two different metal ions. Synergistic effects

From the accumulated results it is evident that the most reactive species usually contain two metal ions per NTP (e.g. Figs. 10, 15 and 28). To evaluate the effect of a metal ion different from that already present in an M^{n+}/ATP 1:1 complex the rate data given in Table 6 were compiled. For this comparison the $(tn)_2Co^{3+}$/ATP and Cu^{2+}/ATP 1:1 systems in 10^{-3} M ATP solutions at pH_0 5.5 were selected, because in both cases the addition of one further equivalent of the same kind of metal ion already present promotes the dephosphorylation rate quite significantly (Tables 5 and 6) [40,64,65]; it seemed therefore interesting to learn something about the effect of other metal ions on the dephosphorylation rate in these two M^{n+}/ATP 1:1 systems.

It is evident from Table 6 that the addition of Mg^{2+} or Ni^{2+} to $(tn)_2Co(ATP)^-$ has nearly no effect on the dephosphorylation rate. With Zn^{2+} the situation is somewhat better: with a fivefold excess a nearly eightfold rate acceleration is achieved. A moderate promotion by a factor of about 40 results with a fivefold excess of Cu^{2+} or $Cu(Bpy)^{2+}$. However, compared with the nearly 300-fold rate enhancement with a single equivalent of $(tn)_2Co^{3+}$, this is not very impressive.

The last result indicates again that the charge of the metal center is important (see Section J(ii)): most probably the extent of complex formation between $(tn)_2Co(ATP)^-$ and M^{n+} is larger for the $1-/3+$ interaction than for a $1-/2+$ interaction. In line with this interpretation, $Cu(Bpy)^{2+}$ is

TABLE 6

Additional promotion of the initial rate of dephosphorylation v_0 (M s^{-1}) of two M^{n+}/ATP 1:1 systems ($[M^{n+}] = [ATP] = 10^{-3}$ M) by the addition of one or five extra equivalents of M^{2+} at pH_0 5.5 ($I = 0.1$ M, $NaClO_4$; 50 °C). [a] All initial rates are given as $v_0 \times 10^8$

M^{n+} of M^{n+}/ATP = 1:1	Extra M^{n+}	$v_0 \times 10^8$	
		At extra $[M^{n+}] = 10^{-3}$ M	At extra $[M^{2+}] = 5 \times 10^{-3}$ M
$(tn)_2Co^{3+}$	None	0.45	0.45
	Mg^{2+}	0.66	0.96
	Ni^{2+}	0.40	0.81
	Zn^{2+}	1.6	3.5
	Cu^{2+}	5.3	16
	$Cu(Bpy)^{2+}$	6.9	18
	$(tn)_2Co^{3+}$	130	
Cu^{2+}	None	2.5 [b]	2.5 [b]
	Mg^{2+}	4.4 [c]	9.7 [c]
	Ni^{2+}	6.2 [d]	9.5 [d]
	Cd^{2+}	10.2 [c]	10 [c,e]
	Zn^{2+}	10.5 [c]	14 [c]
	Cu^{2+}	30 [b]	–

[a] The values for the $(tn)_2Co^{3+}$ systems are from Table III of ref. 40. Regarding the $(tn)_2Co^{3+}$/ATP/Cu^{2+} or $Cu(Bpy)^{2+}$ systems an interesting observation has recently been published (10^{-3} M; 1:1:1; pH 6.5; 25 °C) [78]: in the presence of copper there is in addition to phosphate also an initial production of a small amount of pyrophosphate (see also text in Section J(iii)), a reaction not observed with $Cu(Bpy)^{2+}$. [b] From ref. 64; see also Figs. 13, 15 and 16. [c] Interpolated from the data given in Fig. 6 of ref. 65; see also Fig. 19. [d] Interpolated from the data given in Fig. 5 of ref. 64; see also Fig. 19. [e] Measured despite the appearance of a precipitate.

somewhat more effective than Cu^{2+} in promoting the dephosphorylation of the $(tn)_2Co(ATP)^-$ complex. This result reflects the well-known increased coordination tendency of $Cu(Bpy)^{2+}$ compared with Cu^{2+}_{aq} toward the phosphate moiety and other ligands offering O as donor atoms [15,123,150]. Furthermore, it is interesting to note that with regard to the dephosphorylation of $(tn)_2Co(ATP)^-$, $Cu(Bpy)^{2+}$ is at least as effective as Cu^{2+} (Table 6), while with regard to the simple ATP dephosphorylation at the same pH 5.5 (see Fig. 5), $Cu(Bpy)^{2+}$ is an inhibitor and only Cu^{2+} is a promoter.

The above-mentioned results with $Cu(Bpy)^{2+}$ and $(tn)_2Co(ATP)^-$ are also fascinating from a mechanistic point of view. $Cu(Bpy)^{2+}$ has only two strongly coordinating equatorial binding sites left. From its influence, compared with that of Cu^{2+}, on the reaction rate, it follows that both these binding sites are used for coordination to the triphosphate chain. As the reaction most probably proceeds also in this case via an intramolecular

nucleophilic OH^- attack from an M(OH) unit (Fig. 32), one may tentatively suggest the following composition, structure and mechanistic path for the reactive $[(tn)_2Co(OH)(ATP)(Cu(Bpy)]^0$ species: $Cu(Bpy)^{2+}$ coordinating to the α,β-phosphate groups of ATP^{4-} leads to ring opening of the cobalt chelate and to monodentate coordination of $(tn)_2Co(OH)^{2+}$ at the γ group, thus allowing for an intramolecular attack at the γ phosphorus by the cobalt-bound OH^-.

In contrast with the results with $(tn)_2Co(ATP)^-$, already the addition of one equivalent of Mg^{2+}, Ni^{2+} or Cd^{2+} to the Cu^{2+}/ATP 1:1 system has a remarkable promotional effect (Table 6): at a fivefold excess, all three M^{2+} ions show the same limiting rate which is about 1/3 of the limiting rate obtained with Cu^{2+} itself (Fig. 19). As none of the three added ions form hydroxo complexes at pH 5.5, one has to assume that an intermolecular attack by H_2O occurs at the γ phosphorus (Section E(iv)). However, the ability to provide an $M(OH)^+$ unit has an additional promotive effect as is indicated by Zn^{2+}; in this case a fivefold excess leads to a system which has about 1/2 of the reactivity of the Cu^{2+}/ATP 2:1 system (Table 6).

It is evident from the entries in Table 5 that Cu^{2+} has distinctive properties and that one cannot easily replace both Cu^{2+} ions and obtain a suitably reactive species. The Mg^{2+}/ATP or Ni^{2+}/ATP ratios of 2:1 at pH_0 5.5 are completely unreactive, i.e. the dephosphorylation of ATP is not at all facilitated. Keeping in mind that this is quite different in the Cu^{2+}/ATP/Mg^{2+} or Cu^{2+}/ATP/Ni^{2+} 1:1:1 systems, and especially in the 1:1:5 systems (Table 6), it is evident that here synergistic effects are observed. Evidently Cu^{2+} plays a crucial role in the formation of the reactive intermediate in the ATP system, and this must depend on its pronounced coordination tendency towards N-7 (Sections C(ii), E(i) and E(v)). Hence one is tempted to predict that rate enhancements of a similar magnitude will not be observed in mixed Cu^{2+}/UTP/M^{2+} systems. Here a metal ion–base interaction cannot play any role, and therefore any possible mutual promotion could only occur via facilitated formation of an $M(OH)^+$ unit. In accord with this view, one observes that the promotion of the dephosphorylation of $(tn)_2Co(ATP)^-$ and $(tn)_2Co(UTP)^-$ by $Cu(Bpy)^{2+}$ leads to similar results [151]; in neither cobalt complex is a Co^{3+}–base interaction involved (Section J(ii)).

A final question in connection with the above is the following: why is the dephosphorylation of the Cu^{2+}/ATP 1:1 system, on addition of Mg^{2+}, Ni^{2+} or Zn^{2+}, relatively more pronounced than that of the $(tn)_2Co^{3+}$/ATP 1:1 system on addition of the same ions? Two possible reasons are apparent. One is that complex formation between the M^{2+} and the dinegatively charged $Cu(ATP)^{2-}$ (which is on the pathway to the reactive dimer) is expected to be more pronounced than that between M^{2+} and $(tn)_2Co(ATP)^-$

which carries only a single negative charge. The other reason is that the necessary reorganization to achieve the reactive species from $(tn)_2Co(ATP)^-/M^{2+}$ may be somewhat sluggish (see also Section G). Indeed, this latter suggestion is supported by a recent observation [78] that on addition of Cu^{2+} to pre-formed $(tn)_2Co(ATP)^-$ (10^{-3} M; 1:1:1; pH 6.5; 25°C) there is an initial rapid production of a small amount of pyrophosphate (about 3.5% in the first 5 min) which thereafter does not significantly increase further (after 30 min it is still below 5%). This indicates the initial formation of a complex that promotes *depyro*phosphorylation and which then isomerizes to a complex promoting dephosphorylation.

In conclusion, from the comparisons in this section (Table 6) it is evident that in systems containing two different metal ions, one of these may develop a reactivity towards dephosphorylation of NTPs which it does not possess in the absence of the other metal ion. This observation is of interest because many biological phosphoryl and nucleotidyl transfers occur with enzymic systems which involve two different metal ions [9,10,134–138].

K. INTERRELATIONS BETWEEN SOLVENT POLARITY AND DEPHOSPHORYLATION RATES

In recent years it has been well established that the so-called "effective" or "equivalent solution" dielectric constants in proteins [152,153] or in active-site cavities of metalloenzymes [154] are reduced compared with the situation in bulk water. It is now generally agreed that different types of water exist in cells [155,156]. Proteins reduce the effective dielectric constant, in other words the solvent polarity, at their surface or in clefts via hydrophobic regions, i.e. aliphatic or aromatic side-chains of amino-acid residues at the protein–water interface are responsible for this effect [157–159].

In the above context one should remember that the acidity constants of N and O ligands are clearly dependent upon the polarity of the solvent [124,160]. The basicity of N ligands (with no charge) usually decreases as the polarity of the solvent decreases, while the basicity of O ligands (with a negative charge) increases markedly as the dielectric constant decreases. The change in the stability of complexes [124] is in accord with the change in basicity, but with N ligands the stability decreases usually only slightly, as the polarity of the solvent decreases, while with O ligands the increase in stability may be quite pronounced. Indeed, an example of this latter effect is shown in Fig. 33, where the values for $\log K^{Cu}_{Cu(UTP)}$ vs. $pK^{H}_{H(UTP)}$ [15] and $\log K^{Cu}_{Cu(RiMP)}$ vs. $pK^{H}_{H(RiMP)}$ [161] are plotted [162]. The interrelations between ligand basicity and complex stability, and the effect of the decreasing solvent polarity on these interrelations are clearly seen in Fig. 33. If no extra

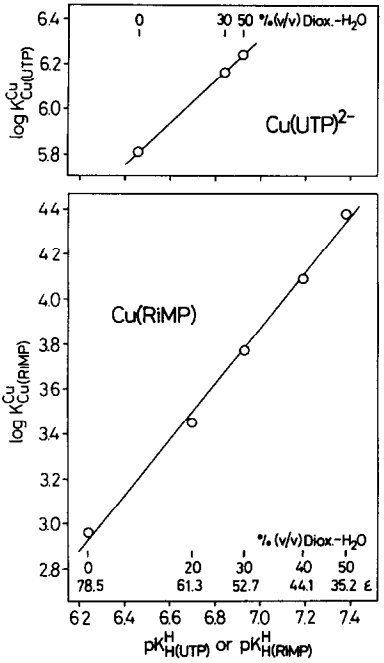

Fig. 33. Relationships between log $K^{Cu}_{Cu(UTP)}$ and $pK^H_{H(UTP)}$, and log $K^{Cu}_{Cu(RiMP)}$ and $pK^H_{H(RiMP)}$ for the $Cu(UTP)^{2-}$ and Cu(RiMP) complexes respectively as they result from the addition of increasing amounts of 1,4-dioxane to the aqueous solutions of the components ($I = 0.1$ M, $NaNO_3$; 25° C). The plotted equilibrium constants are for uridine 5′-triphosphate (UTP) and D-ribose 5′-monophosphate (RiMP) from ref. 15 and ref. 161 respectively. The various percentages of the dioxane–water mixtures (v/v) which correspond to the data points are inserted into the figure; also inserted are the corresponding dielectric constants (ϵ); these latter values are interpolated from the data given in ref. 162.

interactions occur (see for example ref. 15) the slopes of the straight lines are, according to the present experience, always close to unity, at least as far as phosphate or carboxylate ligands are concerned [154,161]. This indicates that the solvent effect on proton binding and on metal ion binding is approximately of the same size.

Results such as those in Fig. 33 suggest that the rate of metal ion promoted dephosphorylations of NTPs is also affected by a decreasing solvent polarity, because the intermediates of these dephosphorylation processes are metal ion complexes (Fig. 32). Moreover, on the basis of the situation indicated for proteins, one may conclude that at the protein–water interface to some extent the properties of a "mixed solvent" are created. Indeed, the "equivalent solution" dielectric constants in the active sites of proteins have been estimated, depending on the protein considered, to be of the order of 70 to 35 [152–154]. Hence an aqueous solution which contains

30% (v/v) 1,4-dioxane seems an appropriate solvent, as the corresponding dielectric constant is close to 50 (see Fig. 33) [162], to mimic in a first rough attempt the polarity existing in the active site of an enzyme.

Unfortunately, so far not many rate data of NTP dephosphorylations have been measured in mixed solvents, but considerations on the dephosphorylation process at reduced solvent polarities are certainly important with regard to the situation in nature. This is why a whole independent section of this review is devoted to this problem, despite the fact that so far only the preliminary data [163(a)] summarized in Table 7 are available [164]. (Added in proof: in the meanwhile further results have been obtained [163(b)].)

Clearly, the relationship between stability, structure and reactivity of the species involved will be difficult to assess, but some conclusions are possible from comparisons between the reaction rates of ATP dephosphorylations valid for water and those valid for 30% (v/v) dioxane–water as solvent (Table 7).

(i) Not only metal ions, but also the proton may facilitate NTP dephosphorylations. This is evident, for example, from the NTP pH–rate profile in the low pH region in Fig. 5. In accord herewith a solvent change from water to 30% dioxane–water changes at pH 7.5 the degree of formation of

TABLE 7

Solvent influence on the initial rate of dephosphorylation v_0 (M s^{-1}) of ATP, and of M^{2+}/ATP 1:1 and 2:1 systems in 10^{-3} M ATP solutions at pH_0 7.50 ($I = 0.1$ M, $NaClO_4$; 50 °C). All initial rates are given as $v_0 \times 10^8$

System	Solvent			
	Water		30% dioxane [a]	
	$v_0 \times 10^8$	PF [b]	$v_0 \times 10^8$	PF [b]
ATP, alone	0.032 [c,d]	*1*	0.073	*2.3*
Mg^{2+}/ATP = 1:1	0.045 [c]	*1.4*	0.085	*2.7*
Mg^{2+}/ATP = 2:1	0.050 [d]	*1.6*	0.098	*3.1*
Zn^{2+}/ATP = 1:1	0.25 [c]	*7.8*	0.77	*24*
Zn^{2+}/ATP = 2:1	1.2 [d]	*38*	4.1 [e]	*130*

[a] Preliminary results obtained in 30% (v/v) dioxane–water mixtures as solvent [163(a)]; this corresponds to a mole fraction of 0.083. The direct pH meter readings were used in the experiments, i.e. no "corrections" were applied for the change in solvent from water to the 30% (v/v) dioxane–water mixture, though correction factors have been published for such [164] and related solvent mixtures [160]. [b] The values given in italics are the promotion factors (PF) based on the dephosphorylation rate of ATP in aqueous solution. For example, 0.045/0.032 = 1.4. [c] From Table 1. [d] From Table 5. [e] This reaction solution appeared slightly milky.

$H(ATP)^{3-}$ from about 9% to 17% (calculated with the constants given in ref. 15) and indeed, the reaction rate is also about double, i.e. the promotion factor, though slightly larger, is close to two.

(ii) The rate enhancements observed in the presence of Mg^{2+} or Zn^{2+} are larger, and these cannot simply be due to an increased degree of formation of the $M(ATP)^{2-}$ complexes, because in aqueous solution at pH 7.5 with 10^{-3} M reactant concentrations, $Mg(ATP)^{2-}$ and $Zn(ATP)^{2-}$ are formed already to about 80% and 90% respectively [17].

(iii) From the data given in Fig. 33 it is evident that the degree of formation of the $M(ATP)^{2-}$ complexes in 30% (v/v) dioxane–water will be about the same or possibly somewhat larger. Hence the differences in rate, observed in the different solvents, cannot be due to different degrees of formation of these complexes. Therefore all promotion factors in Table 7 are based on the dephosphorylation rate of ATP in water. In this way they reflect a solvent effect which is independent of the degree of formation of $M(ATP)^{2-}$.

(iv) The stability of the 2 : 1 complexes is lower and it seems feasible that the $M(ATP)^{2-}/M^{2+}$ interaction is favored by a lower solvent polarity and that therefore part of the observed effect is due to an increased formation of $M_2(ATP)$; at least, $Zn_2(ATP)$ is on the way to the reactive dimer (Section E(ii); Fig. 32).

(v) However, keeping in mind point (iv), it is surprising to find that the rate increases for the 1 : 1 *and* 2 : 1 systems to the same extent, i.e. about twofold for Mg^{2+}/ATP and about threefold for Zn^{2+}/ATP by the solvent change from water to 30% dioxane. On the basis of point (iv), different ratios would have been expected for the 1 : 1 and the 2 : 1 systems.

(vi) A partial explanation of this problem (point (v)) seems possible by taking into account that the concentration of Na^+ is relatively large in all these experiments. It is known (see for example Fig. 32) that in the most reactive intermediates, two positively charged ions are bound to the triphosphate chain, and it seems very probable (see also ref. 165) that owing to the decrease in the polarity of the solvent the coordination tendency of Na^+ increases enough to allow its participation in the formation of a reactive species (see also ref. 163(b)).

(vii) Finally, one should not forget an effect due to differences in the solvation of the NTP species in the two solvents, and also one due to differences in the structure of water (hydrogen bonding). Both these properties will certainly be affected by dioxane and it could be that these effects reduce the activation energy of the dephosphorylation process and hence enhance the reaction rates.

Whatever the final explanations for the facilitated dephosphorylations in the mixed solvent will be, the effects can be remarkable. Addition of two

equivalents of Zn^{2+} to a 10^{-3} M ATP solution facilitates the dephosphorylation in aqueous solution 38-fold (Table 7), but the further addition of dioxane, to give a 30% (v/v) dioxane–water mixture, leads to another factor of 3.5 and thus to a total promotional factor of about 130. Considering this result there seems to be no doubt that polarity changes, as they occur in the active sites of enzymes, are important features in determining the rates of transphosphorylations in nature. Indeed, for a related reaction, the synthesis of ATP from ADP and PO_4 by $(Na^+ + K^+)$-ATPase from sheep kidney, it is suggested [165] that the enzyme undergoes a hydrophobic–hydrophilic transition during the catalytic cycle. In agreement herewith, a 200-fold decrease in PO_4 concentration required for half-maximal phosphorylation of the enzyme is observed when 40% (v/v) dimethyl sulfoxide is added to the assay medium.

L. SOME CONCLUSIONS WITH REGARD TO ENZYMIC SYSTEMS

In vitro studies of the metal ion promoted transfer of a phosphoryl group to water may also provide insight into natural processes as has been repeatedly indicated (Sections I, J(iii) and K). Many more correlations could be made but only some are given below.

One of the most pertinent perceptions follows from the results that lead to structures **A**, **B** and **C** in Fig. 32. All these structures of reactive intermediates formed during NTP dephosphorylation processes have in common the M^{2+}/NTP 2 : 1 composition, i.e. the M(α, β)–M(γ) coordination unit, which is evidently especially suitable to promote the split between the β and γ-group of a triphosphate. The creation of this unit is delicate and therefore only those systems which allow additional interactions facilitating the shift of one metal ion into the α,β position and focusing the other to the terminal γ-phosphate group are highly reactive (structures **B** and **C** in Fig. 32). This "structuring" role [64,65,71] of the N-7 of one of the two ATPs in the $[M_2(ATP)]_2(OH)^-$ dimer, or of the N-6,N-7 site in the reactive $M_2(\epsilon$-ATP)$(OH)^-$ complex, is taken over in nature by enzymes.

A proposal based on the above reasonings is depicted in Fig. 34 showing how nature could achieve selective transphosphorylations. Indeed, a growing number of pertinent enzymic systems containing two or more metal ions are becoming known [9,10,134–138]. There are also examples where the specific function of a divalent metal ion is the formation of an enzyme–metal ion–nucleotide bridged complex [9,166–168]. Furthermore, enzymes may modify the structure of substrate molecules [11,169–171], e.g. Mn^{2+} binds to all three phosphoryl groups of TTP in the binary complex but only to the terminal γ-phosphate group in the ternary complex which involves also DNA polymerase I of *Escherichia coli* [170]. In addition, a recent proposal

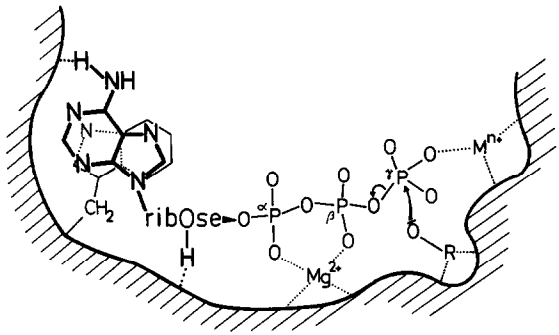

Fig. 34. Tentative view of a reactive $Mg(ATP)^{2-}$ complex at an enzyme, the γ-phosphate group being ready for a nucleophilic attack and transfer to R–O which is sitting in a groove of the enzyme. Obviously, the R–O residue could alternatively be bound to M^{n+} and be correctly positioned towards the γ-phosphate group in this way. ATP may be oriented at the enzyme surface by stacking (e.g. with an indole residue) and hydrogen bonding, forcing Mg^{2+} by this orientation, possibly with the help of protein sites, into the α, β positions of the phosphate chain. Obviously, Mg^{2+} and M^{n+} could interchange their positions or other metal ions could substitute for them, and (at least) one of the two metal ions could even be replaced by an ionic interaction (e.g. with an arginyl group) and a reactive intermediate would still result (see text). The release of ADP from the enzyme could in the example shown be initiated by a stronger coordination of the metal ion to the now twofold negatively charged β group leading thus to a release of $Mg(ADP)^-$ from the enzyme surface. (Reproduced from Fig. 11 in ref. 65 (J. Am. Chem. Soc., 1984) with permission of the American Chemical Society.)

[172] for the complex involving the active site of pyruvate kinase, ATP, Mg^{2+}, Mn^{2+}, and the competitive inhibitor oxalate, which is an analogue of the presumed reactive form of pyruvate, has much in common with the proposal shown in Fig. 34. For the pyruvate kinase complex it is suggested that Mg^{2+} binds to the triphosphate chain of ATP and the enzyme-bound Mn^{2+} bridges the γ-phosphate group and oxalate, facilitating in this way the transphosphorylation in the native complex, where oxalate is replaced by pyruvate. It should be emphasized that it is to be expected [65] that not only coordinated OH^- (Fig. 32) remains a nucleophile of high quality but also other groups, e.g. alcoholic and related residues, that participate in transphosphorylations in nature.

It appears that a selective anchoring interaction between the base moiety of the nucleotide and the enzyme is crucial for the creation of the desired reactive intermediate (Fig. 34), and there are indications of this [171,173,174]. The first step could be to anchor the nucleotide or its complex to the enzyme-protein, e.g. via stacking with an indole residue or by hydrophobic interactions with an isopropyl moiety [20,28,81,91,123,159] but hydrogen-bond formation [175] (e.g. with histidine [176]) and ionic interactions (e.g.

with an arginyl residue [177–180]) also appear feasible. Either of the last two interactions, if it occurs with the phosphate chain, could also replace one of the two metal ions shown in Fig. 34 in leading to the reactive intermediate. Recent results with protonated polyaza macrocycles that bind anionic nucleotide substrates [181] and facilitate the dephosphorylation of ATP [182] support this view.

Such ionic or hydrogen-bond interactions will be favored in low polarity media as they occur in active sites of enzymes (Section K). It should further be emphasized that a low dielectric constant would also allow the replacement of one of the two (possibly even both) metal ions by a monovalent ion such as H^+, Na^+ or K^+. Owing to enhanced binding under these conditions, activation and selectivity would still result (Section K). Considering that, for example, the intracellular pH in human skeletal muscle [183] is close to 7.0, some partial protonation of phosphate groups still appears feasible especially in a low polarity environment. That exclusion of water from the active site cleft of an enzyme favors hydrogen bonding seems certain [184], and that monovalent cations may participate in transphosphorylations is also known [165,172,185]. It should further be pointed out that under conditions with reduced polarity, hydrogen bonds [186] and $R\text{–}O^-/M^{n+}$ complex formations (Section K) [154,161,187] give rise to *cooperativity* with stacking and related interactions [15,16,159,188].

The anchoring process is evidently crucial for locating the two activating "partners", e.g. metal ions, such that the reactive $M(\alpha, \beta)\text{–}M(\gamma)$ structure (Fig. 34) ready for a transphosphorylation results. However, it is also clear from these considerations that an enforced $M(\alpha)\text{–}M(\beta, \gamma)$ coordination would lead to a reactive species ready for the transfer of either a nucleoside monophosphate or a diphosphate group. In fact the concept outlined [65,71] allows selective activation for the transfer of all groups which can be derived from a nucleoside triphosphate, including the transfer of a nucleoside group. Moreover, as purine-nucleotides are much more easily anchored via stacking and hydrophobic interactions than pyrimidine-nucleotides [81,117], this difference may be the main reason why pyrimidine-NTPs, e.g. UTP, are not able to substitute effectively for ATP in many enzymic systems [138,189].

Among the metal ions that activate ATP in nature, Mg^{2+} is the most prominent [3,12]; in fact, on the basis of the results summarized here one is tempted to say [65] that "nature made a good choice" in selecting Mg^{2+} for so many reactions which involve nucleotides. In $Mg(ATP)^{2-}$ the metal ion is mainly coordinated to the β,γ-phosphate groups [11,18,108,109,190]. Hence it is well suited for a shift along the phosphate chain (Fig. 34) and activation is possible with this metal ion (Sections E(iv) and J(iii)). One could speculate that here is one of the origins of the differences between Mg^{2+} and Ca^{2+}. The Ca^{2+} ion with its larger ionic radius [191,192] (which varies also with

the coordination number) and adaptable coordination sphere possibly forms an M(α, β, γ) species, and such a $Ca(NTP)^{2-}$ complex would be more difficult to activate. Indeed, intramitochondrial Ca^{2+} (and Sr^{2+}) inhibits oxidative phosphorylation in intact rat liver mitochondria [193] because $Ca(ATP)^{2-}$ cannot act as substrate, which is in fact $Mg(ATP)^{2-}$. Furthermore, many divalent metal ions promote ATP dephosphorylation as discussed in this review, but they have not been seen as being effective in promoting the *depyro*phosphorylation process, except Ca^{2+} at pH 9 for which pyrophosphate production has been reported [31]. Similarly, addition of Ca^{2+} to $(tn)_2Co(ATP)^-$ [78] at pH 6.5 also leads to the formation of some pyrophosphate.

Coming back to the "natural" advantages of Mg^{2+} one may further add that there is no direct Mg^{2+}–N-7 interaction in $Mg(ATP)^{2-}$ [17,61], and because there is also little tendency for Mg^{2+} to form a hydroxo complex in the physiological pH range (Section E(iv)), no "self-activation" of the $Mg(ATP)^{2-}$ substrate is possible. With most other metal ions, including Zn^{2+} and Mn^{2+}, which have a tendency to interact with N-7 [17,61], this self-activation will occur to some extent. However, there is a "tool" that nature might use to prevent self-activation if one of these metal ions should be desired for a special task: formation of a mixed-ligand complex will inhibit the dephosphorylation reaction (Sections C(iii) and E(iii); Figs. 5, 9, 22 and 23).

In this discussion about the activating role of the metal ion the observations described for the Mn^{2+}/ATP system (Section E(i); Fig. 14) [66] should also be recalled: oxidation of Mn^{2+} to Mn^{3+} creates an excellent activator for the dephosphorylation process. In other words, via redox reactions involving couples such as Mn^{2+}/Mn^{3+} or Fe^{2+}/Fe^{3+}, nature could trigger transphosphorylation events. Under very special natural conditions even Cu^{2+}, which is in vitro an excellent promoter as the many examples in this review show, might be employed. In fact, there are indications that $Cu(ATP)^{2-}$ might be a natural active form of Cu^{2+} [194]. Finally, one may mention that in certain cell compartments, such as in synaptic vesicles [195,196] or chromaffin granules [197], large nucleotide concentrations occur, e.g. the ATP concentration reaches 0.15 M in chromaffin granules of the adrenal medulla [197], and there are also significant amounts of metal ions present, which would allow to trigger a "bombardment" of transphosphorylations.

ACKNOWLEDGEMENT

The financial support of the research of my group on nucleotide complexes by the Swiss National Science Foundation is gratefully acknowledged.

REFERENCES

1 P.D. Boyer, Biochemistry, 26 (1987) 8503–8507.
2 P. Karlson, Kurzes Lehrbuch der Biochemie, 11th edn., Thieme, Stuttgart and New York, 1980, pp. 306 and 365.
3 K. Yoshikawa, Y. Shinohara, H. Terada and S. Kato, Biophys. Chem., 27 (1987) 251–254.
4 E. Gajewski, D.K. Steckler and R.N. Goldberg, J. Biol. Chem., 261 (1986) 12733–12737.
5 O. Meyerhof and K. Lohmann, Biochem. Z., 253 (1932) 431–461.
6 B.S. Cooperman, Met. Ions Biol. Syst., 5 (1976) 79–126.
7 L.G. Marzilli, Prog. Inorg. Chem., 23 (1977) 255–378.
8 A.S. Mildvan, Adv. Enzymol. Relat. Areas Mol. Biol., 49 (1979) 103–126.
9 G.L. Eichhorn, Met. Ions Biol. Syst., 10 (1980) 1–21.
10 F.Y.-H. Wu and C.-W. Wu, Met. Ions Biol. Syst., 15 (1983) 157–192.
11 H.R. Kalbitzer, Met. Ions Biol. Syst., 22 (1987) 81–103.
12 A.S. Mildvan, Magnesium, 6 (1987) 28–33.
13 C.M. Frey and J.E. Stuehr, Met. Ions Biol. Syst., 1 (1974) 51–116.
14 (a) C.M. Frey and J.E. Stuehr, J. Am. Chem. Soc., 100 (1978) 139–145.
(b) K.J. Butenhof, D. Cochenour, J.L. Banyasz and J.E. Stuehr, Inorg. Chem., 25 (1986) 691–696.
15 R. Tribolet, R. Malini-Balakrishnan and H. Sigel, J. Chem. Soc., Dalton Trans., (1985) 2291–2303.
16 H. Sigel, in A.V. Xavier (Ed.), Frontiers in Bioinorganic Chemistry, VCH, Weinheim, 1986, pp. 84–93.
17 H. Sigel, Eur. J. Biochem., 165 (1987) 65–72.
18 R.B. Martin and Y.H. Mariam, Met. Ions Biol. Syst., 8 (1979) 57–124.
19 R.B. Martin, Met. Ions Biol. Syst., 23 (1988) 315–330.
20 H. Sigel, in T.D. Tullius (Ed.), Metal–DNA Chemistry, ACS Symp. Ser., No. 402 (1989) 159–204.
21 H. Sigel, in I. Bertini, R.S. Drago and C. Luchinat (Eds.), The Coordination Chemistry of Metalloenzymes, Reidel, Dordrecht, 1983, pp. 65–78.
22 H. Sigel, Pure Appl. Chem., 55 (1983) 137–144.
23 G.P. Haight, Jr., Coord. Chem. Rev., 79 (1987) 293–319.
24 R.W. Gellert and R. Bau, Met. Ions Biol. Syst., 8 (1979) 1–55.
25 V. Swaminathan and M. Sundaralingam, CRC Crit. Rev. Biochem., 6 (1979) 245–336.
26 H. Diebler, J. Mol. Catal., 23 (1984) 209–217.
27 R.B. Martin, Acc. Chem. Res., 18 (1985) 32–38.
28 H. Sigel, Chimia, 41 (1987) 11–26.
29 H. Sigel, S.S. Massoud and R. Tribolet, J. Am. Chem. Soc., 110 (1988) 6857–6865.
30 Y. Kinjo, R. Tribolet, N.A. Corfù and H. Sigel, Inorg. Chem., 28 (1989) 1480–1489.
31 M. Tetas and J.M. Lowenstein, Biochemistry, 2 (1963) 350–357.
32 M. Hediger and R.M. Milburn, J. Inorg. Biochem., 16 (1982) 165–182.
33 (a) C. Liébecq and M. Jacquemotte-Louis, Bull. Soc. Chim. Biol., 40 (1958) 67–85 and 759–765.
(b) C. Liébecq, Bull. Soc. Chim. Biol., 41 (1959) 1181–1188.
34 P.W. Schneider and H. Brintzinger, Helv. Chim. Acta, 47 (1964) 1717–1733.
35 M.A. Gonzalez, M.R. Webb, K.M. Welsh and B.S. Cooperman, Biochemistry, 23 (1984) 797–801.
36 (a) E. Bamann, F. Fischler and H. Trapmann, Biochem. Z., 325 (1954) 413–428.

(b) E. Bamann and H. Trapmann, Adv. Enzymol. Relat. Areas Mol. Biol., 21 (1959) 169–188.
37 W.J. Bowen and T.D. Kerwin, Proc. Soc. Exp. Biol. Med., 88 (1955) 515–517.
38 M.J. Selwyn, Nature (London), 219 (1968) 490–493.
39 W.W. Butcher and F.H. Westheimer, J. Am. Chem. Soc., 77 (1955) 2420–2424.
40 R.M. Milburn, M. Gautam-Basak, R. Tribolet and H. Sigel, J. Am. Chem. Soc., 107 (1985) 3315–3321.
41 S. Suzuki, T. Higashiyama and A. Nakahara, Bioinorg. Chem., 8 (1978) 277–289.
42 S.H. McClaugherty and C.M. Grisham, Inorg. Chem., 21 (1982) 4133–4138.
43 G.R. Meyer and R. Cornelius, J. Inorg. Biochem., 22 (1984) 249–258.
44 F. Tafesse, S.S. Massoud and R.M. Milburn, Inorg. Chem., 24 (1985) 2591–2593.
45 M. Hediger and R.M. Milburn, ACS Symp. Ser., No. 171 (1981) 211–216.
46 G. Rawji, M. Hediger and R.M. Milburn, Inorg. Chim. Acta, 79 (1983) 247–248.
47 (a) R.D. Cornelius, Inorg. Chem., 19 (1980) 1286–1290.
(b) P.R. Norman and R.D. Cornelius, J. Am. Chem. Soc., 104 (1982) 2356–2361.
48 G.P. Haight, Jr., T.W. Hambley, P. Hendry, G.A. Lawrance and A.M. Sargeson, J. Chem. Soc., Chem. Commun., (1985) 488–491.
49 P.W.A. Hübner and R.M. Milburn, Inorg. Chem., 19 (1980) 1267–1272.
50 I.I. Creaser, G.P. Haight, Jr., R. Peachey, W.T. Robinson and A.M. Sargeson, J. Chem. Soc., Chem. Commun., (1984) 1568–1571.
51 (a) B. Anderson, R.M. Milburn, J.MacB. Harrowfield, G.B. Robertson and A.M. Sargeson, J. Am. Chem. Soc., 99 (1977) 2652–2661.
(b) J.MacB. Harrowfield, D.R. Jones, L.F. Lindoy and A.M. Sargeson, J. Am. Chem. Soc., 102 (1980) 7733–7741.
(c) D.R. Jones, L.F. Lindoy and A.M. Sargeson, J. Am. Chem. Soc., 105 (1983) 7327–7336.
(d) D.R. Jones, L.F. Lindoy and A.M. Sargeson, J. Am. Chem. Soc., 106 (1984) 7807–7819.
(e) J. Chin, M. Banaszczyk and V. Jubian, J. Chem. Soc., Chem. Commun., (1988) 735–736.
(f) J. Chin, M. Banaszczyk, V. Jubian and X. Zou, J. Am. Chem. Soc., 111 (1989) 186–190.
52 (a) G.M. Woltermann, R.A. Scott and G.P. Haight, Jr., J. Am. Chem. Soc., 96 (1974) 7569–7570.
(b) T. Imamura, D.M. Hinton, R.L. Belford, R.I. Gumport and G.P. Haight, Jr., J. Inorg. Biochem., 11 (1979) 241–259.
53 (a) S.H. Gellman, R. Petter and R. Breslow, J. Am. Chem. Soc., 108 (1986) 2388–2394.
(b) R.W. Hay, A.K. Basak, M.P. Pujari and A. Perotti, J. Chem. Soc., Dalton Trans., (1986) 2029–2033.
(c) D. Herschlag and W.P. Jencks, J. Am. Chem. Soc., 109 (1987) 4665–4674.
(d) T. Murakami, Nippon Kagaku Kaishi, (1988) 396–400.
(e) T.H. Fife and M.P. Pujari, J. Am. Chem. Soc., 110 (1988) 7790–7797.
54 B.S. Cooperman, Biochemistry, 8 (1969) 5005–5010.
55 D.H. Buisson and H. Sigel, Biochim. Biophys. Acta, 343 (1974) 45–63.
56 T.G. Spiro, W.A. Kjellstrom, M. Zeydel and R.A. Butow, Biochemistry, 7 (1968) 859–865.
57 I. Feldman, Jerusalem Symp. Quantum Chem. Biochem., 4 (1972) 528–537.
58 I. Feldman and V. Wee, Biochemistry, 13 (1974) 1836–1840.
59 D.L. Miller and F.H. Westheimer, J. Am. Chem. Soc., 88 (1966) 1514–1517.

60 K.H. Scheller, F. Hofstetter, P.R. Mitchell, B. Prijs and H. Sigel, J. Am. Chem. Soc., 103 (1981) 247–260.
61 H. Sigel, R. Tribolet, R. Malini-Balakrishnan and R.B. Martin, Inorg. Chem., 26 (1987) 2149–2157.
62 (a) M.M.T. Khan and A.E. Martell, J. Phys. Chem., 66 (1962) 10–15.
(b) M.M.T. Khan and A.E. Martell, J. Am. Chem. Soc., 88 (1966) 668–671.
63 E.R. Werner and B.M. Rhode, Inorg. Chim. Acta, 80 (1983) 39–46.
64 H. Sigel and P.E. Amsler, J. Am. Chem. Soc., 98 (1976) 7390–7400.
65 H. Sigel, F. Hofstetter, R.B. Martin, R.M. Milburn, V. Scheller-Krattiger and K.H. Scheller, J. Am. Chem. Soc., 106 (1984) 7935–7946.
66 P.E. Amsler and H. Sigel, Eur. J. Biochem., 63 (1976) 569–581.
67 A.A. Hirata and D. Appleman, Anal. Chem., 31 (1959) 2097–2099.
68 E.Z. Utyanskaya and A.E. Shilov, Kinet. Katal., 29 (1988) 136–142 (English translation, pp. 118–123).
69 H. Sigel, D.H. Buisson and B. Prijs, Bioinorg. Chem., 5 (1975) 1–20.
70 (a) B.E. Fischer, U.K. Häring, R. Tribolet and H. Sigel, Eur. J. Biochem., 94 (1979) 523–530.
(b) K.H. Scheller, T.H.J. Abel, P.E. Polanyi, P.K. Wenk, B.E. Fischer and H. Sigel, Eur. J. Biochem., 107 (1980) 455–466.
(c) H. Sigel, K.H. Scheller and B. Prijs, Inorg. Chim. Acta, 66 (1982) 147–155.
71 H. Sigel and F. Hofstetter, Eur. J. Biochem., 132 (1983) 569–577.
72 R. Tribolet and H. Sigel, Eur. J. Biochem., 170 (1988) 617–626.
73 H. Sigel, J. Am. Chem. Soc., 97 (1975) 3209–3214.
74 R. Phillips, S.J., Chem. Rev., 66 (1966) 501–527.
75 T.C. Bruice and S.J. Benkovic, Bioorganic Mechanisms: Vol. 2, Benjamin, New York, 1966.
76 (a) F. Ramirez, J.F. Marecek and J. Szamosi, J. Org. Chem., 45 (1980) 4748–4752.
(b) F. Ramirez and J.F. Marecek, Pure Appl. Chem., 52 (1980) 1021–1045 and 2213–2227.
77 G.J. Hutchings, B.E.C. Banks, M. Mruzek, J.H. Ridd and C.A. Vernon, Biochemistry, 20 (1981) 5809–5816.
78 F. Tafesse and R.M. Milburn, Inorg. Chim. Acta, 135 (1987) 119–122.
79 (a) C.F. Naumann and H. Sigel, J. Am. Chem. Soc., 96 (1974) 2750–2756.
(b) P. Chaudhuri and H. Sigel, J. Am. Chem. Soc., 99 (1977) 3142–3150.
(c) P.R. Mitchell and H. Sigel, J. Am. Chem. Soc., 100 (1978) 1564–1570.
80 Y. Fukuda, P.R. Mitchell and H. Sigel, Helv. Chim. Acta, 61 (1978) 638–647.
81 P.R. Mitchell, B. Prijs and H. Sigel, Helv. Chim. Acta, 62 (1979) 1723–1735.
82 D.H. Buisson and H. Sigel, Angew. Chem., 84 (1972) 1103–1104; Angew. Chem., Int. Ed. Engl., 11 (1972) 1025.
83 (a) P. Orioli, R. Cini, D. Donati and S. Mangani, Inorg. Chim. Acta, 40 (1980) X86–X87.
(b) P. Orioli, R. Cini, D. Donati and S. Mangani, Nature (London), 283 (1980) 691–693.
(c) P. Orioli, R. Cini, D. Donati and S. Mangani, J. Am. Chem. Soc., 103 (1981) 4446–4452.
84 (a) W.S. Sheldrick, Angew. Chem., 93 (1981) 473–474; Angew. Chem., Int. Ed. Engl., 20 (1981) 460.
(b) W.S. Sheldrick, Z. Naturforsch., Teil B, 37 (1982) 863–871.
85 P.E. Amsler, D.H. Buisson and H. Sigel, Z. Naturforsch., Teil C, 29 (1974) 680–682.
86 V. Scheller-Krattiger and H. Sigel, Inorg. Chem., 25 (1986) 2628–2634.
87 R. Tribolet, R.B. Martin and H. Sigel, Inorg. Chem., 26 (1987) 638–643.
88 H. Sigel, K.H. Scheller and R.M. Milburn, Inorg. Chem., 23 (1984) 1933–1938.

89 H. Sigel, Eur. J. Biochem., 3 (1968) 530–537.
90 H. Sigel, J. Inorg. Nucl. Chem., 39 (1977) 1903–1911.
91 H. Sigel, B.E. Fischer and E. Farkas, Inorg. Chem., 22 (1983) 925–934.
92 H. Sigel and C.F. Naumann, J. Am. Chem. Soc., 98 (1976) 730–739.
93 S.S. Massoud and H. Sigel, Inorg. Chem., 27 (1988) 1447–1453.
94 R.B. Martin, J. Inorg. Nucl. Chem., 38 (1976) 511–513.
95 D.A. Buckingham, F.R. Keene and A.M. Sargeson, J. Am. Chem. Soc., 96 (1974) 4981–4983.
96 R.S. Brown, J. Huguet and N.J. Curtis, Met. Ions Biol. Syst., 15 (1983) 55–99.
97 R. Breslow, D.E. McClure, R.S. Brown and J. Eisenach, J. Am. Chem. Soc., 97 (1975) 194–195.
98 W.N. Lipscomb, Acc. Chem. Res., 15 (1982) 232–238.
99 C.J. Boreham, D.A. Buckingham and F.R. Keene, J. Am. Chem. Soc., 101 (1979) 1409–1421; Inorg. Chem., 18 (1979) 28–38.
100 J. Suh, M. Cheong and M.P. Suh, J. Am. Chem. Soc., 104 (1982) 1654–1657.
101 (a) T.H. Fife and T.J. Przystas, J. Am. Chem. Soc., 105 (1983) 1638–1642.
(b) T.H. Fife and T.J. Przystas, J. Am. Chem. Soc., 107 (1985) 1041–1047.
102 P. Job, C.R. Hebd. Séances Acad. Sci., 196 (1933) 181–183.
103 A.A. Frost and R.G. Pearson, Kinetics and Mechanism, Wiley, New York, 1953.
104 (a) M. Eigen, Pure Appl. Chem., 6 (1963) 97–115.
(b) F.A. Cotton and G. Wilkinson, Advanced Inorganic Chemistry, 4th ed., Wiley, New York, 1980, p. 1188.
105 S. Kunugi, H. Hirohara and N. Ise, Eur. J. Biochem., 124 (1982) 157–163.
106 B.A. Connolly and F. Eckstein, J. Biol. Chem., 256 (1981) 9450–9456.
107 R.S. Goody, W. Hofman and M. Konrad, FEBS Lett., 129 (1981) 169–172.
108 (a) M.-D. Tsai, S.L. Huang, J.F. Kozlowski and C.C. Chang, Biochemistry, 19 (1980) 3531–3536.
(b) S.L. Huang and M.-D. Tsai, Biochemistry, 21 (1982) 951–959.
109 B.D. Ray, P. Rösch and B.D.N. Rao, Biochemistry, 27 (1988) 8669–8676.
110 J.I. Watters and I.M. Kolthoff, J. Am. Chem. Soc., 70 (1948) 2455–2460.
111 H. Brintzinger, R. Zell and H. Erlenmeyer, Helv. Chim. Acta, 47 (1964) 1642–1647.
112 M.S. Mohan and G.A. Rechnitz, Arch. Biochem. Biophys., 162 (1974) 194–199.
113 T.A. Glassman, C. Cooper, G.P.P. Kuntz and T.J. Swift, FEBS Lett., 39 (1974) 73–74.
114 E.O. Bishop, S.J. Kimber, D. Orchard and B.E. Smith, Biochim. Biophys. Acta, 635 (1981) 63–72.
115 (a) G. Arena, R. Calì, S. Musumeci, R. Purrello, E. Rizzarelli and S. Sammartano, Proc. Int. Conf. Coord. Chem., 21 (1980) 263.
(b) G. Arena, R. Calì, V. Cucinotta, S. Musumeci, E. Rizzarelli and S. Sammartano, J. Chem. Soc., Dalton Trans., (1983) 1271–1278.
116 K.H. Scheller and H. Sigel, J. Am. Chem. Soc., 105 (1983) 5891–5900.
117 H. Sigel, Biol. Trace Elem. Res., 21 (1989) 49–59.
118 J.E. Coleman, Nature (London), 214 (1967) 193–194.
119 R. Bauer, P. Limkilde and J.T. Johansen, Biochemistry, 15 (1976) 334–342.
120 A. Galdes and B.L. Vallee, Met. Ions Biol. Syst., 15 (1983) 1–54.
121 H. Gampp, H. Sigel and A.D. Zuberbühler, Inorg. Chem., 21 (1982) 1190–1195.
122 E.Z. Utyanskaya and A.E. Shilov, Kinet. Katal., 27 (1986) 124–132 (English translation, pp. 113–121). Note added in proof: Points similar to those given in Section E(v) hold also against the arguments very recently advanced for a dominant role of N-1 by E.Z. Utyanskaya, A.G. Pavlovskii, N.I. Sosfenov and E.E. Shilov, Dokl. Akad. Nauk SSSR,

301 (1988) 149–153 (English translation, pp. 595–598). It should further be noted that Shilov and coworkers (see also ref. 68) consider the 1:1 $[Zn(ATP)]_2^{4-}$ dimer while I emphasize the reactivity of the 2:1 $[M_2(ATP)]_2(OH)^-$ species.
123 H. Sigel, in D. Banerjea (Ed.), Coordination Chemistry—20, published by IUPAC through Pergamon, Oxford and New York, 1980, pp. 27–45.
124 H. Sigel and D.B. McCormick, Acc. Chem. Res., 3 (1970) 201–208.
125 H. Sigel and K.H. Scheller, Eur. J. Biochem., 138 (1984) 291–299.
126 K.H. Scheller and H. Sigel, J. Am. Chem. Soc., 105 (1983) 3005–3014.
127 (a) H. Sigel, Met. Ions Biol. Syst., 8 (1979) 125–158.
(b) H. Sigel and B. Prijs, Helv. Chim. Acta, 50 (1967) 2357–2362.
(c) H. Sigel and H. Brintzinger, Helv. Chim. Acta, 47 (1964) 1701–1717.
128 H. Sigel and F. Hofstetter, to be published.
129 (a) I.R. Jonasson, R.S. Murray, D.R. Stranks and J.K. Yandell, Proc. 12th Int. Conf. Coord. Chem., 1969 p. 32.
(b) I.R. Jonasson, S.F. Lincoln and D.R. Stranks, Aust. J. Chem., 23 (1970) 2267–2278.
(c) A.D. Fowless and D.R. Stranks, Inorg. Chem., 16 (1977) 1276–1281.
(d) S.S. Massoud and R.M. Milburn, Polyhedron, 8 (1989) 275–284.
130 A. Szent-Györgyi, in O.H. Gaebler (Ed.), Enzymes: Units of Biological Structure and Function, Academic Press, New York, 1956, p. 393.
131 T.A. Kaden, K.H. Scheller and H. Sigel, Inorg. Chem., 25 (1986) 1313–1315.
132 K.H. Scheller and H. Sigel, Eur. J. Biochem., 157 (1986) 147–153.
133 H. Sigel, K.H. Scheller, V. Scheller-Krattiger and B. Prijs, J. Am. Chem. Soc., 108 (1986) 4171–4178.
134 T.M. Li, A.S. Mildvan and R.L. Switzer, J. Biol. Chem., 253 (1978) 3918–3923.
135 J.D. Otvos, I.M. Armitage, J.F. Chlebowski and J.E. Coleman, J. Biol. Chem., 254 (1979) 4707–4713.
136 J. Granot, A.S. Mildvan, H.N. Bramson and E.T. Kaiser, Biochemistry, 19 (1980) 3537–3543.
137 B.S. Cooperman, A. Panackal, B. Springs and D.J. Hamm, Biochemistry, 20 (1981) 6051–6060.
138 F.Y.-H. Wu and C.-W. Wu, Adv. Inorg. Biochem., 3 (1981) 143–166.
139 H. Moll, P.W. Schneider and H. Brintzinger, Helv. Chim. Acta, 47 (1964) 1837–1839.
140 M.S. Rohrbach, M.E. Dempsey and J.W. Bodley, J. Biol. Chem., 249 (1974) 5094–5101.
141 M. Cohn and A. Hu, Proc. Natl. Acad. Sci. U.S.A., 75 (1978) 200–203.
142 M.R. Webb, G.G. McDonald and D.R. Trentham, J. Biol. Chem., 253 (1978) 2908–2911.
143 S. Meyerson, E.S. Kuhn, F. Ramirez and J.F. Marecek, J. Am. Chem. Soc., 104 (1982) 7231–7239.
144 K.K. Shukla, H.M. Levy, F. Ramirez, J.F. Marecek, B. McKeever and S.S. Margossian, Biochemistry, 22 (1983) 4822–4830.
145 A.A. Osei, G.W. Everett and R.H. Himes, Biochim. Biophys. Acta, 955 (1988) 269–271.
146 F.H. Westheimer, Acc. Chem. Res., 1 (1968) 70–78.
147 T. Eiki, T. Horiguchi, M. Ono, S. Kawada and W. Tagaki, J. Am. Chem. Soc., 104 (1982) 1986–1991.
148 F.H. Westheimer, Chem. Rev., 81 (1981) 313–326.
149 R.B. Martin, Met. Ions Biol. Syst., 17 (1984) 1–49, see p. 33.
150 (a) H. Sigel, Angew. Chem., 87 (1975) 391–400; Angew. Chem., Int. Ed. Engl., 14 (1975) 394–402.
(b) H. Sigel, B.E. Fischer and B. Prijs, J. Am. Chem. Soc. 99 (1977) 4489–4496.
(c) H. Sigel, Inorg. Chem., 19 (1980) 1411–1413.

(d) H. Sigel, Angew. Chem., 94 (1982) 421–432; Angew. Chem., Int. Ed. Engl., 21 (1982) 389–400.
151 R.M. Milburn and H. Sigel, (1983) unpublished observations.
152 D.C. Rees, J. Mol. Biol., 141 (1980) 323–326.
153 (a) G.R. Moore, FEBS Lett., 161 (1983) 171–175.
(b) N.K. Rogers, G.R. Moore and M.J.E. Sternberg, J. Mol. Biol., 182 (1985) 613–616.
154 H. Sigel, R.B. Martin, R. Tribolet, U.K. Häring and R. Malini-Balakrishnan, Eur. J. Biochem., 152 (1985) 187–193.
155 J.G. Watterson, Biochem. J., 248 (1987) 615–617.
156 C. Tanford, Biochem. Soc. Trans., 15, Suppl. (1987) 1S–7S.
157 B.L. Vallee and R.J.P. Williams, Chem. Br., 4 (1968) 397–402.
158 R.J.P. Williams, Biochem. Soc. Trans., 15, Suppl. (1987) 36S–47S.
159 H. Sigel, Pure Appl. Chem., 61 (1989) 923–932.
160 R.G. Bates, Determination of pH: Theory and Practice, Wiley, New York and London, 1973, p. 223.
161 G. Liang, N.A. Corfù and H. Sigel, Z. Naturforsch., Teil B, 44 (1989) 538–542.
162 (a) G. Åkerlöf and O.A. Short, J. Am. Chem. Soc., 58 (1936) 1241–1243.
(b) F.E. Critchfield, J.A. Gibson, Jr., and J.L. Hall, J. Am. Chem. Soc., 75 (1953) 1991–1992.
(c) G. Åkerlöf and O.A. Short, J. Am. Chem. Soc., 75 (1953) 6357.
163 (a) H. Sigel and R. Tribolet, to be published.
(b) H. Sigel and R. Tribolet, J. Inorg. Biochem., submitted for publication.
164 Y.K. Agrawal, Talanta, 20 (1973) 1354–1356.
165 V.L. Goncalves de Moraes and L. de Meis, FEBS Lett., 222 (1987) 163–166.
166 J.L. Aull, H.H. Daron, M.E. Friedman and P. Melius, Met. Ions Biol. Syst., 11 (1980) 337–376.
167 (a) R. Koren and A.S. Mildvan, Biochemistry, 16 (1977) 241–249.
(b) B.L. Bean, R. Koren and A.S. Mildvan, Biochemistry, 16 (1977) 3322–3333.
168 G.K. Jarori, B.D. Ray and B.D.N. Rao, Biochemistry, 24 (1985) 3487–3494.
169 J. Feuerstein, H.R. Kalbitzer, J. John, R.S. Goody and A. Wittinghofer, Eur. J. Biochem., 162 (1987) 49–55.
170 D.L. Sloan, L.A. Loeb, A.S. Mildvan and R.J. Feldmann, J. Biol. Chem., 250 (1975) 8913–8920.
171 L.J. Ferrin and A.S. Mildvan, Biochemistry, 24 (1985) 6904–6913.
172 D.T. Lodato and G.H. Reed, Biochemistry, 26 (1987) 2243–2250.
173 (a) M. Vašák, K. Nagayama, K. Wüthrich, M.L. Mertens and J.H.R. Kägi, Biochemistry, 18 (1979) 5050–5055.
(b) H. Yoshino, F. Morita and K. Yagi, J. Biochem. (Tokyo), 72 (1972) 1227–1235.
174 D.C. Fry, D.M. Byler, H. Susi, E.M. Brown, S.A. Kuby and A.S. Mildvan, Biochemistry, 27 (1988) 3588–3598.
175 L.G. Marzilli and T.J. Kistenmacher, Acc. Chem. Res., 10 (1977) 146–152.
176 P.R. Rosevear, P. Desmeules, G.L. Kenyon and A.S. Mildvan, Biochemistry, 20 (1981) 6155–6164.
177 (a) D. Mota de Freitas, C. Luchinat, L. Banci, I. Bertini and J.S. Valentine, Inorg. Chem., 26 (1987) 2788–2791.
(b) J.-D. Choi and D.B. McCormick, Biochemistry, 20 (1981) 5722–5728.
178 J.F. Riordan, Mol. Cell. Biochem., 26 (1979) 71–92.
179 B. Springs and P. Haake, Tetrahedron Lett., 37 (1977) 3223–3226.
180 F.A. Cotton, T. la Cour, E.E. Hazen, Jr., and M.J. Legg, Biochim. Biophys. Acta, 481 (1977) 1–5.

181 M.W. Hosseini and J.-M. Lehn, Helv. Chim. Acta, 70 (1987) 1312–1319.
182 (a) M.W. Hosseini, J.-M. Lehn, L. Maggiora, K.B. Mertes and M.P. Mertes, J. Am. Chem. Soc., 109 (1987) 537–544.
(b) G.M. Blackburn, G.R.J. Thatcher, M.W. Hosseini and J.-M. Lehn, Tetrahedron Lett., 28 (1987) 2779–2782.
(c) P.G. Yohannes, K.E. Plute, M.P. Mertes and K.B. Mertes, Inorg. Chem., 26 (1987) 1751–1755.
(d) M.W. Hosseini, J.A. Blacker and J.-M. Lehn, J. Chem. Soc., Chem. Commun., (1988) 596–598.
183 J.W. Pan, J.R. Hamm, D.L. Rothman and R.G. Shulman, Proc. Natl. Acad. Sci. U.S.A., 85 (1988) 7836–7839.
184 J. Petruska, L.C. Sowers and M.F. Goodman, Proc. Natl. Acad. Sci., U.S.A., 83 (1986) 1559–1562.
185 D. Dunaway-Mariano, J.L. Benovic, W.W. Cleland, R.K. Gupta and A.S. Mildvan, Biochemistry, 18 (1979) 4347–4354.
186 M.P. Williamson and D.H. Williams, Eur. J. Biochem., 138 (1984) 345–348.
187 H. Sigel, R. Malini-Balakrishnan and U.K. Häring, J. Am. Chem. Soc., 107 (1985) 5137–5148.
188 G. Liang, R. Tribolet and H. Sigel, Inorg. Chem., 27 (1988) 2877–2887.
189 (a) G.M. Weinstock, K. McEntee and I.R. Lehman, J. Biol. Chem., 256 (1981) 8856–8858.
(b) J.C. Gerhart and A.B. Pardee, J. Biol. Chem., 237 (1962) 891–896.
190 (a) F. Ramirez and J.F. Marecek, Biochem. Biophys. Acta, 589 (1980) 21–29.
(b) H. Takeuchi, H. Murata and I. Harada, J. Am. Chem. Soc., 110 (1988) 392–397.
191 R.B. Martin, Met. Ions Biol. Syst., 17 (1984) 1–49, see p. 5.
192 Y. Marcus, Chem. Rev., 88 (1988) 1475–1498.
193 M.M. Fagian, L.P. da Silva and A.E. Vercesi, Biochim. Biophys. Acta, 852 (1986) 262–268.
194 C. Tallineau, M. Barriere, M. Boulard, P. Boulard-Heitzmann, R. Pontcharraud, D. Reiss and O. Guillard, Biochim. Biophys. Acta, 775 (1984) 51–56.
195 (a) K.S. Rajan, R.W. Colburn and J.M. Davis, Met. Ions Biol. Syst., 6 (1976) 291–321.
(b) R.W. Colburn and J.W. Maas, Nature (London), 208 (1965) 37–41.
196 N.A. Thorn, J.T. Russell and M. Treiman, in A.M. Poisner and J.M. Trifaró (Eds.), The Secretory Granule, Elsevier, Amsterdam, 1982, pp. 119–151.
197 H. Winkler and S.W. Carmichael, in A.M. Poisner and J.M. Trifaró (Eds.), The Secretory Granule, Elsevier, Amsterdam, 1982, pp. 3–79.